ZESZYTY NAUKOWE POLITECHNIKI RZESZOWSKIEJ NR 274
Mechanika z. 81 2010

Paweł KRZACZEK
Wiesław PIEKARSKI

Uniwersytet Przyrodniczy w Lublinie

UTILIZATION OF VEHICLE CONTROL-DIAGNOSTIC SYSTEM IN EVALUATION OF ENERGETIC PARAMETERS

In modern tractors and farm machinery newest electronic and information technologies, controlling not only engine work parameters but also operation of other sub-assemblies of the vehicle, are used. It enables real time exchange of information between controllers of tractor engine or whole agricultural unit. Evaluation of technical condition is possible on level of real time monitoring of diagnostic parameters, as well as by means of portable diagnostic systems. Utilization of on-board control-diagnostic systems, with installed automatic tests algorithms controlling operation of particular sub-assemblies, is also possible. Goal of this paper was evaluation of energetic parameters of John Deere 6920 tractor by means of on-board diagnostic system utilization. Tractor engine energetic parameters obtained as a result of such investigations enable evaluation of energetic "saturation" of a tractor. Establishing characteristics of changes course for: torque, power and unitary fuel consumption enables determination of rotation speed range for optimal operation of an engine. Using on board diagnostics of agricultural tractor as well as additional external diagnostic system Service ADVISOR eases location of damages and failure repair in tractors and farming machinery. It also enables determination of unitary fuel consumption ge, precisely enough to be used in establishing its value for practical purposes.

INTRODUCTION

Analysing present situation and tendencies taking place in the word of motorization, increase in electronics, information techniques and mechatronics utilization becomes clearly noticeable It has significant effect on development of constructional solutions as well as quality of operation of cars and commercial or agricultural vehicles. On one hand, it enables increase of work efficiency of exploited equipment, and on the other hand it leads to significant complication of construction [9]. Increasing number of various steering systems for particular subassemblies is introduced in vehicles It should be emphasised that areas of their operation often overlap, what results in necessity of integration of these system operation [1]. That is why, since 1980s, in cars, introduction of, based on various communication protocols, serial data buses has begun. Subsequently, unification of cars steering systems into common on-board diagnostic system (OBD), later adopted for commercial and agricultural vehicles, took place [2, 5, 10].

Introduction of serial data bus, for example CAN type, enabled operation, on the same set of data, of even dozen or so controllers responsible for work of vehicle subassemblies. Utilization of data transmission protocols enables real time exchange of information between controllers. Moreover, its introduction simplifies assessment of cars technical condition [7,8]. It is especially important when exploited vehicles are scattered over significant area, and there are difficulties to use some of other measurement methods.

Utilization of serial data bus enables evaluation of technical condition of vehicle through monitoring diagnostic parameters in real time. Moreover, serial bus makes possible cooperation with external diagnostic system and is a basis for on-board control-diagnostic system, which is programmed to perform auto-tests of particular subassemblies [4].

Knowledge of energetic parameters, from the vehicle user point of view, is necessary to obtain good economics of vehicle work and is a basis for determination of its technical condition [6]. There are many methods of measuring energetic parameters such as power or torque. Some of them require transporting vehicle to particular place or disassembly of some of vehicle subassemblies. That is why, in this paper, method of measuring energetic parameters in place where vehicle is used was utilized. In order to measure fuel consumption, control-diagnostic system cooperating with mobile diagnostic system was used. Equipped with on-board diagnostic system, John Deere 6920 agricultural tractor was object of this research.

METHODS

In order to evaluate energetic parameters such as torque and power output of agricultural tractor, PT 301 MES device was used. It enabled measurements of these parameters on power take-off shaft (PTO) (Fig. 1). This device is a mobile dynamometric stand enabling measurements in vehicle workplace. The only limitation for its use is possibility of connecting it to a source of, depending on its load level, 400 or 240V current supply. Measuring range for maximal torque and maximal power, that can be absorbed by the brake, reaches 5800Nm and 340kW respectively, and depends on time of operation and conditions at the site.

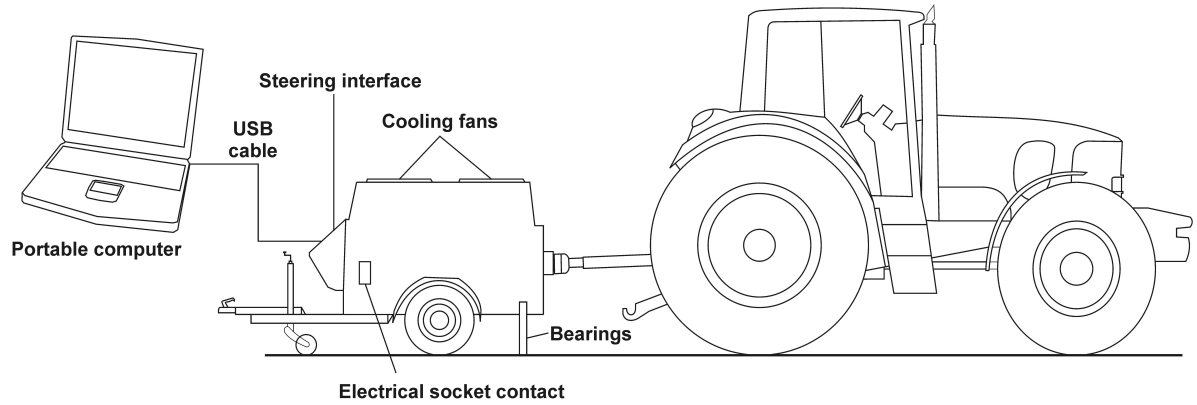

Fig. 1. Diagram showing mobile PT 301 MES dynamometric station [4]

Investigated tractor reflects tendencies in modern construction solutions of vehicles. John Deere 6920 tractor is based on modular design. Its diesel engine is fully electronically controlled and equipped with eight, connected into common steering-diagnostic system, controllers managing particular subassemblies. The system enables, through diagnostic connector, two-way communication with external diagnostic system Service Advisor.

Before conducting research, equipment and technical condition of investigated tractor had been checked by means of visual inspection and interview with tractor user. Next action was communication through diagnostic connector between engine steering units and portable computer equipped with diagnostic system Service ADVISOR. After connection with on board diagnostic system was established, verification of previously gathered informations was conducted. Subsequently, it was determined what steering units are available in the system and what parameters can be monitored.

In order to take measurements, the tractor was placed on even surface and in line with the brake axis and power take-off shaft of the tractor was connected with a terminal of the brake by properly chosen transmission shaft. Following task was determining rotation speed ratio of the engine and the dynamometric stand by establishing ratio of rotational speed between the tractor engine crankshaft and power take-off shaft i_{wom} = 1,995. Measurements of torque M_o and power N_e were carried out under full load and variable rotational speed. Readings of surrounding temperature T_{ot} and atmospheric pressure p_a were also registered.

During conducted research, in real time, following diagnostic parameters were registered in Service ADVISOR diagnostic system: hourly fuel consumption G_l [l·h^{-1}], engine rotational speed , power take-off shaft rotational speed, air temperature T_{ot}, atmospheric pressure p_a, fuel temperature T_p, coolant temperature T_{ch} and temperature of hydraulic oil T_h. At the same time load, was put on the power take-off shaft by means of engine test bench PT 301 MES, and value of breaking power and rotational speed of the brake were registered.

Relying on above mentioned data, reduced torque M_{ozr} and reduced power N_{ezr} were calculated. Obtained maximal values of measured parameters were compared with producer specifications. Measurements of energetic parameters: power and torque were carried out in conformity with DIN 70020 standard, while calculating them to reduced conditions according ISO 3046 standard.

Measurements of hourly fuel consumption G_l were conducted simultaneously with measurement of torque M_o and power N_e. Obtained results of hourly fuel consumption G_l [l·h^{-1}] were registered in Service ADVISOR diagnostic system. At the same time readings of air temperature T_{ot}, atmospheric pressure p_a and, in order to determine fuel density ρ_p, fuel temperature T_p were registered. Based on these measurements hourly fuel consumption G_c expressed in [kg · h^{-1}] was calculated according to formula:

$$G_c = G_l \cdot \rho_p \ [\text{kg} \cdot \text{h}^{-1}]; \tag{1}$$

Than specific fuel consumption was determined according to formula:

$$g_e = \frac{1000 \cdot G_c}{N_e} = \frac{1000 \cdot G_c}{M_o \cdot 2\pi \cdot n} \ [\text{g} \cdot \text{kWh}^{-1}]; \tag{2}$$

where: G_c – hourly fuel consumption [kg · h^{-1}], N_e – power output [kW], M_o – torque [Nm], n – engine rotational speed [rpm].

Moreover, flexibility coefficient *e* (3), enabling evaluation of suitability of vehicle for traction tasks, was determined. This coefficient is product of torque flexibility coefficient e_m (3) and rotational speed flexibility coefficient e_n (3).

$$e = e_m \cdot e_n = \frac{M_{\max}}{M_N} \cdot \frac{n_N}{n_M}; \tag{3}$$

where: M_{max} – maximal torque [Nm], M_N – torque at maximal power [Nm], n_N – maximal power rotational speed [obr · min^{-1}], n_M – maximal torque rotational speed [obr · min^{-1}].

EXPERIMENTAL RESULTS AND DISCUSSION

Course of, registered in Service ADVISOR diagnostic system, hourly fuel consumption G_l and engine rotational speed *n* during taking measurements for John Deere 6920 tractor were presented in Figure 2. In order to make tractor measurement results analysis more accurate, measurement intervals were plotted on curves of course of both measured parameters, and whole measurement was divided into four periods. Analogous analysis was used for evaluation of John Deere 6820 tractor [4]. Obtained results are presented in Table 1 and Figure 3.

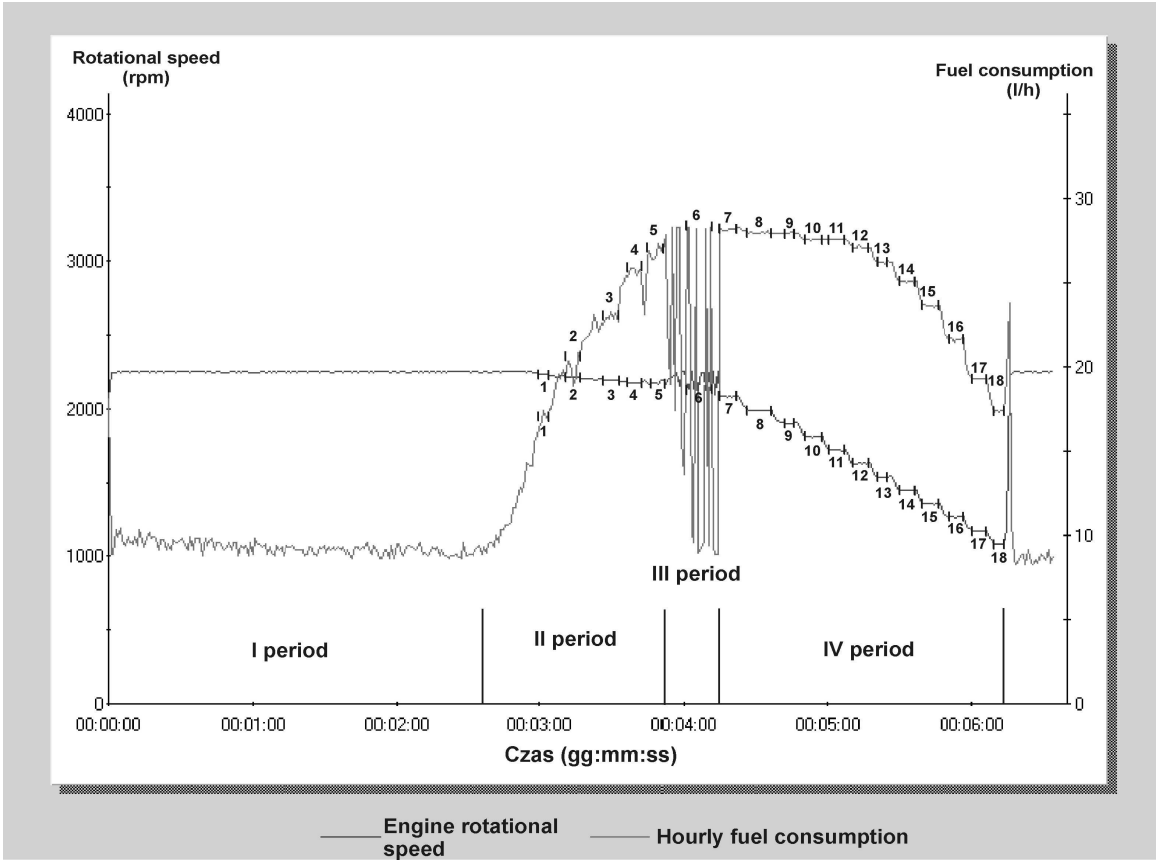

Fig. 2. Progress of changes in hour fuel consumption G_l and engine speed *n* while preparing external speed characteristics for John Deere 6920 tractor (registered in the Service Advisor diagnostic system

In order to ensure proper measurements conditions, thermal state of engine, by means of registering temperature of coolant T_{ch}, was monitored. Simultaneously, during measuring fuel consumption, temperature of fuel T_p, which was later used to recalculate volumetric fuel consumption ($l \cdot h^{-1}$) to, expressed in ($kg \cdot h^{-1}$), mass fuel consumption. Obtained results were presented in table 1.

First period included beginning of registration of parameters in Service ADVISOR diagnostic system and preparation of the investigated tractor for measurements. During this period, check-up of diagnostic parameters determining thermal condition of the engine and drive transmission system were conducted. In case of investigated vehicle these were: coolant, engine oil and hydraulic oil temperature. Second period, although the engine did not work with maximal possible fuel charge, represents increase of engine load with simultaneous increase of fuel consumption. Compared with investigation of John Deere 6820 tractor [4], this period comprised greater amount of measurement intervals, and rotational speed ranged from 2150 to 2250 rpm.

Table 1. Fuel consumption measuring results for John Deere 6920 tractor at maximum load and variable engine speed on the basis of data from the Service Advisor diagnostic system

Vehicle mileage P = 850 hours. PTO nominal rotational speed n = 1000 obr/min. PTO ratio i_{WOM} = 1,995. Weather conditions: p_a = 1016 hPa, T_p = -4 °C.												
On.	**Measured quantities**								**Reduced quantities**			
	n [rpm]	M_o [Nm]	N_e [kW]	G_l [$l \cdot h^{-1}$]	T_p [°C]	ρ_p [$kg \cdot m^{-3}$]	G_c [$kg \cdot h^{-1}$]	g_p [$g \cdot kWh^{-1}$]	M_{oz} [Nm]	N_{ez} [kW]	G_c [$kg \cdot h^{-1}$]	g_{pz} [$g \cdot kWh^{-1}$]
1	2246	12,7	3,0	17,9	21,0	831	14,87	4986,8	12,1	2,8	14,87	5221,8
2	2210	253,6	58,7	20,5	21,0	831	17,04	290,2	242,2	56,1	17,04	303,8
3	2195	328,8	75,6	23,3	21,0	831	19,36	256,2	314,0	72,2	19,36	268,3
4	2167	407,6	92,5	27,3	21,0	831	22,69	245,3	389,3	88,3	22,69	256,9
5	2147	437,1	98,2	28,5	20,0	832	23,71	241,4	417,4	93,8	23,71	252,7
6	2123	447,0	99,4	28,4	20,0	832	23,63	237,8	426,9	94,9	23,63	249,0
7	2079	462,9	100,8	28,2	20,0	832	23,46	232,9	442,0	96,2	23,46	243,8
8	1983	481,4	100,0	28,0	20,0	832	23,30	233,0	459,8	95,5	23,30	244,0
9	1899	508,2	101,1	28,0	20,0	832	23,30	230,5	485,3	96,5	23,30	241,4
10	1803	534,4	100,9	27,7	20,0	832	23,05	228,3	510,4	96,4	23,05	239,1
11	1712	553,0	99,1	27,7	20,0	832	23,05	232,5	528,1	94,7	23,05	243,5
12	1624	557,1	94,7	27,1	20,0	832	22,55	238,0	532,0	90,5	22,55	249,2
13	1528	562,5	90,0	26,3	19,0	833	21,91	243,4	537,2	86,0	21,91	254,8
14	1444	565,2	85,5	25,8	19,0	833	21,49	251,4	539,8	81,6	21,49	263,2
15	1357	574,7	81,6	24,2	19,0	833	20,16	246,9	548,9	78,0	20,16	258,5
16	1261	572,5	75,6	21,7	19,0	833	18,08	239,1	546,7	72,2	18,08	250,4
17	1173	567,0	69,7	19,3	19,0	833	16,08	230,8	529,4	64,8	16,08	241,7
18	1081	534,4	60,5	17,4	19,0	833	14,49	239,5	358,1	41,0	14,49	250,8

Third period, similarly to one for 6820 tractor [4], included irregular course of both parameters. Increase of load governed by controller of dynamometric stand, causes variable reaction of the engine resulting from its work with maximal fuel charge, what makes it difficult to stabilize the load during the course of measurement. It should be noted that in case of 6920 tractor rotational speed range, for this period, was narrower (2050 - 2150 rpm), and variability of fuel consumption was significantly grater. It

enables statement that work of the engine with rotational speed grater than 2000 rpm is not beneficial. It should also be mentioned that significant increase of unitary fuel consumption occurred, after above mentioned rotational speed was exceeded.

Course of hourly fuel consumption G_l and rotational speed of the engine was stable in fourth period. In this period, rotational speed ranged from 1100 to 2000 rpm. For this interval, course of torque curve (Fig. 3) was flat, and at the same time specific fuel consumption was the lowest. However, analysing course of external characteristics of power N_{ez}, torque M_{oz} and specific fuel consumption, it was noted that the most favourable conditions for work of 6920 model are when rotational speed ranges from 1500 to 2000 rpm.

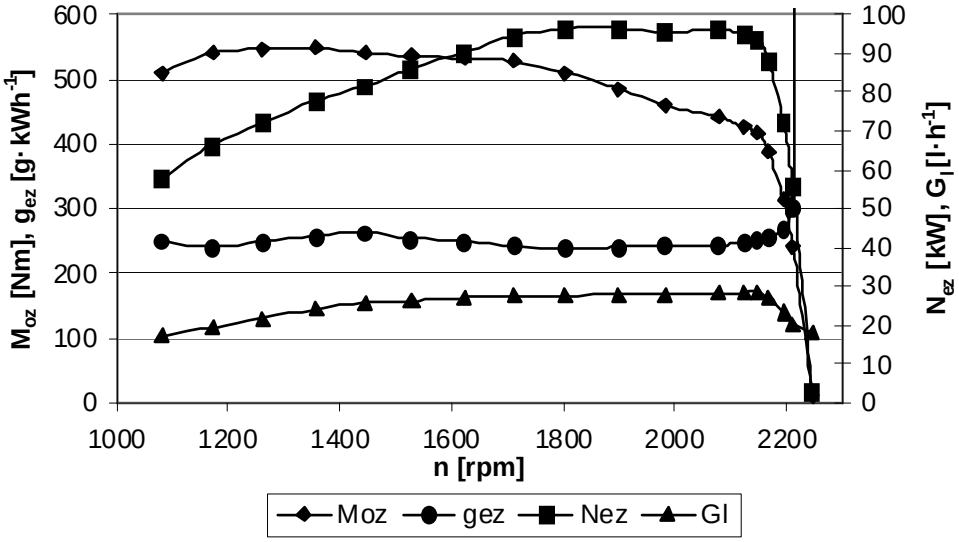

Fig. 3. Progress of changes in torque M_{oz}, power N_{ez}, hourly G_l and specific fuel consumption g_{ez} for John Deere 6920 tractor external speed characteristics on the basis of data from the Service Advisor diagnostic system

Obtained readings of minimal specific fuel consumption g_{emin} for the investigated tractor were 239,3 g·kWh^{-1} for rotational speed of about 1800 rpm. Conducted research shows that minimal specific fuel consumption was obtained with the engine working with rotational speed for which maximal power is delivered. Comparison of obtained values of specific fuel consumption with research of Kamiński [3] (from 225 to 273 g·kWh^{-1}) shows that for the investigated tractor specific fuel consumption was below mean values. Analysing course of specific fuel consumption curve it can be stated that optimal rotational speed, for this engine work, ranges form about 1500 to 2100 rpm. However, taking into consideration discussed before course of process of increasing load put on the power take-off shaft, this range should be narrowed to 2000 rpm.

In order to evaluate technical condition of the investigated tractor, comparison of obtained result with factory specifications for effective power N_{wom} at nominal range of revolution of power take-off shaft was conducted. In investigated vehicle, N_{wom} was 96,2 kW which is 97,5% of value stated by a producer. Therefore, vehicle technical condition can be considered good.

Results show that torque flexibility e_m = 1,13 and rotational speed flexibility e_n = 1,39, while flexibility of the engine as a whole e = 1,57. When compared with research of Kamiński [3], obtained coefficients are relatively low. It is related to course of torque and power curves, which in case of investigated vehicle have different character than in case of older generation vehicles, what results from a method of controlling work of ,powered with common-rail system, engine. It is clearly visible that nominal power is not equal to maximal power, and for rotational speed ranging from 1700 to 2100 rpm power is at similar level. Torque curve characterizes with flat course for rotational speed ranging from 1200 to 1700 rpm. Based on analysis of course of all curves it is possible to determine range of the engine work optimum rotational speed to be from 1500 to 2000 rpm.

CONCLUSIONS

Measurements of energetic parameters: effective power N_e, torque M_o, by means of utilization PT 301 MES dynamometric stand, in range of nominal rotational speed of power take-off shaft, enable precise evaluation of technical condition of investigated tractors in place where they are used. For the investigated vehicle difference was 2,5%, when compared with producer specifications , what proves its good technical condition.

Determining characteristics of torque, power and unitary fuel consumption course, and taking into consideration course of measurement registered in diagnostic system, enabled determination of engine work optimum rotational speed range, which, in case of John Deere 6920, was from 1500 to 2000 rpm.

Utilizing control-diagnostic system in vehicle with simultaneous use of external diagnostic system enables, accurate enough for practical purposes, determination of course of specific fuel consumption g_e and its dependence on rotational speed. This system enables elimination of need for utilization of, interfering with engine powering system, research apparatus. That, thanks to lack of necessity of its installation, rationalizes measurement, and therefore, eliminates risk of accidental malfunctions. Its only necessary to carry out research which aim is to determine accuracy with which fuel consumption is measured by control-diagnostic system.

Moreover, introduction of diagnostic system, thanks to communication with vehicle on-board diagnostic system, contributes to significant facilitation of detection and removal of failures both in cars as well as tractors or agricultural equipment. System enables identification of faults generated by tractor control systems, monitoring and recording of all vehicle work parameters. It can be used while servicing a vehicle, but it also enables, if necessary, analysis of recorded data in off-line mode.

REFERENCES

1. Jantos J., Mamala J.: *Identyfikacja protokołów transmisji magistrali CAN w pojazdach rolniczych*. Inżynieria Rolnicza. Kraków 2007. Nr 6 (94). s. 57-63.
2. Jankowski M.: *Wprowadzenie do pokładowego diagnozowania pojazdów samochodowych*. Artykuł XII Konferencji „Diagnostyka Maszyn Roboczych i Pojazdów". Diagnostyka vol. 33. 2005 r.

3. Kamiński J.R.: *Analiza parametrów energetycznych ciągnika URSUS 1134*. Inżynieria Rolnicza 3(91), 2007. s. 67-73.
4. Krzaczek P.: *Assessment of energy parameters for John Deere 6820 farm tractor carried out using on-board diagnostics*. Inżynieria Rolnicza. Kraków 2009. Nr 8 (117). s. 91-98.
5. Merkisz J., Mazurek S.: *Pokładowe systemy diagnostyczne pojazdów samochodowych*. Wydawnictwa Komunikacji i Łączności. Warszawa 2007.
6. Rychlik A.: *Metody pomiaru zużycia paliwa pojazdów użytkowych*. Eksploatacja i Niezawodność. Maintenance and Reliability. Nr 4/(32), 2006. s. 37-41.
7. Scarlett A. J.: *Integred control of agricultural tractor and implements: a review of potential opportunities relating to cultivation and crop establishment machinery*. Computers and electronics in agriculture, 30 (2001), 167-191.
8. Speckmann H., Jahns G.: *Development and application of an agricultural BUS for data transfer*. Computers and Electronics in Agriculture, 23, 1999. str. 219-237.
9. Zhang Q.: *Mechatronics and its applocation to off-road vehicels*. Strona internetowa: http://ageweb.age.uiuc.edu/faculty/research/mechatronics.htm. (2003)
10. Zimmermann W., Schmidgall R.: *Magistrale danych w pojazdach. Protokoły i standardy*. Wydawnictwa Komunikacji i Łączności. Warszawa, 2008.

ZESZYTY NAUKOWE POLITECHNIKI RZESZOWSKIEJ NR 274
Mechanika z. 81 2010

Valeriy KYRYLOVYCH
Artyom SAZONOV

Zhytomyr State Technologycal University, Ukraine

UNIT OF ADAPTATION GRIPPERS OF INDUSTRIAL ROBOTS

In the paper presents a new approach to decision the problem of adaptation grippers of industrial robots to changing negative force-torque loads at the time of technical robotized kit fixing in the device of position working. Capabilities and basic elements of unit of adaptation grippers for industrial robots presented.

INTRODUCTION

One of the major problems with the use of industrial robots (IR) in machining flexible automated production is a problem of adaptation grippers IR (GrIR) to changing negative force-torque loads arising from the adjustment of each t-th position working PW_{t-1} at the time of fixing technical robotized kit (TRK), which includes long handling object HO_{t-1}, which is clamping in grippers of IR (GrIR+HO_{t-1}), clamping elements PW_t accessories.

The interaction of technological items robotized system: on one side – the influence of a force HO_t GrIR clamp on the other – force clamp HO_t $GrIR_{t-1}$ is called "dual connection" [5]. Intensity clamp HO_{t-1} device of PW_t far outstrips the amount of clamp force HO_t by device of PW_t, which is obvious. The result of this interaction is force conflict (FC) [7].

Analysis of information sources showed that over the research of many researchers involved. Proposed some methods to adapt ShPR FC phenomena represented in many information sources [5, 6, 7, 8]. Methods of adaptation are mostly passive in nature.

THE AIM

The aim of this work is to present the proposed construction the unit of adaptation GrIR to FC, which is mounted on GrIR and reduces the negative impact of force-torque excitation on elements of IR.

The analysis of existing methods of adapting past can be divided into the following types [2, 3, 6, 8]: passive, active, combined and integrated.

Passive adaptation – involves in the construction GrIR compensating mechanical devices that react to the occurrence of unwanted effects force-torque and due to the ductility of structural elements compensate for installation errors that arise while fixing HO_{t-1} in device of PW_t. This kind of adaptation of a number of disadvantages that reduce the possibility of

using it to systems that are moving manipulation of IR occurs at high speeds, due to presence of unwanted vibration ultimate level of manipulation, the need to re-establish the compensation of errors when serving each PW_t, but at the same time adapting this method is very simple in implementation.

Active adaptation – is realized by practicing corrective movements all degrees of mobility IR. This kind of adaptation is limited primarily kinematic features junctions parts of IR manipulation, relatively large energy consumption of corrective movements drive train parts, requires certain hardware and software control systems improvements IR. Indisputable advantage of this type is reliability adaptation and lack of critical loads on the elements and components of IR manipulation.

To combine the advantages outlined above approximation methods suggested to use the *combined type of adaptation* that does not require improvements IR and control systems through the use of mechanical devices compensating simplifies implementation and operation.

THE PRESENTATION OF THE MAIN PART

As an example hardware implementation of the combined type of adaptation method presented unit of adaptation (UA), which conditionally divided into two blocks: Mechanical and Information. Mechanical block compensating role played by the compliance unit, which includes compensators angular and linear errors installing HO to avoid unwanted vibrational processes in the endpoint trajectory displacement of IR manipulation unit compliance mechanism for fixing the fixed position (MFFP). Pliability joints secured by using their spring design elements.

Information recording unit provides information about available installation error, converting mechanical quantities of forces and moments in the electric signal, further processing and signal control output to enable or disable the MFFP. The specified function is achieved by using force-torque sensor as a sensitive and perceptive about forces and moments that occur during consolidation HO_{t-1} device of PW_t clamping elements. Sketches of the basic units and units represented in Figure 1.

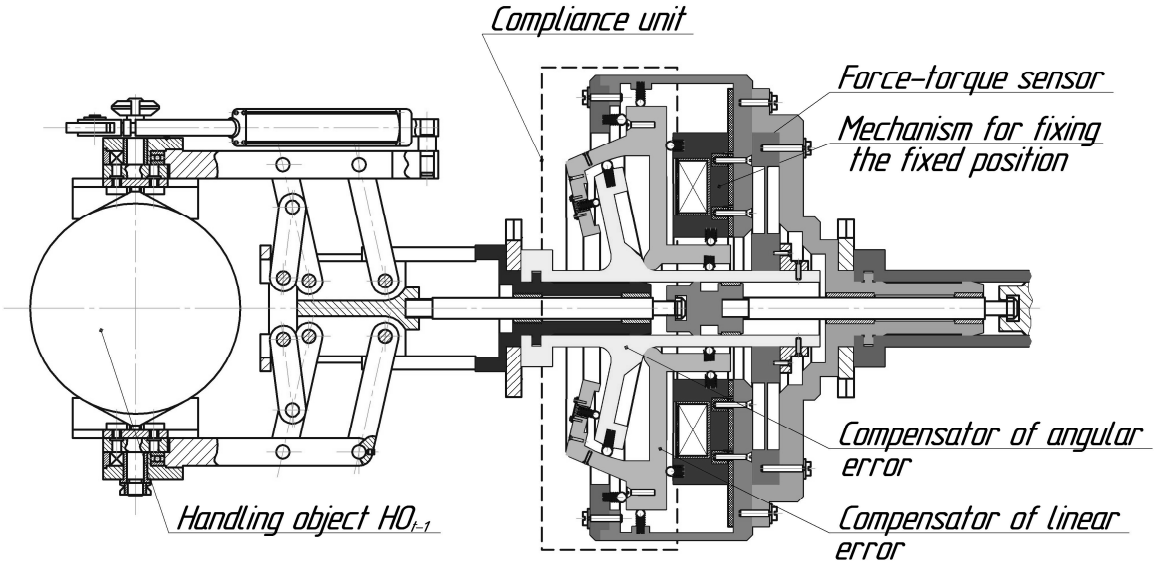

Fig. 1. Basic elements of UA GrIR to the effect of FC

Moving TRK (GrOR + HO_{t-1}) in the service area of device of PW_t compliance recorded MFFP unit that provides opportunities to move at high speeds and at the same time avoid unwanted vibrational processes in endpoint positioning GrIR. When clamping HO_{t-1} device of PW_t HO_{t-1} attached force-torque to load from the clamping device elements. Moment of load application is fixed information block, which produces singhalese unfastening of MFFP to provide certain elements compensating compliance. Thus, since the vast majority are device of PW_t force-torque, is centering and setting compensation of errors. Change force-torques loads on HO_{t-1} shows the passage of time fixing process, where the change signal from the sensor is constant. This suggests that the transition is set to take place, all the error installing themselves compensated, so an information pack produces signal to turn on MFFP and recording site in compliance compensated position, the final link of IR removed from service area device of PW_t.

CONCLUSIONS

Using the combined method of adapting the example of the proposed UA increases flexibility of automated production technology enables to increase the functionality of the conversion process in establishing long HO in device of PW_t.

REFERENCES

1. Бауманн Э.: *Измерение силы электрическими методами*, пер. с нем. А. С. Вищенкова и С. Н. Герасимова, под ред. И. И. Смыслова, М.: Мир 1978. 430 с.
2. Кирилович В.А., Черепанська І.Ю., Сазонов А.Ю.: *Адаптивність схватів промислових роботів як напрям підвищення ефективності роботизованих механоскладальних технологій* . Вісник ЖДТУ. Житомир, 2010 р. № I(52). С.17 – 24.
3. Кирилович В.А., Черепанська І.Ю., Сазонов А.Ю.: *Адаптивність схватів промислових роботів механообробних ГВК*. Методи розв'язування прикладних задач механіки деформованого твердого тіла. Збірник наукових праць Дніпропетровського національного університету. Дніпропетровськ, 2010 р. № 11. С. 119 – 125.
4. Проць Я.І.: *Захоплювальні пристрої промислових роботів*: [навчальний посібник]. Тернопіль, Тернопільськй державний технічний університет ім. І. Пулюя, 2008. 232с.
5. Тютюнник А.Г., Кирилович В.А., Чевпотенко О.В.: *До питання адаптивності захватних пристроїв промислових роботів при синтезі роботизованих механоскладальних технологій.* Вісник ЖДТУ. Житомир, 2004 р. № IV(31). С.168 – 173.
6. Coiffet Ph.: *Interaction with the environment. Robot technology*. Volume 2. London, Kogan Page Ltd., 1983, – 240 c.
7. Monkman. G. J., Hesse. S., Steinmann. R., Schunk. H.: *Robot grippers*. Weinheim: WILEY-VCH Verlag GmbH & Co. KGaA, 2007. – 452 c.
8. Xiong Ch., Ding H., Xiong Y..: *Fundamentals of robotic grasping and fixturing.* USA: World Scientific Publishing Co. Pte. Ltd., 2007 – 229 c.

ZESZYTY NAUKOWE POLITECHNIKI RZESZOWSKIEJ NR 274
Mechanika z. 81 2010

Janusz LUBAS

Rzeszow University, Poland

A COMPARISON OF THE TRIBOLOGICAL BEHAVIOURS MATERIALS MODIFIED OF BORON IN THE SLIDING PAIRS

The aim of the present work is to determine the influence of technologically produced boron surface layers on the friction parameters in the sliding pairs under lubricated friction conditions. The tribological evaluation included ion nitriding, powder-pack boronizing, laser boronizing, hardening and tempering surface layers and TiB_2 coating deposited on 38CrAlMo5-10, 46Cr2 and 30MnB4 steels. Modified surface layers of annular samples were matched under test conditions with counter-sample made from AlSn20 bearing alloy. Tested sliding pairs were lubricated with 15W/40 Lotos mineral engine oil. The tribological tests were conducted on a T-05 block on ring tester. The applied steel surface layer modification with boron allowed creating surface layers with pre-determined tribological characteristics required for the elements of sliding pairs operating under lubricated friction conditions. Boronizing reduces the friction coefficient during the start-up of the frictional pair and the maximum start-up resistance level is similar to the levels of pairs with ion nitride surface layers.

1. Introduction

The surface of engineering components are subjected to higher stresses and greater fatigue, abrasion and corrosive damages than the interior. Therefore, more than 90 pct of the service failures of engineering components are initiated at the surface. Surface modification techniques are employed to improve the resistance to failure by producing a hard and wear resistance layer around a soft and tough core. Two major classes of treatments available for enhancing the surface properties are thermal and thermochemical. Thermal treatment, such as flame and induction hardening, modify the microstructure without modifying the surface chemistry, whereas in thermochemical methods, the surface chemistry is altered. Nitriding and quenching and tempering are well know surface treatment methods [1].

The boride layer is formed by diffusion of boron atoms in the base metal at high temperature [2-5]. Diffusion of boron into the surface of various metals and alloys results in the formation of metallic borides which provide extremely hard (up to 2000HV), wear and corrosion resistant surface [6, 7]. This treatment is a thermochemical treatment in which a material is kept in a boron-giving environment from 850 to 1000^{o}C for 2-10 h [3, 8]. Various processes adopted for boronizing include pack boriding, molten salt boriding, vacuum boriding, laser boriding, etc. The resulting layer may consist of either single-phase boride (FeB or FeB_2) or polyphase boride layer (FeB and FeB_2). The tribological properties variations of FeB and FeB_2 layers depend on physical state of boride source used, boronizing temperature, treatment

time, and properties of the boronized material [9]. Industrial boriding can be carried out on most ferrous and non-ferrous materials. Boronizing is very effective, especially on grey and ductile iron or low alloy steel with chromium. If boronizing is applied to a material surface the resultant boride layer increases the wear resistance considerably. Furthermore, it decreases the friction coefficient [8]. The use of ceramic materials for many tribological applications has increased considerably over the past two decades. This is the effect of the unique combination of properties of these materials, such as low bulk density, high corrosion resistance, low thermal expansion and high hardness over a wide range of temperature. Titanium diboride (TiB_2) belongs to this group of materials and is well known for its high hardness, high melting point, a relatively high strength, high chemical stability at high temperature and high wear resistance [10, 11]. Titanium diboride is promising class of advanced materials which have a great potential for tribological application.

The current boronizing processes allow obtaining surface layers of high hardness and high resistance to corrosion and wear, with low brittleness and no tendencies towards cracking [4]. However, the operation characteristics of these layers depend on the chemical composition, the structure of the surface layer, the method and parameters of their production, as well as any possible thermal treatment. The modification of the surface layer with boron should be selected upon the required operating characteristics and the operating conditions of the kinematic sliding pairs [5-7]. Thus, it is crucial to determine the influence the boron modification the elements of the sliding pair has on the operating conditions and wear during the lubricated friction.

2. Experimental

The aim of this work is to determine the influence of technologically produced boron surface layers on the friction parameters in the sliding pair. The tribological tests were conducted on a T-05 block on ring tester (Fig. 1). Three types of steel were used in the creation of annular samples, 38CrAlMo5-10, 46Cr2 and 30MnB4 (Fig. 1).

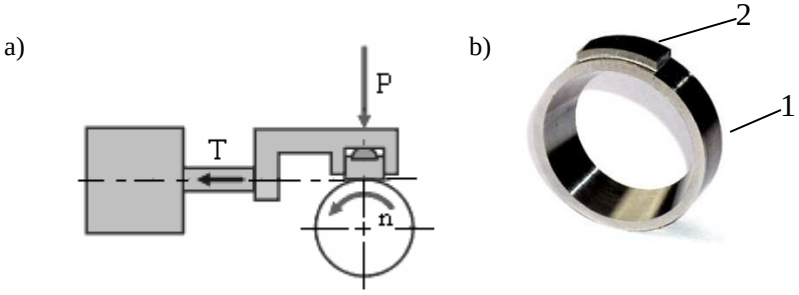

Fig 1. Simplified scheme of the block-on-ring tester (a) and the sliding pair; 1-annual sample, 2-counter-sample (b)

Annular samples from 38CrAlMo5-10 steel were ion nitrided in the atmosphere H_2 + N_2, in the temperature of 500^{o}C and in the time of 6h. Annular samples from 46Cr2 steel were borided in powder, in the temperature of 950 ^{o}C in the time of 8h, and then were isothermally quenched and hardened. In the boronizing process, powder of the following composition was used, B4C (30%), Al2O3 (68%), NH4Cl and NaF). Annular samples from 46Cr2 steel were also laser-borided, with the use of CO_2 laser (power of beam P = 2 kW, spot diameter d = 4 mm, energy density 160 W/mm^2,

tracking speed v = 16 mm/s, gas carrier –argon). The boronizing process consisted in covering the annular sample with the layer of amorphous boron and liquid glass, and melting with the laser beam. Also, the annular samples from steel 46Cr2 were covered with the TiB_2 coating using PVD method (temperature 400^{o}C, time 40min, pressure in ionization chamber p = 2,5 x 10^{-2} bar). Annular samples from 30MnB4 steel were hardened and tempered, hardening in the temperature of 800^{o}C and drawing temper in the temperature of 450^{o}C. Modified surface layers of annular samples were matched under test conditions with counter samples made from AlSn20 bearing alloy. Tested sliding pairs were lubricated 15W/40 Lotos mineral engine oil.

The on-site tests were executed by following a specified algorithm, which included the initial grind-in of the samples and the correct co-operation process at the pre-determined load parameters. The grind-in was executed on a test site at a load of 5 MPa until a complete adhesion of the annular sample and the counter-sample was achieved. It was assumed for the starting phase that the pair would be accelerated from a speed of n = 0 to 500 rpm in 30 seconds. The friction coefficient to temperature ratio was measured as a function of pressure, while the measurements of the pair co-operation under the pre-determined friction conditions were taken at the annular sample rotational speed of 100 rpm and at a jump unit pressure p = 5, 10, 15 and 20 MPa. The course of the friction coefficient, temperature and wear as a function of variable load were registered at real-time during the tests.

3. Results and discussion

The co-operation of a sliding pair is characterised by the large dynamics of the measured parameters' values, due to external forces. Determination of these changes' tendencies is especially important in the start-up stage of the frictional work. The assessment of the occurring changes is possible by registering the friction coefficient as a function of variable sliding speed (Fig. 2). The registered charts present the typical courses of the friction coefficient for the 'ring-block' frictional pairs under the load of 20 MPa. During the first start-up phase, a rapid increase in the frictional resistance occurs, followed by its significant drop. The registered courses of the friction coefficient for the higher sliding speeds are diversified. There are sliding pairs, with an increase in the sliding speed of the annular sample, which cause the increase in the friction coefficient. These variations occur in the pairs with nitrided surface layers, after exceeding the sliding speed of 0.6 m/s and after 0.2 m/s for the pairs with the TiB2 coating. The measured value of the friction coefficient level in the associations with the laser borided layer and TiB2 coating equals approximately 0.11. As for the pairs with 30MnB4 steel annular samples, an increase in the sliding speeds leads to the stabilisation of the friction coefficient values, while the powder-park boronizing pairs exhibited a decrease in this value (to its lowest possible level μ = 0,02) along with an increase in the sliding speed.

Another significant aspect pertaining to sliding pairs is to determine the value of the start-up moment (Fig. 3). During the tests, the lowest friction resistances were recorded for the pairs with ion nitrided, powder-pack borided and hardened and tempered surface layers, which have similar values of approximately 8 Nm (at 20 MPa). Significant increases of the friction moment (by about 20%) occur in pairs with TiB_2 coating and laser borided surface layer of annular samples. Similar moment

changes are observed at the pressure of 10 and 15 MPa. The pairs with nitrided surface layers and TiB_2 coating reach the friction moment value at about 2 Nm under singular pressures (at 5 MPa), while the pairs with laser and powder-pack borided surface layers have the friction resistance values higher by 15%. The observation of the friction parameter changes during the start-up phase tells about the behaviour of the system during its further work. The most favourable operating conditions are present in sliding pairs in which the friction coefficient increases in the initial stage of start-up, and then decreases significantly and stabilises itself at a constant level. The value of the moment determines the energy demand of the system upon its start-up. Those sliding pairs which exhibited the tribochemical equilibrium within the shortest time generate optimal conditions for their further operation. The changes registered are the result of physiochemical processes and the changes in the friction surface micro-geometry due to the adaptation of the system to the conditions of external forces [12, 13]. In the sliding pairs, which exhibit a significant decrease in the friction coefficient, the improvement in the friction conditions depends on the increase in the effectiveness of the lubrication by the oil coat, due to the existing tribochemical changes. These changes are shaped by the existing load state of the kinematic sliding pair, the temperature levels and the chemical reaction occurring within the area of friction. As an effect of the changes in the oil chemical composition and the synthesis of new chemical compounds, a boundary layer is created, which strengthens the anti-wear layer by changing its structure and decreases the movement resistances. These changes lead to the further decrease in the friction resistance, accompanied by the increase in the sliding speed of the annular sample [12, 13]. The pairs with stable courses of the friction coefficient the surface layer of the element provides sliding characteristics, which allow the equilibrium of tribochemical phenomena within the contact area. This equilibrium allows inherent regulation of the processes occurring within the friction area, which stabilises the resistance values despite the increase in the sliding speed.

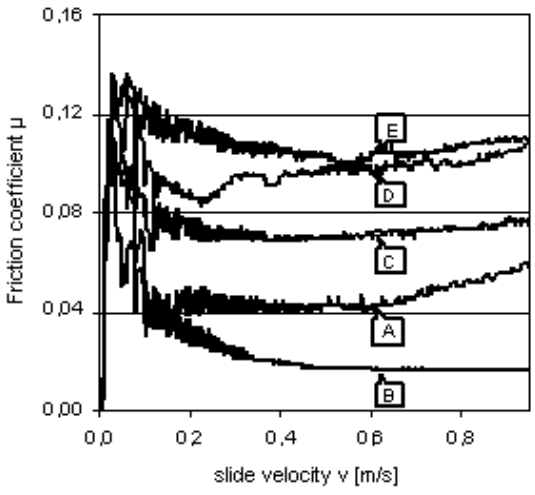

Fig. 2. Influence of surface treatment annular sample on change of friction coefficient vs. rotation speed and load 20MPa; A – ion nitrided, B – pack borided, C – quenched and tempered, D – coated TiB_2, E – laser borided

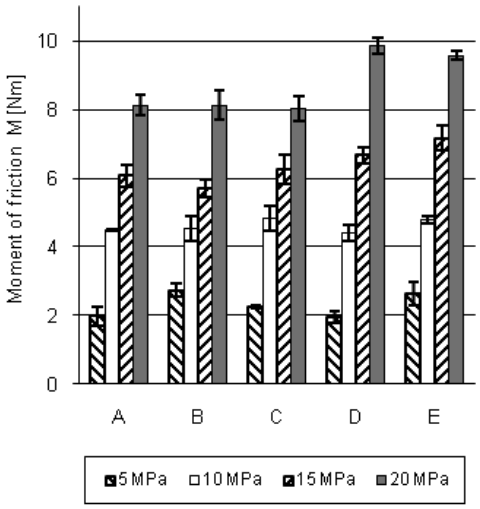

Fig. 3. Influence of surface treatment annular sample on moment of friction in function load of kinematics pair; A – ion nitrided, B – pack borided, C – quenched and tempered, D – coated TiB_2, E – laser borided

In order to determine the effect of the test duration on the friction processes, the measurements of friction resistances were made in pre-determined load conditions (Fig. 4). The registered courses of the friction coefficient indicate a similar character of changes in the surface layer of pairs with nitrided, powder-pack borided, hardened and tempered layers. Despite the initial differences between the friction resistances after 300 seconds of operation, the level and the character of these changes is uniform, and the friction coefficient value is about 0.09. In the surface layer of other pairs, a significant increase in the friction resistance is noted; the pairs with powder-pack boronizing annular sample have the resistance coefficient of approximately 0.15, and 0.17 for the TiB_2 coating. The temperature values taken in the friction areas at the end of the test fall between 80 and 90 °C and can be ranged ascending, for the annular samples used as follows: hardening and tempering, powder-pack boronizing, ion nitriding, laser boronizing and TiB_2 coating .

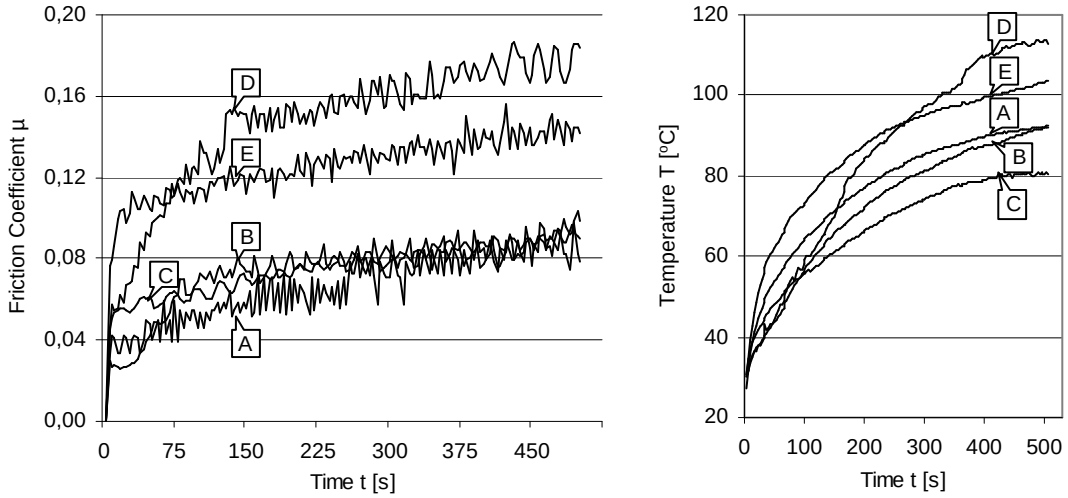

Fig. 4. Influence of surface treatment annular sample on friction coefficient and temperature in function time of test; A – ion nitrided, B – pack borided, C – quenched and tempered, D – coated TiB_2, E – laser borided

In order to determine the effect of the test duration on the friction processes, the measurements of friction resistances were made in pre-determined load conditions (Fig. 4). The registered courses of the friction coefficient indicate a similar character of changes in the surface layer of pairs with nitrided, powder-pack borided, hardened and tempered layers. Despite the initial differences between the friction resistances after 300 seconds of operation, the level and the character of these changes is uniform, and the friction coefficient value is about 0.09. In the surface layer of other pairs, a significant increase in the friction resistance is noted; the pairs with powder-pack boronizing annular sample have the resistance coefficient of approximately 0.15, and 0.17 for the TiB_2 coating. The temperature values taken in the friction areas at the end of the test fall between 80 and 90 °C and can be ranged ascending, for the annular samples used as follows: hardening and tempering, powder-pack boronizing, ion nitriding, laser boronizing and TiB_2 coating .

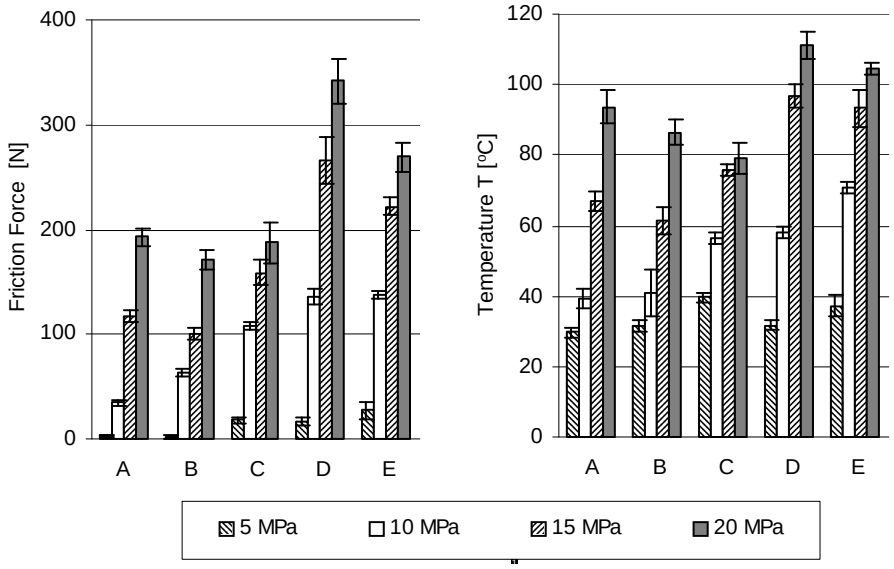

Fig. 5. Influence of surface treatment annular sample on friction forces and temperature depending on load and rotation speed 100 rpm annular sample; A – ion nitrided, B – pack borided, C – quenched and tempered, D – coated TiB_2, E – laser borided

Significant changes of the friction force and temperature values within the friction area occur under singular pressures p = 5, 10, 15 and 20 MPa (Fig. 5). The friction-force level values for the pairs with ion nitriding, powder-pack boronizing, hardening and tempering samples are similar and do not exceed 200 N (at 200 MPa). Its value for the laser boronizing pairs is 270 N and amounts to 341 N for the TiB_2 pairs. The lowest friction force values at low-pressure conditions (at 5 MPa) were measured in pairs with nitriding and powder-pack boronizing samples. At the pressure of 10 MPa, the friction force increases by 50% in pairs with powder-pack borided surface layer in comparison to the pairs with nitrided layer. Further increase of pressure up to 15 MPa in a pair with powder-pack borided surface layer decreases the tendency toward the rise of the friction force. The hardening and tempering, laser boronizing and TiB_2 coating pairs exhibit the intensity of changes within the pressure range of 5 to 10 MPa at a similar level. The temperature measurements following the conclusion of the tests have indicated the lowest heat in sliding pairs with the hardening and tempering samples (below 80^oC). The highest temperature values were noted for the pairs with the TiB_2 coating (about 111^oC) and powder-pack borided surface layer (104^oC) . The change of the surface pressure affects the temperature increase within the pair's adhesion area proportionally. In the nitrided and powder-pack borided surface layer pairs, the intensity of the temperature increase is smaller for the low-pressure range (5-10 MPa) than for the higher pressures (10-20 MPa). In the surface layer of all other pairs tested, however, the changes tend to be quite the opposite; higher singular pressures will decrease the intensity of the temperature increase within the friction area.

The registered courses of the friction force and temperature reveal the ability of the sliding pairs to adapt to the friction conditions in the extension of the pair's operation time. The changes occurring in the reaction of the pair to the stabilised forcing upon the start-up, and to the time flow, explain whether the system allows for a long-term and reliable operation or not. In the initial period of the pair's operation, there is

always an intense increase in the friction coefficient, followed by its drop and stabilisation or increase. The stabilisation of the friction resistances indicates the adaptation of the pair composition to the existing forces and the generation of stable anti-wear and anti-seizure layers. The layers ensure the separation of the co-operating surface layer areas and a reduced rate of direct adhesion between the surface irregularities [12]. These conditions create a state of equilibrium between the processes of layer destruction and creation within the tribochemical processes occurring in the friction pair. The changes of the friction resistance and temperature allow assessing the probability of the kinematic sliding pair's failure caused by the acting external forces and the emergency use of the pair [13].

These load conditions were also used for the wear measurements of the AlSn20 bearing alloy. The lowest wear was measured for pairs with nitrided, pack borided, quenched and tempered samples and did not exceed 0.01 mg of the bearing alloy's mass, while the value dispersion was below 20% (Fig. 6). The pairs with the TiB_2 coating and laser borided surface layer exhibit almost twice the wear of the AlSn20 above, amounting to 0.015 mg for the laser borided surface layer and 0.018 mg for the TiB_2 coating.

The occurring differences in the wear of bearing alloy and the absence of measurable surface layer annular sample wear changes are the effect of the interaction between the co-operating surface layers, as well as of the physiochemical changes of their surfaces, induced by external forces. These phenomena result from the elementary wear processes occurring within the contact area of the sliding pair, on the elementary surfaces of the cooperating layers. The lubrication factor is crucial for these processes, as it creates favourable or unfavourable friction conditions, depending on its transformation. These changes contribute to the generation of boundary layers on the layers created, which are either highly resistant to ruptures or are quickly destroyed under variable operating conditions. The co-operation conditions also include the secondary phenomena of the friction and wear process. Among these are the effects of the wear products on the frictional surface layers, transmission of one element's particles onto the other, electron emissions and the corrosion current flow [14]. The material transmission processes were observed mostly in sliding pair with pack borided surface layer and TiB_2 coating (Fig. 7).

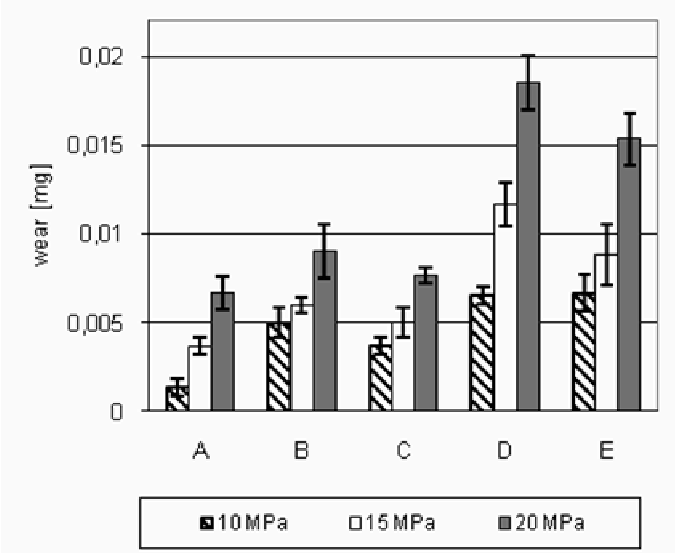

Fig. 6. Influence of surface treatment annular sample on wear of AlSn20 bearing alloy under various load conditions: A – ion nitrided, B – pack borided, C – quenched and tempered, D – coated TiB_2, E – laser borided

Despite the presence of a lubricating factor, oxidation processes are also present in the mixed friction conditions and create oxides on the surface layers of the cooperating elements (Fig. 8). The oxides lead to the decrease of the friction and wear factors within the friction processes; however, in unfavourable conditions, hard and brittle oxides increase the wear [15]. The high wear of bearing alloy observed in pairs with the TiB_2 coating is explained by the increased initial surface roughness and the load of the system. Due to the influence of the hard areas on the areas of the second material, a

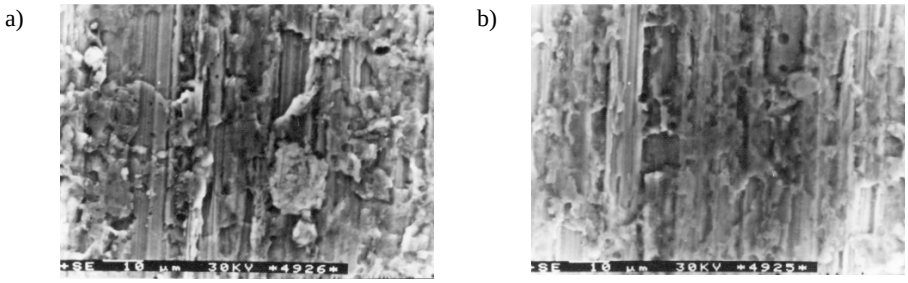

Fig. 7. SEM images of (a) pack borided surface layer and (b) TiB_2 coating layer after test

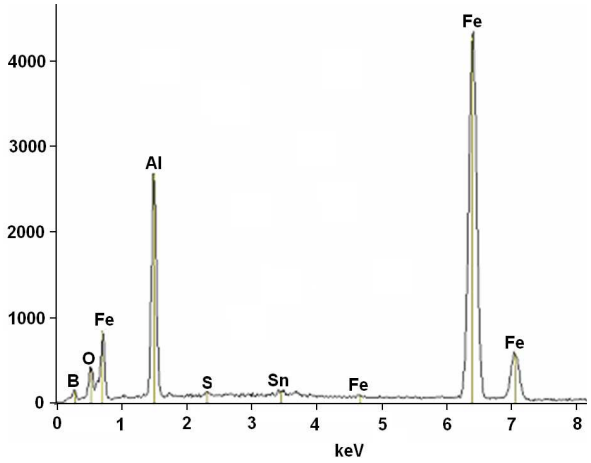

Fig. 8. SEM analysis of pack borided surface layer after test

stress concentration occurs, which leads to the interaction between the two surface layers and a more intense abrasion of the softer material. These changes may lead to smoothening of the surface and removal of its irregularities which eliminates the potential sources of further material transfer and stabilises the wear process. However, the hard wear products created in the friction process induce chipping, slicing and grinding, which intensify the wear process. The phenomenon of macroscopic diffuse aluminium flow occurring in the section of the surface plastic deformation may lead to increased aluminium concentration, in the TiB_2 coating, adhering directly to the friction surfaces [16]. This increases the bearing alloy wear, especially because the created TiB_2 coating is characterised by a non-uniform and undirected distribution of the peak-to-valley height. The examination of the rough layers indicates that the wear of the surface layer in the friction process depends not only on the peak-to-valley heights, but also on their shape and the direction of the machining lines. Decreased surface wear is observed with the greater surface roughness when the co-operating surface layers have the machining lines parallel to the sliding direction [17].

4. Conclusions

On the basis of these investigation, the results of this study can be summarised as follows:

1. The applied steel surface layer modification with boron allow creating surface layers with pre-determined tribological characteristics required for the elements of kinematic sliding pairs operating in the conditions of mixed friction.
2. The process surface layers on annular samples, generated by nitriding, boronizing and hardening and tempering, as well as by PVD, did not demonstrate measurable wear.
3. Powder-pack boronizing reduces the friction coefficient during the start-up of the frictional pair and the maximum start-up resistance level is similar to the levels of pairs with ion nitrided surface layers.
4. The use of hardening and tempering 30MnB4 steel in sliding pairs ensures the operating parameters and bearing alloy wear ratio are similar to the sets with nitrided steel.
5. The highest friction resistance and bearing alloy wear levels were measured in sliding pairs with laser borided surface layer and the TiB_2 coating samples.

References

1. Zwierzycki W.: *Wybrane zagadnienia zużywania się materiałów w slizgowych węzłach maszyn.* PWN, Warszawa-Poznan, 1990.
2. Sen U., Sen S., Yilmaz F.: *Structural characterizations of boride layer on boronized ductile irons.* Surf. Coat. Technol. 176 (2000) 223-228.
3. Przybyłowicz K.: *Teoria i praktyka borowania stali*. Politechnika Swietokrzyska, Kielce, 2000.
4. Kulka M., Pertek A.: *The importance of carbon content beneath iron borides after boriding of chromium and nickel-based low carbon steel*. Applied Surf. Sci. 214 (2003) 161-171.
5. Sen U., Sen S., Yilmaz F.: *The fracture toughness of borides formed on boronized cold work tool steel*. Mater. Characterization. 50 (2003) 261-267.
6. Bejar M.A., Moreno E.: *Abrasive wear resistance of boronized carbon and low-alloy stell*. J. of Mater. Processing Technology, 173 (2006) 352-358.
7. Martini C., Palombarini G., Poli G., Prandstraller D.: *Sliding and abrasive wear behaviour of boride coating*. Wear, 256 (2004) 608-613.
8. Atik E., Yunker U., Meric C.: *The effect of conventional heat treatment and boronizing on abrasive wear and corrosion of SAE 1010, SAE 1040, D2 and 304 steels*. Tribology Intern. 36 (2003) 155-161.
9. Meric C., Sahina S., Yilmazb S.: *Investigation of the effect on boride layer of powder particle size used in boronizing with solid boron-yielding substances*. Mater. Res. Bulletin, 35 (2000) 2165–2172.
10. Panish N., Wangyao P., Hannongbua S., Sricharoenchai P., Sun Y.: *Tribological study of nano-multilayer ultra-hard coatings based on TiB_2*. Rev. Adv. Mater Sci, 13 (2006) 117-124.
11. Basu B., Vleugels J., Van Der Biest O.: *Fretting wear behavior of TiB2-based materials against bearing steel under water and oil lubrication*. Wear, 250 (2001) 631–641.
12. Ozimina D.: *Przeciwzużyciowe warstwy wierzchnie w układach tribologicznych*. Politechnika Swiętokrzyska, Kielce, 2002.
13. Szczerek M., Wiśniewski M: *Tribologia i tribochemia*. ITE, Radom, 2000.

14. Schouwenaars R., Jacobo V.H., Ortiz A.: *Microstructure aspect of wear in soft tribological alloys*. Wear, 263 (2007) 727-735.
15. Pranay A., Liang H., Usta M., Ucisik A.H.: *Wear and surface charakterization of boronized pure iron*. J. of Tribology, 129 (2007) 1-10.
16. Berger M., Hogmark S.: *Evaluation of TiB_2 coatings in sliding contact against aluminium*. Surf. Coat. Technol. 149 (2002) 14-20.
17. Guha D., Chowdhuri R.: *The effect of surface roughness on the temperature at the contact between sliding bodies*. Wear, 197 (1996) 63-73.

ZESZYTY NAUKOWE POLITECHNIKI RZESZOWSKIEJ NR 274
Mechanika z. 81 2010

Peter MALEGA

Technical University of Košice, Slovakia

MODEL THAT RATES TECHNICAL EFFECTIVENESS OF PRODUCTION

This paper is about the model that rates technical effectiveness of production. This paper is applied on selected company, which has problems with technical criteria that are important for technical effectiveness of production. The last section of this paper presents proposed model that rates the technical effectiveness of production, which could be used (maybe with modification) in the production companies.

INTRODUCTION

Maximising productivity and the effectiveness of operations are a key element of companies' strategic plans and is a key concern for business managers in every industry. Developments in technology, globalisation and pay-for-performance compensation programs have led to unprecedented improvements in worker productivity, shareholder value and worldwide standards of living [2].

The pace of change has been very rapid with companies needing to adapt very quickly to these changes in order to prosper, or in some cases even to survive. One of the three conditions necessary for an economy to be economically efficient is to be on its production-possibilities frontier. If it is not on the production-possibilities frontier, more could be produced with the given resources and technology. Any position below the production-possibilities frontier is inefficient, because we can increase production and value [1].

THE LEVEL OF EFFECTIVENESS

Effectiveness is functional characterization of business activities. It characterises overall rationality of business activities as an individual system, which operates only on the base of effectively assured marginal relations with surroundings. [4] Effectiveness is the term, which reflects some conditions of company development. Their change in actual time will change contents of effectiveness too. Globosity and heterogeneousness of objective conditions causes, that effectiveness is synthetic and heterogeneous term.

Synthetic is described by focus of effectiveness on substantial issues of company's economic development, beginning with discovering and use of resources (labour force, working resources and working things), their transformation on useful things and ending with their consumption.

Application of the term effectiveness in various context causes, that it practically gets heterogeneous character. Effectiveness could be understood as a successful manufacturing activity, use of a new technology or work organization, decrease of the rate of production usage and total costs, increase of the side-run, uniformity of production

and products quality, elimination of work difficulty and raising workers performance etc. So effectiveness reflects the new qualitative elements in the manufacturing activities, eventually in other parts of reproduction process. Effectiveness could be understood as the ratio of achieved results and amount incurred, and this ratio should be maximised. It means to achieve the maximum or optimal results with minimum or optimal resources. In general effectiveness could be understood as the optimal utilisation of sources, means and human work results by exploiting laws of nature, society and thinking in achievement of socially useful goals [6].

The level of effectiveness reflects quantitative and qualitative rate of conformity of goals (estimated on the base of knowledge and objective socio–economic laws) and resources necessary for their achievement [5].

The theory is using various terms of effectiveness [7]:

- Technical effectiveness – consist in exploitation and transformation of natural forces and material to the human applicable forms,
- Economic effectiveness – is based on use of social laws (especially economic) for universal development of economy,
- Social effectiveness – reflects effectiveness of given social system in compare with former system, as well as effectiveness of currently developing economic systems.

THE QUALITY AS THE IMPORTANT FACTOR OF TECHNICAL EFFECTIVENESS

The quality is the important factor of technical effectiveness, because it represents the ratio between the inputs and outputs.

It should be noted that the production of certain types of mouldings there is a huge waste in the selected company. Even if the company declares that it uses almost all of the waste through re-injection of the rigrid material, that material is no longer anything like as good properties as the original material was [3]. The evaluation assessed the quality of mouldings based on data the company obtained from the company for a period of 31 days (randomly selected days) and the data were compiled from 3-the shift operation.

The production process was rated for a random 31 days and it showed that in each reporting date, there have been a large number of rejects, which suggests that in the production is an ongoing problem with low-quality products.

The production in the selected company is in compliance with all legal requirements that are imposed on different types of manufactured products. However, it is possible to observe in the company's quality management system's many weaknesses. In the manufacture of products the company should implement a system of comprehensive quality management, but this system should not only be a stated objective of the company, but should prove to be as real acts, which the company would have to prove their interest in the Quality Management System (QMS) [6].

Quality control extends to all levels of flow (processing) of materials, because the total control process includes an input control of raw materials, intermediate control of semi-continuous production and final product inspection (Fig. 1). If the material does not comply with quality requirements, it should not be released for processing, respectively to distribution.

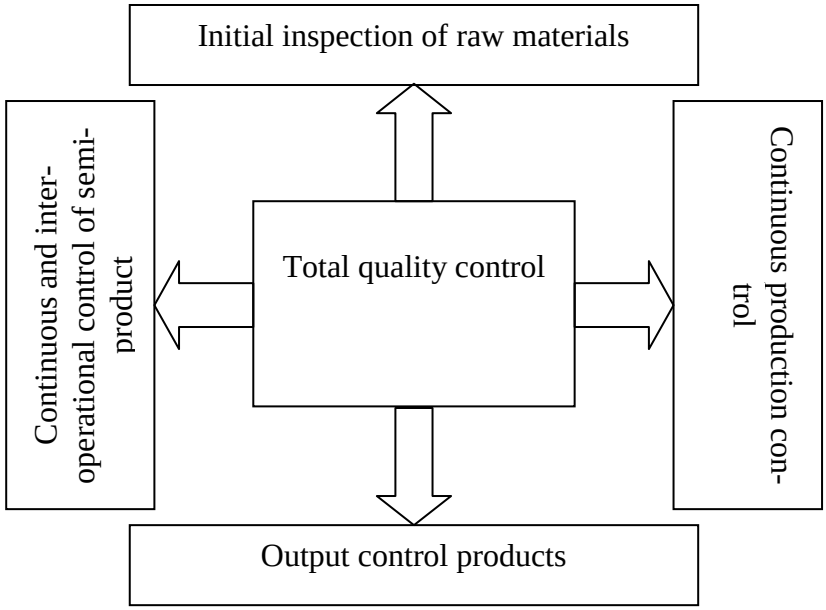

Fig. 1. Total quality control [6]

THE PROPOSED MODEL OF TECHNICAL EFFECTIVENESS

It can be stated that at present it is not yet developed a comprehensive evaluation model of technical effectiveness of production of plastic moldings, and therefore can not be used in the practice. The companies don't intend with technical effectiveness in many cases, respectively they involved with the technical effectiveness only when it is quite obvious, that the production did not meet even the minimum criteria of effectiveness. This fact makes the reality that in many companies is often impractical spend huge investments and eventually these companies haven't got benefit from this activity because their use is not on the production frontier and technical effectiveness of production is not at the desired level [6].

Proposed model was applied to the selected company, but it can be stated that after adjusting the input parameters, the model can be used with other companies that specialize in the manufacture of plastic moldings.

Proposed model for the rating of technical effectiveness of production of plastic moldings consist of a number of successive steps and consistent practice respecting all the steps of the model should contribute to a substantial increase in production effectiveness in production companies.

Model that rates the technical effectiveness is based both on the procedures that rate technical and technological parameters of injection moulding process, as well as the previously known procedures used in the evaluation of technical effectiveness. The model tries to find an adequate link between these two evaluations and to combine them into a single unit desired level. The proposed model is showed in the Fig. 2 [6].

MODEL THAT RATES TECHNICAL EFFECTIVENESS

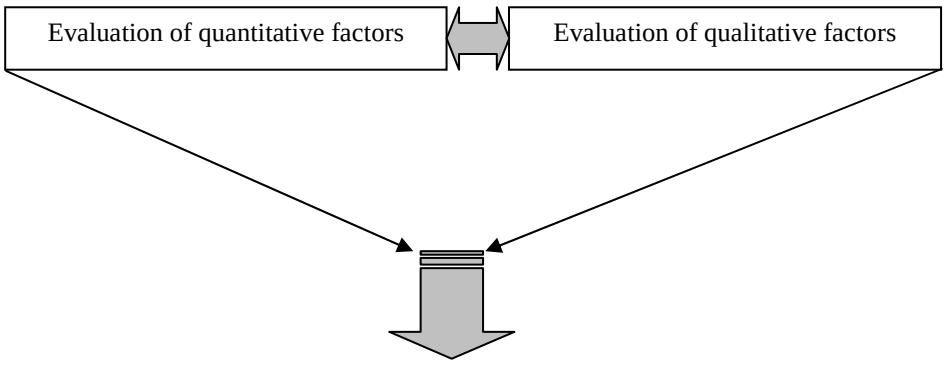

Criteria	Technical effectiveness	Rating
All qualitative and quantitative criteria on the asking level	Very good level	1
All quantitative on the asking level and at least half of the qualitative criteria on the asking level	Good level	2
All qualitative on the asking level and at least half of the quantitative criteria on the asking level	Sufficient level	3
At least half of the quantitative and half of the qualitative criteria on the asking level	Technical effectiveness frontier	4
At least half of the quantitative criteria on the asking level and more than half qualitative criteria under the asking level	Small problems	5
At least half of the qualitative criteria on the asking level and more than half quantitative criteria under the asking level	Middle problems	6
More than half quantitative and qualitative criteria under the asking level	Big problems	7

Quantitative factors	Weight of criteria	The required indicator values	Qualitative factors	Weight of criteria
Machine failure	0,08	effort to minimize	Machine type	0,09
Machine Maintenance	0,04	effort to minimize		
Rebuilding of the machine	0,06	effort to minimize	Machine Operator	0,08
Machine Performance	0,08	effort to maximize	Staffing	0,15
Defective products	0,08	effort to minimize		
Energy Consumption	0,08	effort to minimize	Readiness for Innovation	0,1
Sprue system	0,1	effort to minimize		
Type and multiplicity of the form	0,09	effort to minimize	The geometry of the product	0,15
Duration of cooling	0,02	effort to minimize	Acceptance of the production plan	0,13
Consumption of material	0,08	effort to minimize	Type of material	0,15
Injection Time	0,07	effort to minimize		
The level of product quality	0,1	effort to maximize	Required characteristics of the final product	0,08
Operable time of the machine	0,04	effort to maximize	Machine availability	0,07
Stoppages	0,08	effort to minimize	Overall	1,00
Overall	1,00			

Fig. 2. The proposed model of technical effectiveness [6]

CONCLUSION

This article is based on the need to monitor and rate the technical effectiveness of production as one of the most important competitiveness aspect of mechanical businesses and their application on the global market. This work is oriented on the rating of effectiveness of production by moldings from plastics and as the most deciding aspects were selected especially technical and also economic effectiveness.

By rating the effectiveness of production was laid the big stress on the fact, that effectiveness is the combination of the technical and the economic effectiveness.

Technical effectiveness was mostly rated with the simulation software Moldflow Plastics Insight. The most important section is the proposed model, that rate technical effectiveness of production. This model was applied to selected company, where was well founded the assumption, that effectiveness of production is not on the desired level [6].

REFERENCES

1. Beaumont J.P., Nagel R., Sherman R.: *Successful injection molding*. Hanser publisher, Mníchov, 2002.
2. Greškovič F., Spišák E., Dulebová Ľ.: *Vplyv regranulátu na zmenu vlastnosti plastov*. In: Acta Mechanica Slovaca. roč. 10, č. 2b (2006), s. 135-140. ISSN 1335-2393.
3. Greškovič F., Spišák E.: *Vplyv množstva regranulátu na vlastnosti plastu*. In: PRO-TECH-MA 05 : Progressive technologies and materials : International scientific conference : Rzeszów - Bezmiechova, Poland, 28th June-30th June, 2005. Rzeszów : Oficyna Wydawnicza Politechniki Rzeszowskiej, 2005. p. 44-48. ISBN 83-7199-356-0.
4. Krylov A.I.: *Analysis of production efficiency, technical progress and economic mechanism*. Monograph. - M., Finance and Statistics, 168 p., 1991.
5. Malega P., Spišák E., Greškovič F.: *Economic effectiveness by plastics injection molding process*. In: PRO-TECH-MA ´07, Rzeszóv – Bezmiechova, Poland, p. 39 – 40, 28th June – 30th June 2007, ISBN 978-83-7199-443-2.
6. Malega P.: *Príspevok k metódam hodnotenia ekonomickej efektívnosti výroby výliskov z plastov*. Písomná práca k dizertačnej skúške na získanie vedecko – akademickej hodnosti philisophiae doctor, 2006.
7. Vidová J.: *Metodika hodnotenia efektívnosti nekonvenčných technológií*. Písomná práca k dizertačnej skúške, Košice, 2000.

Jozef MALEJČÍK
Janette BREZINOVÁ
Anna GUZANOVÁ

Technical University of Košice, Slovakia

HIGH SOLID COATINGS QUALITY IN SELECTED CORROSION MEDIA

The ecological approach to surface treatments with organic coatings requires a reduction in the proportion of coatings containing volatile organic solvents, VOCs - Volatile organic compounds. One of possible solutions is to substitute solvent paints by water diluted and high-proof materials. The contribution presents the results of research aimed at establishing high solid coatings quality by accelerated laboratory tests in conditions of artificial atmosphere.

INTRODUCTION

Environmental protection and particularly big economical costs for production of coatings with high content of volatile organic solvents have a major impact on the development and use of new - ecological (green) coatings. The objective of this effort is to reduce the amount of volatile organic compounds (VOCs - Volatile organic compounds) released in any production process into the atmosphere as much as possible. One form of solution is the substitution of this paint by water-based high solid (HIGH SOLID) materials. [1,4]

The paper deals with features evaluation of high solid coating compared to synthetic paint coatings after exposure to corrosive environment. Electro-chemical characteristics of the pre-treated blasted surfaces on the basis of electrode potentials were evaluated [2].

MATERIAL AND METHODS

For the experimental work hot-rolled steel sheet S235JRG2 with thickness of 2 mm was used. Pretreatment of the surface was carried out by a laboratory pneumatic blasting machine TJVP - 320 at a pressure of 0.4 MPa and the nozzle distance from the sample 200 mm. Pretreatment of surfaces was carried out using two types of angular abrasives:

a) GBM natural garnet - almandine - $Fe_3Al_2(SiO_4)_3$, grain size 0.56 mm,
b) brown corundum - Al2O3, grain size 0.56 mm.

Roughness parameters were determined by stylus profilometer Surftest SJ - 301, Mitutoyo, according to EN ISO 4287 - Profile method. The activity of the blasted surface was evaluated on the basis of changes in electrode potential versus saturated calomel electrode i mmediately after blasting, also after 1, 3, 6, 12, 24, 72, 120, 240 and 576 hours of exposure of the samples in the interior and exterior. The test electrolyte - SARS “simulated acid rain" of pH = 5.0 was used, which by containing present ions simulates a slightly acidic atmospheric rain. Its composition is shown in Tab. 1.

Table 1. Composition of SARS solution at pH = 5. 0

Chemical	Concentration [mmol . l^{-1}]
HNO_3	0.01
NaCl	1
$(NH_4)_2SO_4$	1

On the blasted surfaces, at 0.2 MPa pressure following coatings were applied by spraying:
- S2330 - the dispersion of pigments and fillers in a mixture of epoxy resins based on bisphenol A and low-viscous epoxy resin reactive diluent modified with the addition of solvents and additives. -
- S2556 FERRO COLOR S - synthetic anti-corrosion coating (2in1).

Average thickness of the dried coating was 95 µm. To evaluate the adhesion of the coatings after exposure to the corrosive environments two methods were used – Cross-cut test - STN EN ISO 2409 and Pull-Off Adhesion Test - EN ISO 4624. To determine the quality of the coating samples were exposed to two environments, in a humid environment with the presence of sulfur dioxide (SO_2) according to EN ISO 3231 and by the full i mmersion of the samples in 20% solution of potassium ferrocyanide (K_4 [Fe(CN)6]) in distilled water (STN 03 8135). To assess the protection effectiveness of selected coating, on part of the samples was made experimental cut before entering into the corrosive environment, according to DIN 53167.

RESULTS

Arithmetic mean deviation of the profile (Ra) measured after blasting with brown corundum reached the value of 6.03 mm and after blasting with almandine 5.23 mm. Fig. 1 shows measured values of specimen potential after blasting by corundum and almandine. Blasted surfaces reached approximately the same value of the surface activity. For both surfaces, the decline in activity more pronounced in exterior exposure samples, which showed an increase in the measured corrosion potential. Corrosion processes on the metal surface run more intensively due to the nature of the environment in the exterior. Surface activity decreases with increasing time of exposure of the samples.

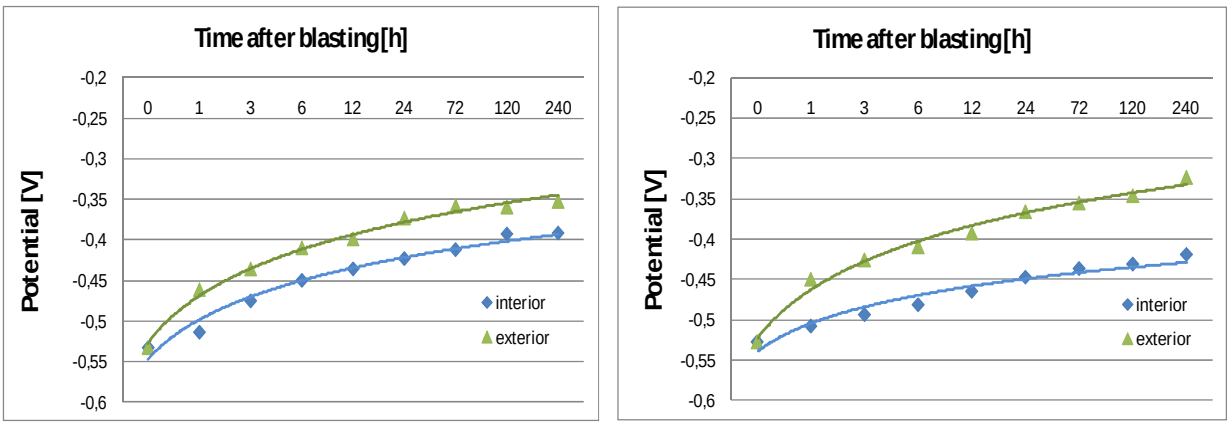

a) b)

Fig. 1. Surface activity in the interior and exterior after blasting by a) brown corundum, b) almandine

Adhesion of each coating was evaluated on samples in the unexposed state and after 576 hours of exposure in corrosive environments by cross-cut test and pull-off test.

Table 2 shows the preview of the final appearance of the samples after 576 hours in a humid atmosphere with sulphur dioxide, after the grid examination. In another, the quality of coatings was evaluated by pull-off test, the results graphically shows figure 2.

environment / pretreatment		S 2330	S 2556
After 576 hour of exposition in wet atmosphere polluted by SO_2	C		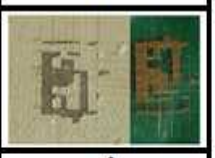
	classification	2	4
	G	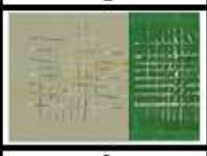	
	classification	2	3

Table 2. Cross-cut test of the samples before and after exposure in simulated aggressive environments

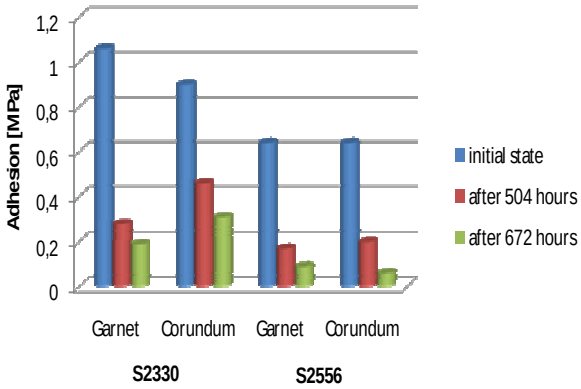

Fig. 2. Change in adhesion before and after exposure of samples in corrosive environment

BM - coating	Appearance: The first defect manifestation	Appearance: At the end of exposition	Evaluation at the first defect manifestation	The first defect manifestation after [h]	
garnet - S 2556			Medium density of osmotic blisters of site < 5 mm	168	a)
corundum - S 2556			Large density of osmotic blisters of site < 5 mm	72	a)
garnet - S 2556			Very low density of osmotic blisters, just visible in the normal projection	504	b)
corundum - S 2556			Medium density of osmotic blisters, just visible in the normal projection	504	b)

Fig. 3. Evaluation of protective efficiency of applied coatings on the samples after exposure in: a) condensing chamber containing SO_2, b) 20% NaCl

Effect of the pretreatment on the decrease of coatings adhesion did not significantly express. Adhesion of both applied coatings due to their exposure in the corrosive environment decreased. Higher adhesion was reached for high solid coating (S2330) after exposure of samples in both corrosive environments. Coatings were degraded by forming of osmotic blisters (Fig. 3), the number and size with increasing exposure time was expanding.

In the next phase of experiments corrosion in the vicinity of artificially created test sections was evaluated (Fig. 3). Corrosion and corrosion distance from this section gives an indication of the electrochemical influence of anticorrosive pigment used in the coating [3]. More protective effect in selected type of corrosion environment was showed for high solid coatings.

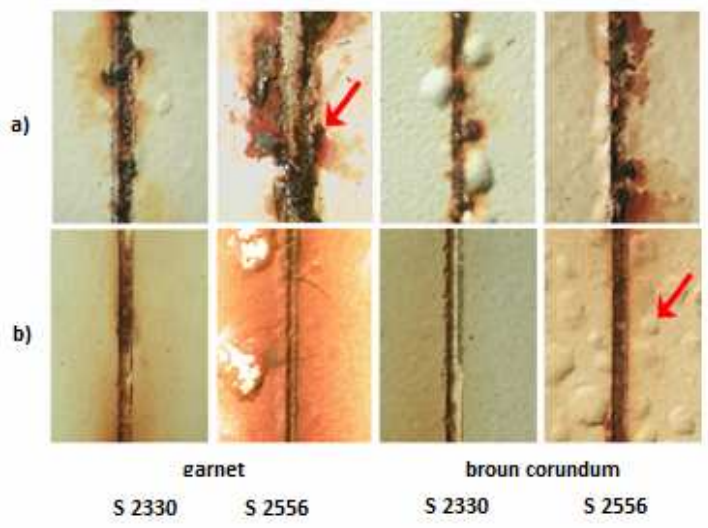

Fig. 4. View of the cuts on the samples after exposure in: a) condensing chamber containing SO_2 , b) 20% NaCl solution, mag. 40x

CONCLUSION

Results of the experiment confirm, that almandine - mineral blasting medium can be used for pretreatment of steel surfaces, though it is necessary to consider his lower durability and secondary pollution of the surface. Experimental results showed improved quality of high solid coating materials with low solvent content. Because of their environmental aspects, they represent the future of the barrier coatings to protect steel surfaces.

REFERENCES

1 Kalendová A., Veselý D., Houšková V.: *Zvýšení korozne-inhibiční ochrany organických povlaku pomoci funkčních pigmentu*. Acta Mechanica Slovaca, Interantikor 2005, 3-A/2005, roč.9, TU Košice, s.117-122, ISSN 1335-2393.

2 Ábel, M., Brezinová J., Draganovská D.: *Vlastnosti povrchu predupraveného tryskaním* [online].[cit. 2009-10-10]. Dostupné na internete: http://www.sjf.tuke.sk/transferinovacii/pages/archiv/transfer/6-2003/pdf/84-87.pdf

3 Hadzima B., Liptáková T.: *Základy elektrochemickej korózie kovov*. 1.vyd. Žilina: Edis,2008.112 s. ISBN 978-80-8070-876-4.

4 Hochmannová L.: *Antikorozní pigmenty a plnivá ve vysokosušinových epoxidových nátěrových hmotách*. In: XIX. Ročník konference povrchové úpravy, 2005.

Contribution was processed within the frame of Grant Scientific Project VEGA No. 1/0144/2008 and 1/0510/2010.

Alexander MALYARENKO
Maxim MITENKOV
Sergey KVASUK

Byelorussian State Polytechnic Academy, Minsk, Byeloruss

RESEARCH OF LAP THERMAL DEFORMATION AT OPERATIONAL DEVELOPMENT OF OPTICAL SURFACES AT THE EXPENSE OF A TEMPERATURE VARIATION OF POLISHING SLURRY

The outcomes of experimental research of temperature influencing of polishing slurry on machining accuracy of optical surfaces are resulted at different rotational speeds of the lower link at operational development by laps with a different profile of cross section. The guidelines on perfection and implementation of optical surfaces operational development at the expense of a temperature variation of polishing slurry are given.

INTRODUCTION

Nowadays in the sphere of optical-mechanical industry, the production of complex and unmanufacturable, the so called “high-tech” lenses, which demands machinery accuracy, gathers pace. Taking into account labour and material resources, the task of advanced manufacturing process creation of optical details that will allow to reduce workers’ qualification and to increase the quality of output goods, is of current importance.

The most labour-intensive process of the workflow is tweaking; it takes up to 40% of time spent on part cutting. The fundamental quality rating of workpieces is achieved at this stage, so its perfection gives a promising lead for the problem solving.

Currently, at the tweaking stage of optical details, pitches of different mixture are mostly used as polishing materials. However, the process control as well as the form of the workpiece surface is based mainly on practical methods. These methods are not clearly characterized and their efficiency is defined purely by the performer’s skills and experience, considering strong requirements for the form accuracy of the optical surface [1].

From the authors’ point of view, at the tweaking stage, the use of tools with membraneous foamed polyurethane substrates gives a chance to reduce the time spent on polishing from 1,5 to 5; to increase the yield by 85%, to cut the use of accessory materials; in other words, to intensify the process of final treatment of sensitive optical surfaces and to stabilize the derivable accuracy parameters.

Owing to the research done before, it is evident that while using the polishing foamed polyurethane substrates, we can successfully control the tweaking process at the expense of thermal variations of polishing suspension in the cutting zone. At the same time, this process of control in combination with the above mentioned advantages, can decrease the performer’s qualification because of its realization simplicity. That is why, doing research in this field is of interest.

THE OBJECTIVE OF THE GIVEN RESEARCH

Nowadays at the tweaking stage of optical surfaces, there are no guidelines concerning the choice of optimal form of a lap body. The constructions of lap bodies that are used can be theoretically divided into three groups with different forms of cold face, that is with different profile of cross section: dilative, concentric and convergent from the centre to the brim.

According to the theoretical research carried out by the authors [3], intended thermal deformations for these types of lap bodies are different. That is why, for using thermally controlled tweaking, the choice of optimal form of a lap body is essential.

The aim of the research work was to define the influence of a lap body profile on machinery accuracy of optical surfaces and the stability of the achievement of desired precision parameters in the terms of tweaking thermal variations.

THE OUTCOMES OF THE EXPERIMENT AND THEIR DISCUSSIONS

As test subjects, laps of different constructions have been used (Fig. 1), made of aluminum alloy AL2 State Standard 1521-76. The polishing foamed polyurethane substrate PPM-1-1 TC OP.004, adjusted in compliance with recommendations, was put on the interior lap surface [2].

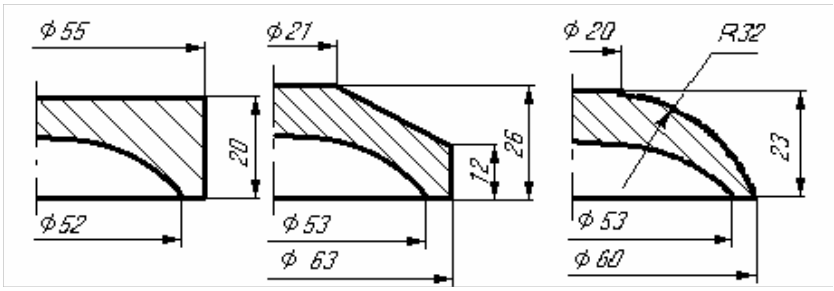

Fig. 1. The constructions of the lap bodies used in the research work: a – with the dilative profile; b – with the concentric profile; c – with the convergent from the centre to the brim profile.

During the research process, the treatment of convex spherical surfaces within a radius of 39,02 mm and optical lenses $57^{\pm 0.3}$ mm in diameter made of glass LK7 fixed in devices on a pitch layer with the help of elastic methods has been carried out. As a preliminary, the intermediates were polished with free abrasive on a steel tool; aqueous suspension of white electrocorundum M10 with the relationship between solid and liquid phase S:L = 1:3 was used as abrasive. The divergence of the intermediates from the standard following the flexure pointer was sustained within $h = -4^{\pm 0.5}$mkm. The quality control of the polishing process on the lack of scratches, popouts and the smoothness of microrelief was implemented visually with the help of a sixfold magnifying glass.

The tweaking of optical surfaces was carried out on a batch-produced machine model 6SHP-100M on the following conditions: the detail rotational speed is 90, 180 and 360 revolutions per minute; the tool sweep frequency on a detail is 40 double strokes per minute; the tool amplitude is 45 mm; the time spent on one detail polishing is 30 minutes; the pressure in the cutting zone is 0,013 MPa.

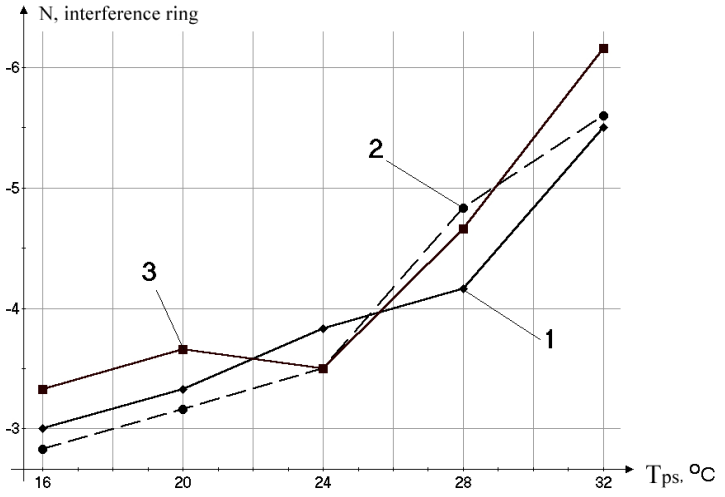

a)

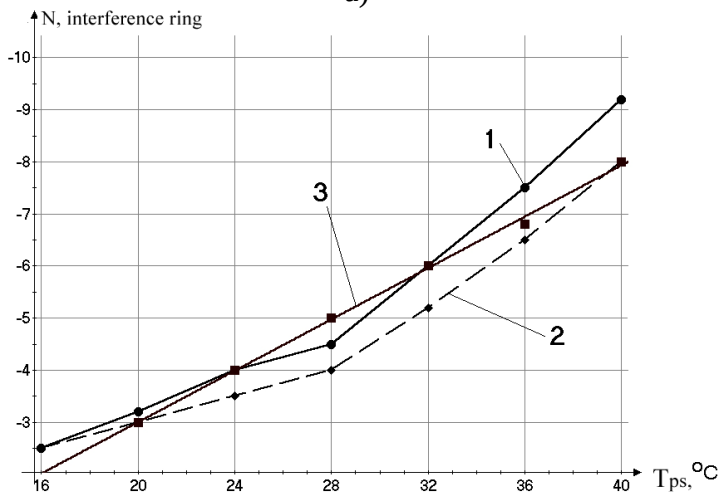

b)

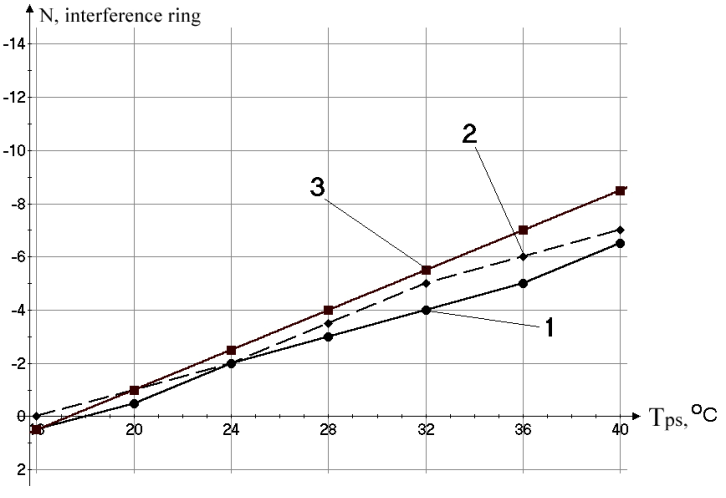

c)

Fig. 2. The dependence of the form N total error of the machined surface of the optical lenses on the temperature of the polishing suspension at lower link rotational speed of 90 (a), 180 (b), 360 min^{-1}(c) while using a lap with: 1 – the dilative profile; 2 – the concentric profile; 3 – the convergent profile from the centre to the brim profile

At this stage, the polishing suspension with the relationship between solid and liquid phase S:L = 1:40 was used as a technological medium. Up-to-date batcher PAS-30T provided the polishing suspension delivery with the consumption of two litres per minute and its temperature in the range from 16 to 40°C accurate within $^{\pm 0,5^o}$C.

The form accuracy of machined surface was checked with interferometric method with the help of trial glass and the polishing quality considering tape, thin coating, scratches, spots was controlled by means of a sixfold magnifying glass.

Figure 2 shows the dependence of form N work surface total error at different temperature variations of the polishing suspension and at different detail rotational speed at operational development by laps with a different profile of cross section. According to the research, irrespective of lap bodies constructions, temperature increase of cooling mixture from 16 to 40°C entails work surface radius rise, so it leads to form N total error increase.

While treating at low speed (n_d = 90 revolutions per minute), it was noted that at temperature above 28°C matt layer didn't come off but remained in the centre of the work surface after treatment time. Besides, lustre was seen on a lap work surface, and it's because of the prevalence of the detail influence on the lap. At the same time, the detail is a tool against the laps. The increase of treatment time and the pressure in the cutting zone leads to partial metal transition in the centre, that is to "matt ring" formation. This phenomenon was observed while using all three types of lap bodies. The presence of short finish precluded the form accuracy control by means of work trial glass, that is why form N total error control was fulfilled with the help of indicated spherometer, and it also didn't help to conclude about form ΔN site error at given temperature variations (Fig. 3). Hence, we can conclude that the tweaking with the foamed polyurethane substrates use is not effective at this rotational speed of the detail.

At the detail rotational speed of 180 revolutions per minute, the defective layer made at the previous treatment came off completely. According to figure 2b, while using a lap with the convergent profile at the given rotational speed, the dependence of the form total error is linear, besides, one interference ring change took place at 4°C. The form site error is constant at all temperature variations and does not exceed 0,3 interference rings. The linearity is broken for the other two types of laps: while treating the polishing suspension at temperatures above 28°C, the treatment is more intensive. So, for a lap with the dilative profile of cross section (Fig. 2a), the change of N total error on one interference ring at temperatures below 28°C occurs every 8°C, and at temperatures above 28°C occurs every 4°C. While using a lap with the concentric profile of cross section (Fig. 2b) at temperatures of cooling mixture above 28°C the same change of N total error takes place every 3°C. The form ΔN site error (Figs. 3a, 3b) for these laps ranges from 0,3 to 0,8 interference rings at all temperature variations and the intermediates rotational speed. According to the research, one can realize the tweaking process control at the given rotational speed, using a lap with the convergent profile.

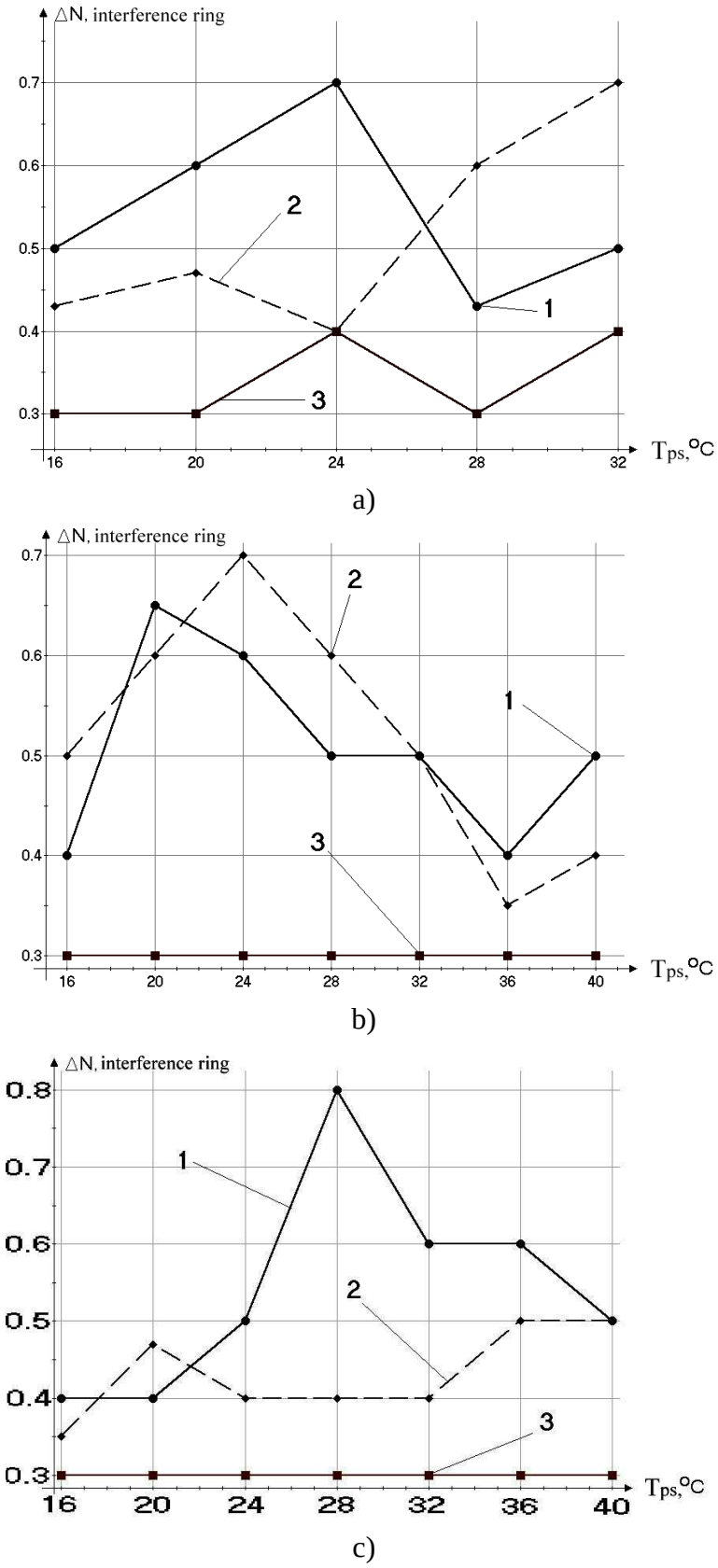

Fig. 3. The dependence of the form ΔN site error of the machined surface of the optical lenses on the temperature of the polishing suspension at lower link rotational speed of 90 (a), 180 (b), 360 min^{-1}(c) while using a lap with: 1 – the dilative profile; 2 – the concentric profile; 3 – the convergent profile from the centre to the brim profile

The dependence of the form total error formation on the temperature levels off at higher rotational speed (n_d = 360 revolutions per minute) for the dilative and concentric laps: the change of N on one interference ring occurs every 4°C and 3,5°C accordingly. It is preferable to use these types of laps at high rotational speed to get the optical surfaces of mid-coefficient accuracy, as the form site error (Figs. 3a, 3b) varies in a wide range and is not stable.

The laps of the convergent profile illustrate the most stable operation and the linear error dependence on the temperature at the rotational speed of 360 revolutions per minute (Fig. 2b), in this way the change of the form total error on one interference ring occurs every 3°C, and the site error doesn't exceed 0,3. So, 1°C of temperature variation of the polishing suspension leads to the change of the curvature radius of the work surface by 6,8 μm. In other words, the coefficient of the curvature radius change (Crc) of the work surface is constant at all temperature variations and makes Crc = 0,592 μm/°C, while using the above mentioned type of the lap. So, we have come to the conclusion that it is preferable to use the given form of the lap body to get the desired characteristics of high-precision optical surfaces.

CONCLUSIONS

1. The radius of the work surface increases with the temperature rise of the polishing suspension that results in the form N total error increase. The dependence for the laps with the convergent profile is linear.
2. It is not effective to treat the tweaking with the foamed polyurethane substrates at lower link rotational speed of 90 revolutions per minute.
3. It is possible to get the desired precise characteristics of sensitive optical surfaces while using the laps with the convergent profile at the rotational speed of 180 revolutions per minute and 360 revolutions per minute.
4. The coefficient of the curvature radius change (Crc) of the work surface while using the lap with this profile is constant at all temperature variations and makes Crc = 0,592 μm/°C.

Abbreviations

T_{ps} – temperature of the polishing suspension in the cutting zone; n_d – the detail rotational speed; N – the form total error of the optical surface; ΔN – the form site error; Crc – the coefficient of the curvature radius change of the work surface.

REFERENCES

1. Kumanin K.G.: *Shaping of the optical surfaces*. Collected articles. M.: Oborongiz, 1962 – p. 157.
2. Busarnova S.M., Mamonov S.K., Nehochen A.S, Panphilov V.I., Fedin B.E.: *The treatment of the einzel lenses with the help of the polyurethane polisher*. Optical-mechanical industry. 1990. №6, p. 55.
3. Malyarenko A.D., Filonov I.P.: *The technological basis of the optical surfaces shaping*. Mn.: VYZ-UNITI BSPA, 1999. p. 212.

Mariana OLEXOVÁ
Ján SLOTA
Attila HERDITZKY

Technical University of Košice, Slovakia

MICROSTRUCTURE EVALUATION OF TRIP STEEL USED IN A CAR CRASH ZONES

The paper deals with evaluation of TRIP (transformation induced plasticity) steel microstructure. These special steels are commonly used mainly in automotive industry for crash zones of car's bodies. The TRIP steel has high strength compared to AHSS steel, but on the other hand a good plastic properties. The microstructure properties of TRIP steel were investigated by a light microscope and evaluated by a computer program ImageJ. Microstructure charakteristics of TRIP steel was investigated on shape-complicated part made by deep drawing process.

INTRODUCTION

In the automobile industry, great attention focused to the development of materials. Steel is still one of the major materials which is needed for car production. Current safety requirements bring increase of using stronger steels and decrease the total weight of the car. In another direction is there effort to reduce fuel consumption and to increase the operational reach of the car. Deep drawing process is one of technologies which is used in the manufacture of cars. [1]

TRIP steels have high strength and excellent plastic properties. The microstructure of TRIP steels is retained austenite embedded in a matrix of primary ferrite (Fig. 1). [3, 5]

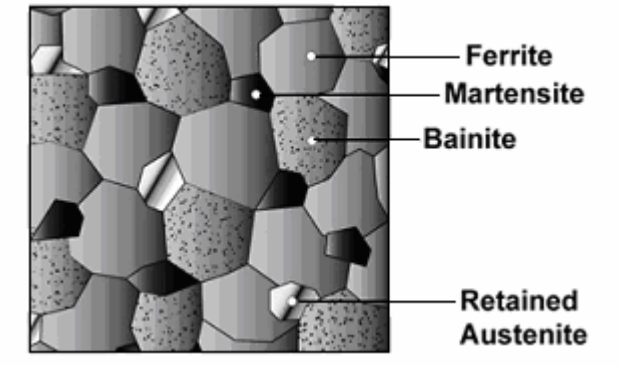

Fig. 1. Microstructure TRIP steel

The driving force for the spread of cracks in the TRIP steel is low, so it is resistant to brittle fracture. Suitable for high energy absorption during deformation (crash - test). The disadvantage is the relatively low yield point. [1]

EXPERIMENTAL MATERIAL

TRIP steel with transformation induced plasticity, steel labeled RAK 40/70 and thickness of a_0 = 0,75 mm was evaluated in experimental work. Steel plate which was evaluated was on both sides galvanized. Samples were tested in directions 0°, 45°, 90° against the rolling direction. Flat bar according to STN EN 10002-1, L_0 = 80 mm was used for testing. Chemical composition and mechanical properties of tested steel are listed in Tab. 1 and 2.

Table 1. Chemical composition of the RAK 40/70 steel

Chemical element	C	Mn	P	S	Ti	Si	Al	Cr	Cu	Ni	Nb	Mo	Zr
Coeficient [%]	0,204	1,638	0,018	0,003	0,009	0,200	1,730	0,055	0,028	0,018	0,004	0,008	0,007

Table 2. Mechanical properties of the RAK 40/70 steel

Direction	Yield strength $Rp_{0,2}$ [MPa]	Tensile strength R_m [MPa]	Ultimate elongation A_{80} [%]	Coefficient of normal anisotropy r [-]	Strain hardening exponent n [-]
0º	442	771	27,7	0,686	0,259
45º	441	762	25,4	0,870	0,294
90º	450	766	25,9	0,838	0,278

5 cornered cups were drawed (pressured) by the hydraulic press Fritz MULLER BZE 100. (Fig. 2).

Fig. 2. Designation of cup cormers

Samples of TRIP steel RAK 40/70 for light microscopy were prepared by the procedure:

- hand cutting,
- identification of borders (for better orientation), to distinguish from the bottom side wall proceeds,
- with the help of taxidermist dentakryl resin,
- a gradual grinding (grain abrasive paper 400, 600 and 1600),

- polishing,
- etching solution of 2% HNO_3 in Nitric acid (Nital).

Optical microscopy was performed on a light microscope Neophot 2. Program ImageJ analyzer was used for image processing and image analysis. This program supports image processing functions such as contrast adjustment, sharpen, smoothing, edge detection, and others. To evaluate the visual structure of the samples by using Image J program, it is necessary that each structure are sufficiently contrasting.

EXPERIMENTAL RESULTS

Symmetrical sample was cut in all five corners. Samples were taken from the corners and the proceeds are marked from 1 –5. The material samples was taken from the wall, rounded the corner and the bottom of the proceeds. In Table 3 is evaluate the composition of phases program ImageJ. Graphical representation of % austenit of the phases in microstructure is shown in Figures 3 – 7.

Table 3. % Evaluate the composition of phases program ImageJ

	Sample 1	LUT	Invert LUT
a)	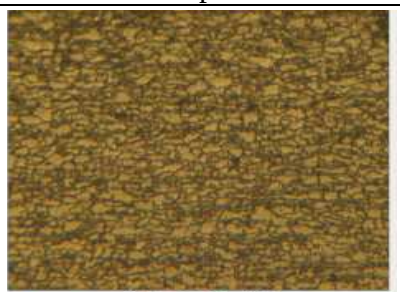	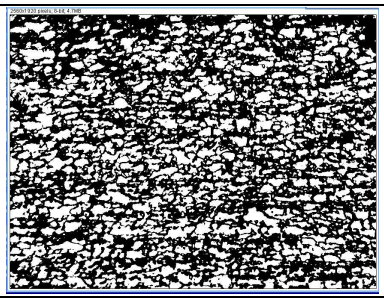	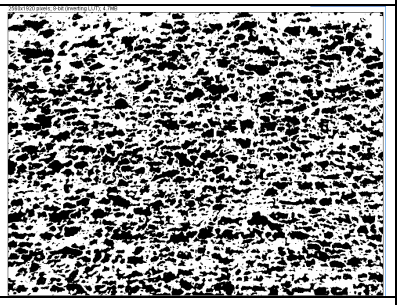
		56,11%	43,88%
b)	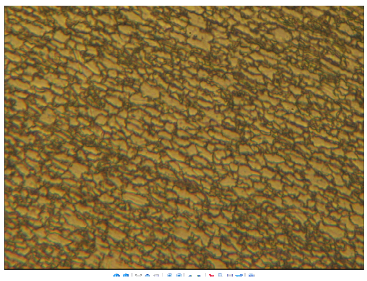		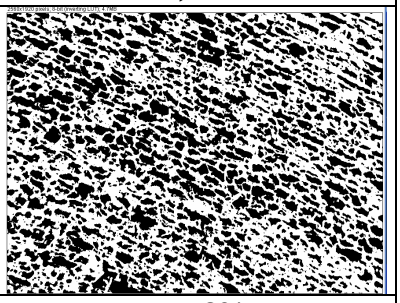
		55,51%	44,48%
c)	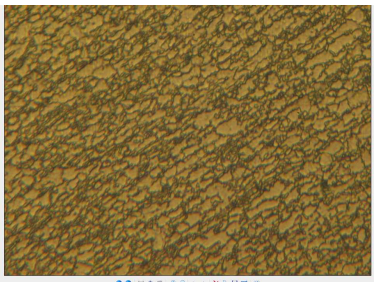		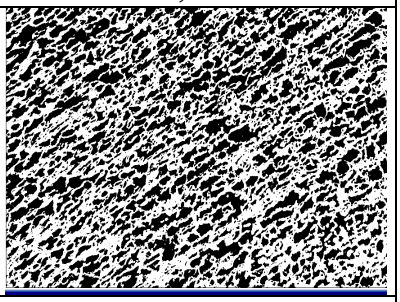
		51,76%	48,23%

Both windows show a modification of the default LUT (gray level scale) in the window no longer runs from the lower left to the upper right corner, and the LUT ramp graduated area has been squeezed toward the middle. So far it is possible to

adjust linearly bringhtness and contrast. Invert LUT – show the darker background. Analyze LUT evaluate martenzit and bainit, analyze invert LUT evaluate martenzit and residual austenite in the identified locations cup.

Samples were tested at three locations: in radius of cup, in bottom of cup and in wall of cup. Radius of cup is space between the wall and bottom of each corner ot the samples cup.

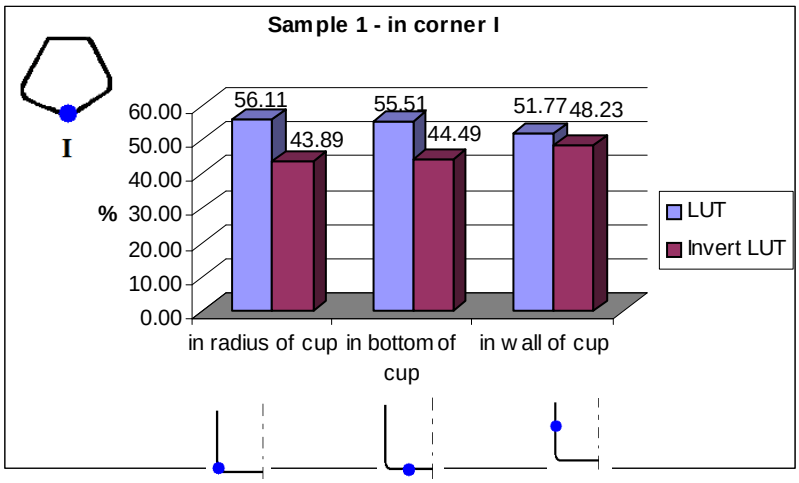

Fig. 3. Evaluating of sample No. 1

In the sample in a radius of measuring cup by LUT method, which includes matrenzit and bainiti - 56.11%. 43.89% is ferrite and residual austenite, which were determined by a method invert LUT. In bottom of the cup measured by LUT, there is 55.51% martensite and bainit and the remaining 44.49% is ferrite and residual austenite measured by invert LUT method. In wall of cup, martensite and bainit is 51.77% and 48.23% is ferit and residual austenite.

In the transition from corner I to corner II, those currency rates are changing as shown in Figure 4

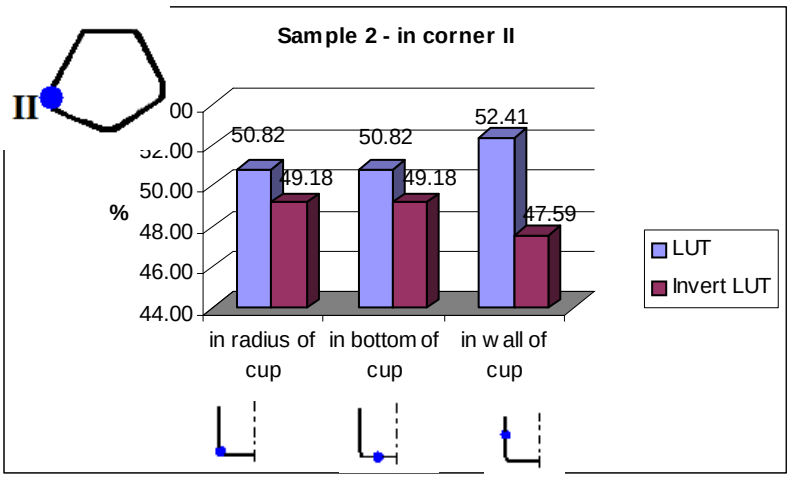

Fig. 4. Evaluating of sample No. 2

In the transition from corner II to corner III, those currency rates are changing as shown in Figure 5.

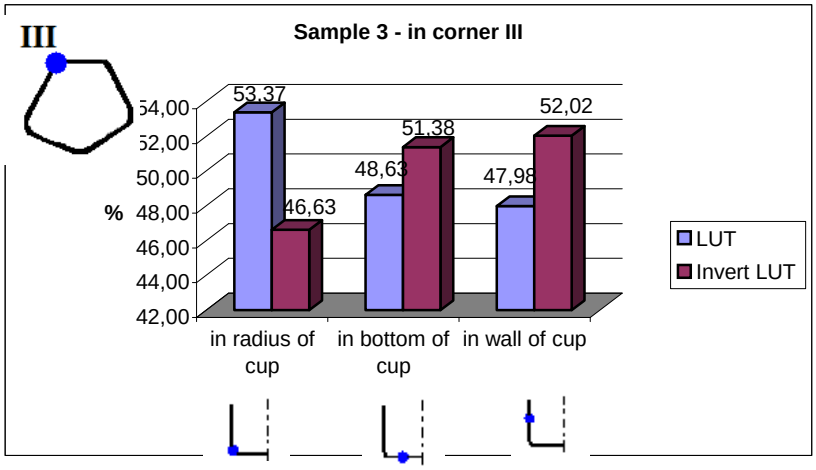

Fig. 5. Evaluating of sample No. 3

In the transition from corner III to corner IV, those currency rates are changing as shown in Figure 6.

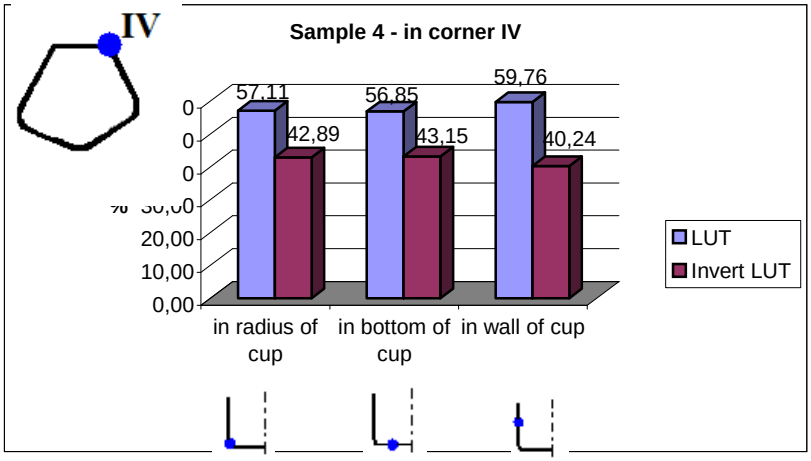

Fig. 6. Evaluating of sample No. 4

In the transition from corner IV to corner V, those currency rates are changing as shown in Figure 7.

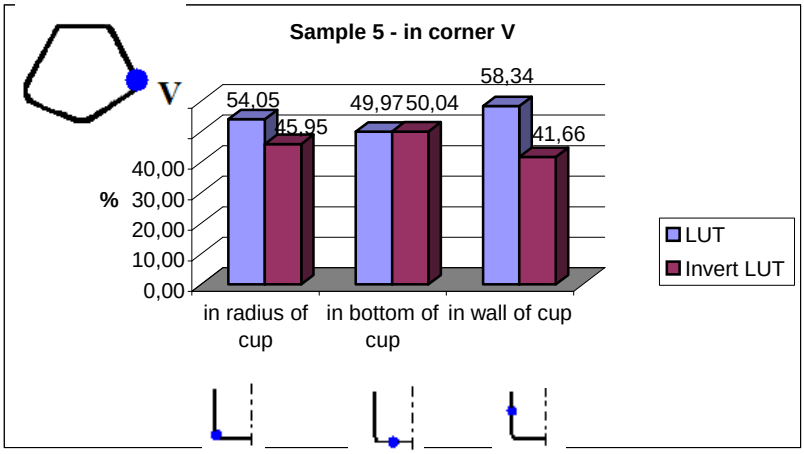

Fig. 7. Evaluating of sample No. 5

DISCUSSION

Condition of successful application of image analysis is metallographic cut, where individual structural components were sufficiently contrastive. Contrast between ferrite and martensite was achieved by etching in 2% Nital. After this etching islands of martensite was show as compact surface blocks and this is convenient for successful application of image analysis by software ImageJ.

CONCLUSIONS

In evaluation of the visual microstructure of the samples by using the ImageJ program, it is neccessary that each structure was contrast enough. On the basis of its experimental research and evaluation of achievements can be found:

1. The biggest values of the martensite volume fraction were measured in the sample 4 in measurement of wall of cup – 59,76 % martenzit and bainit of metode LUT and 40,24% is ferit and retained austenite of metoe invert LUT. The samples were evaluated by the percentage of ingredients.

2. This result is not final because TRIP steel consists of four components: martenzit, bainit, ferit and retained austenite. Using image is appropriate to examine the steel, which have two phases.

REFERENCES

1. Spišák E., Greškovič F., Slota J.: *Špeciálne technológie v automobilovej výrobe*. TU Košice, Strojnícka fakulta, Edícia EQUAL, ISBN 80-8073-753-3.
2. Slota J., Gajdoš I., Olexová M.: *Numerická simulácia procesu hlbokého ťahania a jej verifikácia*. MMaMS '2009, s. 588-591. Dostupné na internete: http://web.tuke.sk/sjf-kamam/mmams2009/Zbornik_MMaMS_2009.pdf.
3. *World auto steel*. Dotupné na internete [online] http://www.worldautosteel.org/SteelBasics/Steel-Types/TRIP.aspx. [15.5.2010]
4. Spišák E. a kol.: *Dizajn moderne koncipovaných ocelí na základe charakteristík lisovateľnosti*. APVV-0629-06
5. Buriková K. Džupon M., Parilák Ľ: *Spôsoby leptania pre obrazovú analýzu dvojfázových nízkouhlíkových feriticko-martenzitických ocelí*. Metal 2008, s. 1-6. Dostupné na internete: http://www.nanocon.cz/data/metal2008/sbornik/Lists/Papers/064.pdf

Acknowledgments: this paper was supported by the Slovak Research and Development Agenci under the contrect No. APVV-0629-06. [4]

ZESZYTY NAUKOWE POLITECHNIKI RZESZOWSKIEJ NR 274
Mechanika z. 81 2010

Iaroslav PASTERNAK
Heorhiy SULYM*

Lutsk National Technical University, Ukraine; *Białystok Technical University, Poland

THE UNIFIED APPROACH FOR THE ANALYSIS OF ELASTIC EQUILIBRIUM OF SOLIDS CONTAINING THIN INTERNAL AND SURFACE HETEROGENEITIES

This paper develops the unified approach for the analysis of plane elastostatic problems for solids containing thin elastic inclusions or overlays. The approach is based on the previously developed integral equation method for the solution of plane elastostatic problems for solids with perfectly embedded inclusions. In this paper the method is extended to the case of delaminated inclusion and elastic enforcing overlay. Thus, the wide class of problems can be solved basing on the developed technique.

INTRODUCTION

Thin heterogeneities are common in engineering practice. Those are cracks; thin inclusions; various cavities filled with gas, liquid or solid substance; technological defects etc. However, the prevalence of thin heterogeneities is caused not only by the undesirable effects of imperfect manufacturing or materials processing. Wide applications have got, for example, thin stringers [1], fiber reinforcement of composite materials [2], thin plate-like reinforcement elements [3] etc. Problems for solids with thin heterogeneities are concerned with the methods of calculation of piles in a ground [4], elastic fastenings of console beams and anchors [9], fiber pullout problems (Reissner problem) [8], reinforcement of walls of underground buildings and mines, holes enforced with thin elements [13] etc.

The abovementioned problems are usually considered with the previous determination of the boundary conditions or geometrical features and the further solution is based on the appropriately constructed equations. However, as it is specified in the monograph [10], all these problems are very close to the problems of the thin inclusions theory. In particular, stringers are surface heterogeneities that unilaterally contact with the medium; piles, anchors and elastic fastenings are inclusions, which end face is outside the medium; reinforcing fibers are the inclusions completely embedded into the medium. Thus, it would be useful to adopt the unified approach, in particular basing on the numerical method [5], which would allow studying of all these problems.

PROBLEM FORMULATION AND SOLUTION STRATEGY

Consider a plane problem of elastostatics for an isotropic solid containing thin elastic inclusion from other material. Between a solid and inclusion at the certain part of their interface the conditions of perfect mechanical contact are satisfied, and at its complement the inclusion is completely delaminated (the mechanical contact between the materials is absent). Consider the general scheme of modeling of such defect using the principle of coupling of different dimensionality continuums [10] (Fig. 1).

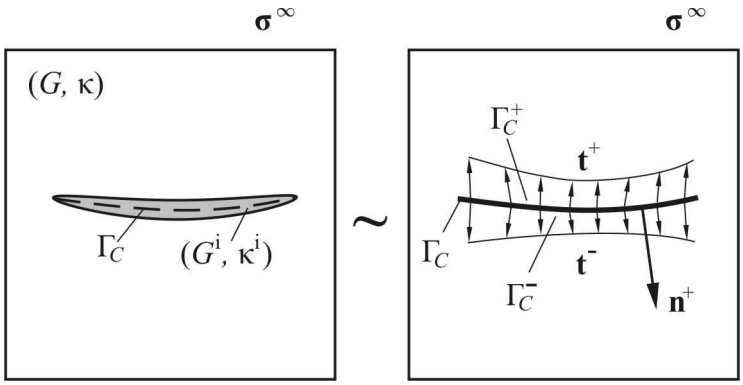

Fig. 1. Schemes of the problem and the inclusion modeling approach by a coupling principle

Adopting the lined model of inclusion, withdraw the consideration of inclusion as a geometrical object, and transfer the contact tractions and displacements onto its median surface Γ_C (accordingly onto faces Γ_C^+ and Γ_C^-, Fig. 1). The own boundary of a solid is denoted as Γ. According to the approach [10] the displacement field in a solid with a cut is defined within the following Somigliana identity:

$$u_i(\boldsymbol{\xi}) = \int_{\Gamma_C^+} \left[U_{ij}(\mathbf{x},\boldsymbol{\xi}) \Sigma t_j(\mathbf{x}) - T_{ij}(\mathbf{x},\boldsymbol{\xi}) \Delta u_j(\mathbf{x}) \right] d\Gamma(\mathbf{x}) + \int_{\Gamma} \left[U_{ij} t_j(\mathbf{x}) - T_{ij} u_j(\mathbf{x}) \right] d\Gamma, \qquad (1)$$

where u_i, t_i are the components of displacement and traction vectors respectively; $\Delta u_i = u_i^+ - u_i^-$, $\Delta t_i = t_i^+ - t_i^-$, $\Sigma u_i = u_i^+ + u_i^-$, $\Sigma t_i = t_i^+ + t_i^-$; the signs "+" and "–" denote values concerned with the surfaces Γ_C^+ and Γ_C^- formed with a cut Γ_C (see Fig. 1). Indexes in notations correspond to the projections of vectors onto the axes of global coordinate system Ox_1x_2. The Einstein summation convention is used. Kernels of the integral equations are explicitly written in [7].

Approaching the field point $\boldsymbol{\xi}$ to the source boundary point $\mathbf{y} \in \Gamma$ of a solid and considering, that at a point $\mathbf{y}$ the curve Γ is smooth, similarly to [7] one can obtain from Eq. (1) the singular displacement integral equation:

$$\frac{1}{2} u_i(\mathbf{y}) = \int_{\Gamma_C^+} \left[U_{ij}(\mathbf{x},\mathbf{y}) \Sigma t_j - T_{ij}(\mathbf{x},\mathbf{y}) \Delta u_j \right] d\Gamma + \mathrm{RPV} \int_{\Gamma} U_{ij} t_j d\Gamma - \mathrm{CPV} \int_{\Gamma} T_{ij} u_j d\Gamma, \qquad (2)$$

where the notation RPV stands for the Riemann principal value, and CPV for the Cauchy principal value. As for the collocation point $\mathbf{y}$ that lays on a smooth part of

the cut Γ_C one can obtain the following integral equation:

$$\frac{1}{2}\Sigma u_i(\mathbf{y}) = \mathrm{RPV}\int_{\Gamma_C^+} U_{ij}\Sigma t_j d\Gamma - \mathrm{CPV}\int_{\Gamma_C^+} T_{ij}\Delta u_j d\Gamma + \int_{\Gamma}\left[U_{ij}t_j - T_{ij}u_j\right]d\Gamma. \quad (3)$$

Differentiating (3) by y_k, using Hook's law and considering, that $n_i^+ = -n_i^-$, the following integral equation is received:

$$\frac{1}{2}\Delta t_i(\mathbf{y}) = n_j^+(\mathbf{y})\left[\mathrm{CPV}\int_{\Gamma_C^+} D_{ijk}\Sigma t_k d\Gamma - \mathrm{HPV}\int_{\Gamma_C^+} S_{ijk}\Delta u_k d\Gamma + \int_{\Gamma}\left[D_{ijk}t_k - S_{ijk}u_k\right]d\Gamma\right], \quad (4)$$

where HPV stands for the Hadamard principal value (finite part) of an integral.

Integral equations (2), (3) and (4) are not enough for the solution of formulated problem. It is also necessary to develop the mechanical model of thin delaminated inclusion. Assume that the model of thin delaminated inclusion allows to receive the explicit form of the boundary functions Σu_i and Δt_i on Γ_C, i.e. to obtain expressions

$$\Sigma u_i(\mathbf{y}) = F_i^u\left(\mathbf{y}, \Sigma t_j, \Delta u_j\right), \quad \Delta t_i(\mathbf{y}) = F_i^t\left(\mathbf{y}, \Sigma t_j, \Delta u_j\right) \quad (i, j = 1,..,2). \quad (5)$$

Then the system of equations (2)–(5) is full for the solution of the problem.

The system of boundary integral equations (2)–(5) is solved numerically using the boundary element method [7]. Thus, the system of singular integral equations is reduced to the system of linear algebraic equations concerning the nodal values of the boundary functions t_j, u_j, Σt_j and Δu_j.

MODEL OF THIN DELAMINATED INCLUSION OR ELASTIC ENFORCING OVERLAY

The model of thin elastic inclusion $F_i^u(\mathbf{y}) = \tilde{F}_i^u(\mathbf{y})$, $F_i^t(\mathbf{y}) = \tilde{F}_i^t(\mathbf{y})$ satisfying the conditions of perfect mechanical contact with the medium is developed by the authors in the paper [5]. Basing on it the imperfect contact models are developed here.

Assume that thin inclusion is completely delaminated from the face Γ_C^- at the segments $\gamma_C^- \subset \Gamma_C^-$ (no contact tractions are considered at these segments). Then at the collocation point $\mathbf{y} \in \gamma_C^-$ the following boundary conditions are satisfied:

$$t_i^-(\mathbf{y}) = 0, \quad u_i^+(\mathbf{y}) = u_i^{i+}(\mathbf{y}) \quad (i = 1,2). \quad (6)$$

The first of the conditions (6) taking into account the used notations $\Sigma t_i = t_i^+ + t_i^-$ and $\Delta t_i = t_i^+ - t_i^-$ allow to obtain the first equation of the model of thin inclusion completely delaminated at the surface $\gamma_C^- \subset \Gamma_C^-$:

$$F_i^{t-}(\mathbf{y}) \equiv \Delta t_i(\mathbf{y}) = \Sigma t_i(\mathbf{y}). \quad (7)$$

As thin inclusion contact with one face (Γ_C^+) of a cut it is necessary to consider its tension, shear and bending along its axis. For this purpose the second equation of perfectly contacting inclusion model can be used. Assuming that the displacements of inclusion's median surface due to its small thickness are close to the displacements u_i^{i+} of the face Γ_C^+, one can obtain the second equation of the delaminating model at γ_C^-:

$$F_i^{u-}(\mathbf{y}) \equiv \Sigma u_i(\mathbf{y}) = \tilde{F}_i^u(\mathbf{y}) - \Delta u_i(\mathbf{y}). \tag{8}$$

Similarly, if inclusion is delaminated from the face Γ_C^+ at the segments $\gamma_C^+ \subset \Gamma_C^+$ for the collocation points $\mathbf{y} \in \gamma_C^+$ one can directly obtain the equation of model of the full delaminating at the segments γ_C^+:

$$F_i^{t+}(\mathbf{y}) \equiv \Delta t_i(\mathbf{y}) = -\Sigma t_i(\mathbf{y}); \quad F_i^{u+}(\mathbf{y}) \equiv \Sigma u_i(\mathbf{y}) = \tilde{F}_i^u(\mathbf{y}) + \Delta u_i(\mathbf{y}).$$

The model (7), (8) of inclusion completely delaminated from a face Γ_C^- are enough adequate and entirely suitable for modeling of thin elastic overlays with additional conditions of absence of a material in the domain, which borders with Γ_C^-, for example, for a traction-free surface $t_i^- \equiv 0$, $u_i^- \equiv 0$.

STRESS CONCENTRATION AT THE TIP OF THIN INCLUSION, WHICH IS IN PERFECT MECHANICAL CONTACT WITH THE MEDIUM

Consider the elastic equilibrium of the inclusion's end part under the assumptions that the inclusion tip is rounded and in the perfect contact with the medium. The reference coordinate system is depicted in Fig. 2. The equilibrium equation of the inclusion tip with the account of perfect mechanical contact conditions between inclusion and the medium are the following

$$\int_{-h(r)}^{h(r)} \sigma_{xx}(r, y)\, dy = -\int_0^r \Sigma t_x(r)\, dr. \tag{9}$$

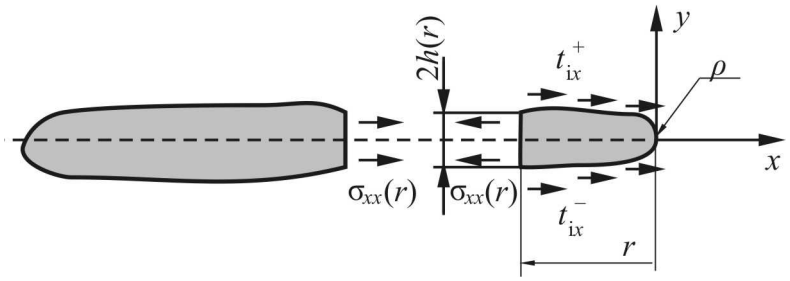

Fig. 2. Determination of stress concentration at the tip of inclusion

When $r \to 0$ the halfthickness equals $h(r) = \sqrt{r}\sqrt{2\rho - r} + O(r^2)$, where ρ is the rounding radius at inclusion's tip, and the left-hand side of (9) is possible to present in the approximate form

$$\int_{-h(r)}^{h(r)} \sigma_{xx}(r, y)\, dy \approx 2h(r)\sigma_{xx}(r).$$

Thus, the stress $\sigma_{xx} = \sigma_{xx}(r)\big|_{r=0}$ at the inclusion tip, according to (9) equals

$$\sigma_{xx} = -\lim_{r\to 0}\left[\int_0^r \Sigma t_x(r)\, dr\right] \Big/ \left[2h(r)\right] = -\frac{1}{\sqrt{2\rho}} \lim_{r\to 0} \sqrt{r}\Sigma t_x(r). \qquad (10)$$

For determination of stress σ_{yy} in a matrix at the thin elastic inclusion tip consider the strains of inclusion when $r \to 0$. One can simply write that

$$\varepsilon_{yy}(r) \approx \Delta u_y(r) \big/ \left[2h(r)\right],$$

thus,

$$\varepsilon_{yy} = \lim_{r\to 0} \Delta u_y(r) \big/ \left[2h(r)\right] = \frac{1}{\sqrt{8\rho}} \lim_{r\to 0} \frac{\Delta u_y(r)}{\sqrt{r}}. \qquad (11)$$

According to the Hook's law for an isotropic solid the stress σ_{yy} in a matrix at the tip of thin inclusion basing on (10) and (11) is as follows:

$$\sigma_{yy} = \frac{\sqrt{8}G}{(\kappa+1)\sqrt{\rho}} \lim_{r\to 0} \frac{\Delta u_y(r)}{\sqrt{r}} + \frac{(\kappa-3)}{(\kappa+1)\sqrt{2\rho}} \lim_{r\to 0} \sqrt{r}\Sigma t_x(r). \qquad (12)$$

Here κ is a Muskhelishvili constant.

According to the definitions of generalized stress intensity factors (SIF) [10]

$$\lim_{r\to 0} \sqrt{r}\Sigma t_x(r) = \frac{\sqrt{2}(\kappa+1)}{\sqrt{\pi}(\kappa-1)} K_{12}, \quad \lim_{r\to 0} \frac{\Delta u_y(r)}{\sqrt{r}} = \frac{\kappa+1}{\sqrt{2\pi}G} K_{11},$$

and from (10) and (12) the following relations are obtained

$$\sigma_{xx} = -\frac{\kappa+1}{\sqrt{\pi\rho}(\kappa-1)} K_{12}, \quad \sigma_{yy} = \frac{2}{\sqrt{\pi\rho}} K_{11} + \frac{\kappa-3}{\sqrt{\pi\rho}(\kappa-1)} K_{12}.$$

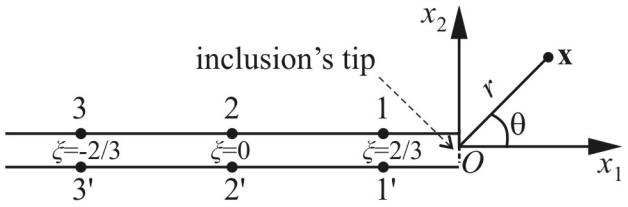

Fig. 3. System of nodes at the end boundary element

The lined modeling approach for thin heterogeneities allows to adopt the technique for calculation of the generalized SIF basing on the extrapolation of the boundary functions [5], which calculation formulas for the system of nodes 2-2', 3-3' (Fig. 3) at the end discontinuous boundary element are as follows:

$$K_{i1} = \frac{\sqrt{\pi} G \left(3\Delta u_j^{2-2} + \sqrt{15}\Delta u_j^{3-3} \right)}{4\sqrt{2J}\left(\kappa+1\right)} \ \left(i \neq j\right); \ \ K_{i2} = \left(-1\right)^{i+1} \frac{\sqrt{2\pi J}\left(5\Sigma t_i^{2-2} + \sqrt{15}\Sigma t_i^{3-3} \right)}{8\kappa_* \left(\kappa+1\right)}. \quad (13)$$

Here J is a Jacobian of the boundary element. For the application of expressions (13) it is necessary to use the values of functions Δu_i and Σt_i given in the local coordinate system depicted in Fig. 3.

EXTRAPOLATION TECHNIQUE FOR ESTIMATION OF THE INTEGRAL EQUATIONS SOLUTION SINGULARITY

The study of thin rigid inclusions completely delaminated from the medium at one face [6] has shown that the tractions near the tips of such inclusion possess not a square root as for a crack or elastic inclusion, but a stronger one, $O\left(r^{-3/4}\right)$ singularity. Consider the general extrapolation approach for determination of the type of a power singularity of the stress field. For this purpose approximate the values of boundary functions Δu_i and Σt_i at the system of nodes 2-2', 3-3' within the following functions

$$\Delta \tilde{u}_i = \delta_i r^{n_i^u}, \ \ \Sigma t_i = \chi_i r^{n_i^t - 1}. \quad (14)$$

Applying the least square method procedure one can obtain the following formulas for determination of unknown exponents in the approximations (14)

$$n_i^u = \log_{5/3}\left(\Delta u_i^{3-3'} / \Delta u_i^{2-2'} \right), \ \ n_i^t = 1 + \log_{5/3}\left(\Sigma t_i^{3-3'} / \Sigma t_i^{2-2'} \right). \quad (15)$$

The unknown factors δ_i and χ_i are estimated similarly:

$$\delta_i = \Delta u_i^{2-2'} J^{\log_{5/3}\left(\Delta u_i^{2-2'}/\Delta u_i^{3-3'}\right)}, \ \ \chi_i = \Sigma t_i^{2-2'} J^{\log_{5/3}\left(\Sigma t_i^{2-2'}/\Sigma t_i^{3-3'}\right)}.$$

NUMERICAL EXAMPLES

To show the efficiency of the proposed approach, consider a few variants of its possible application.

Thin inclusion completely embedded into the matrix with a perfect contact. To show the efficiency of application of the developed approach, consider a plane problem for the elastic unbounded medium containing thin rectilinear elastic inclusion of finite length. Relative rigidity of inclusion is characterized by the value of $k = E^{\mathrm{i}} / E^{\mathrm{m}}$, where E^{m} is the elastic modulus of matrix material, and E^{i} of inclusion one. The Poisson ratios of matrix and inclusion are assumed to be the same and equal $\nu^{\mathrm{i}} = \nu^{\mathrm{m}} = 0.3$. The problem scheme is depicted in Fig. 4. The thickness of inclusion equals 0.01 of its length. Generalized SIF are determined within the approach (13). The data obtained with the developed approach is compared with the results of direct calculations of thin rectangular inclusion of the corresponding size using the regularization BEM [11] with determination of generalized SIF using the approximation approach [12].

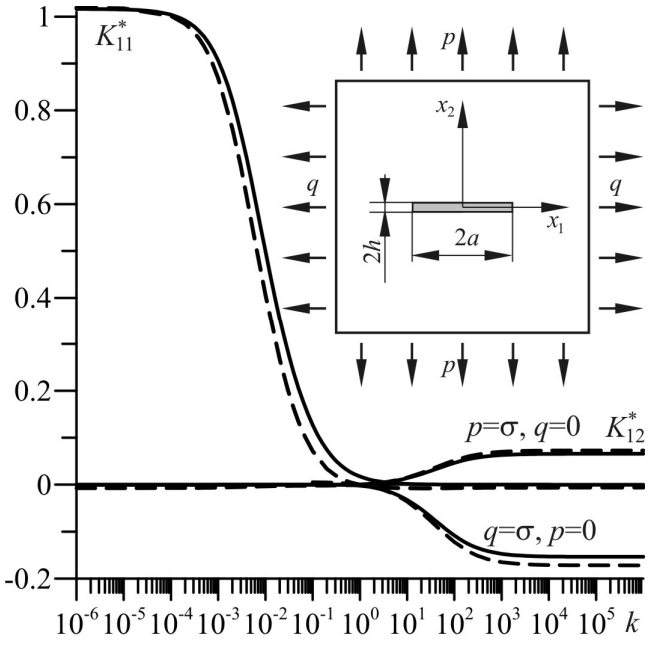

Fig. 4. Normalized generalized SIF $K_{ij}^* = K_{ij} \Big/ \left(\sigma \sqrt{\pi a} \right)$ of thin elastic inclusion

The results of the numerical analysis of a problem using the specified approaches are plotted in Fig. 4. Continuous lines correspond to the proposed method that is based on the thin inclusion model [5], and dashed one to the direct calculations of thin rectangular inclusion using the regularization BEM.

For the cases close to the limit values of inclusion's relative rigidity k (zero, one, infinity), the deviations of generalized SIF calculated for a crack and absolutely rigid inclusion using the proposed approach from the analytical solution is less than 1.2 %. Generalized SIF obtained using the direct method for very soft and very rigid

inclusions differs from the analytical one a little more: 2 % is a deviation for the case of a crack and 5.3 % for absolutely rigid inclusion. Such results are caused by the influence of a real nonzero thickness of inclusion, and also the intermediate asymptotic, that depends on the size and the shape of inclusion's tip. In general, Fig. 4 shows a good agreement of the results of thin inclusion study using the model [5] and a direct approach. Though, the latter gives bigger generalized SIF values for rigid inclusions, and smaller for soft ones. Thus for the latter the proposed approach gives certain "safety factor".

One-side completely delaminated thin elastic inclusion. Consider the previous example under the condition that the inclusion is completely debonded at Γ_C^- from a matrix, and perfectly contacts with it at Γ_C^+. At the infinity the following load is applied: $p = \sigma$, $q = 0$. When the inclusion's relative rigidity varies from zero to one, the singularity of the solution should be the same as for a crack, which is a square root one. With the increase in inclusion's relative rigidity the singularity should become the $O\left(r^{-3/4}\right)$ one [1, 6]. Consider the change of solution's singularity depending on the inclusion's relative rigidity k using the extrapolation formulas (15) basing on the nodal values of the boundary function Δu_2. Numerical results of this study are presented in Table 1.

Table 1. The change of an exponent n of stress field singularity $O\left(r^{n-1}\right)$

k	n with (15)	n (theory)	Relative error, %
0 (10^{-10})	0.444	0.50	11.2
1	0.403	0.50	19.4
∞ (10^{10})	0.225	0.25	10.0

Table 1 shows that the estimation of solution singularity for the limit cases of inclusion's relative rigidity gives the error of about 10 % that is small enough with the account of complexity of direct numerical methods application for the determination of the stress field singularity. For a homogeneous case ($k = 1$) the singularity estimation error is bigger because the basic influence in this case has the reduced rigidity kh/a. In general, with the account of the chosen polynomial base functions, extrapolation approach (15) gives results good enough to serve as the auxiliary tool for the theoretical study of solution's singularity, and also for the choice of the appropriate base functions for modeling of inclusion's end boundary elements.

Partially enforced hole. In the work [13] the practical importance of study of holes enforced with thin overlays is shown and the approach for the research of curvilinear holes, which can be mapped onto the unit circle with the function $\omega(\zeta) = R_0\left(\zeta + \varepsilon/\zeta^{N+1}\right)$, is proposed. This approach allows studying symmetrically enforced holes with the shape of regular polygon with rounded vertices. The model of an overlay set by expressions (7) and (8) is free of these restrictions and allows studying partially enforced holes of arbitrary shape, and also solids with thin surface overlays and stringers.

As an example, consider the distribution of hoop stresses $\sigma_{\theta\theta}$ at the circular hole, which is symmetrically enforced along the half of the circle with the opened stiffening rib. The scheme of the problem and the dependence of hoop stresses on a polar angle θ and overlay's relative rigidity k are depicted in Fig. 5.

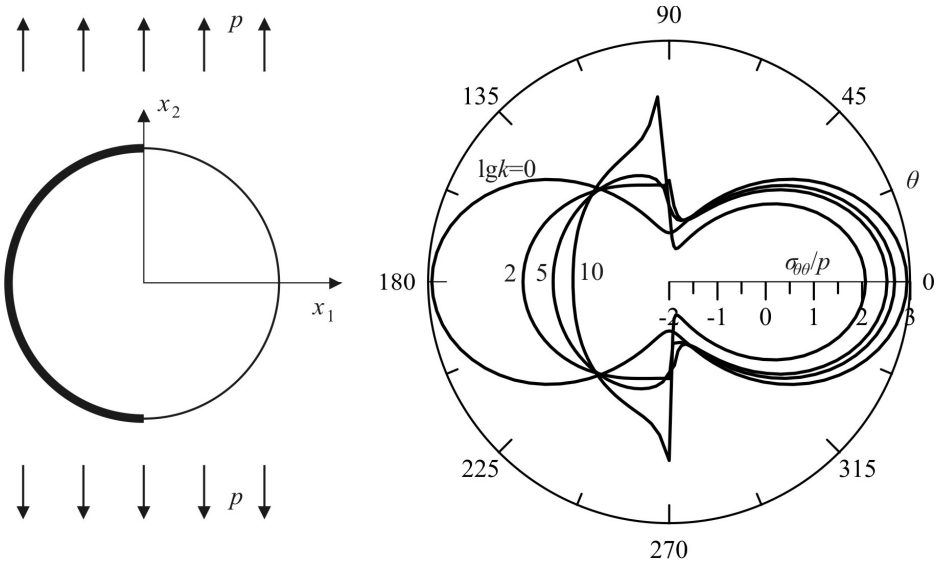

Fig. 5. Hoop stresses $\sigma_{\theta\theta}$ at a hole enforced with a thin overlay

Fig. 5 shows that the increase in enforcement's relative rigidity causes the reduction of stress concentration, given by the Kirsch problem solution; and mostly at the enforced part of a hole. The desired notable effect of stress concentration reduction is provided with the overlay's relative rigidity of $k = 10^2 \div 10^5$ (for its halfthickness $h = 0.01R$, where R is a radius of a hole). However, it is necessary to simultaneously take into account that with the increase in overlay's relative rigidity k the increase in hoop stress concentration is observed under an overlay near its end faces. This is explained with the occurrence of the square root singularity of stress field, the same as for the problems of rigid stamps indention.

CONCLUSION

The authors' approach for studying of solids containing thin elastic perfectly embedded inclusions is extended to the case of delaminated inclusions and elastic enforcing overlays. Basing on the simplified model of thin elastic inclusion the relations between generalized stress intensity factors and stress concentration at the rounded tip of thin inclusion are obtained. The extrapolation approach is developed for the numerical estimation of a power singularity of hypersingular integral equations solution. The numerical examples are presented to show the possible application of the proposed approach for the analysis of a wide class of problems.

REFERENCES

1. Alexandrov V.M., Smetanin B.I., Sobol B.V.: *Thin stress concentrators in elastic solids*. Moscow 1993. (in Russian)

2. Aliabadi M.H., Saleh A.L.: F*racture mechanics analysis of cracking in plain and reinforced concrete using the boundary element method*. Eng. Fract. Mech. 2002, 69, P. 267–280.

3. Leite L.G.S., Venturini W.S.: *Boundary element formulation for 2D solids with stiff and soft thin inclusions*. Eng. Anal. Bound. Elem. 2005, 29, P. 257–267.

4. Padron L.A., Aznarez J.J., Maeso O.: *BEM–FEM coupling model for the dynamic analysis of piles and pile groups*. Eng. Anal. Bound. Elem. 2007, 31, P. 473–484.

5. Pasternak I.M., Sulym H.T.: *Dual boundary element method in the problems of thin inclusions theory*. Proc. Int. Conf. “In-Service Damage of Materials, its Diagnostics and Prediction”, Ternopil 2009, P. 137–143. (in Ukrainian)

6. Popov G.Ya.: *Concentration of elastic stresses near stamps, cuts, thin inclusions and enforcements*. Nauka, Moscow 1982. (in Russian)

7. Portela A., Aliabadi M.H., Rooke D.P.: *The dual boundary element method: Effective implementation for crack problems*. Int. J. Numer. Meth. Engng. 1992, 33, P. 1269–1287.

8. Reissner E.: *Note on the problem of the distribution of stress in a thin stiffened elastic sheet*. Proc.of the National Academy of Sciences 1940, 26, P. 300–305.

9. Riederer K., Duenser C., Beer G.: *Simulation of linear inclusions with the BEM*. Eng. Anal. Bound. Elem. 2009, 33, P. 959–965.

10. Sulym H.T.: *Bases of mathematical theory of thermoelastic equilibrium of deformable solids with thin inclusions*. Research-and-Publishing Center, NTSh, Lviv 2007. (in Ukrainian)

11. Sulym H.T., Pasternak I.M.: *Regularized Somigliana identity for elastic problems with thin shapes.* Herald of Lviv university 2007, 13, P. 142–150. (in Ukrainian)

12. Sulym H.T., Pasternak I.M.: *Determination of the limit state parameters of elastic solids containing thin inclusions basing on the numerical solution of the problem*. Herald of the Ternopil state technical university 2009, 14(1), P. 15–22. (in Ukrainian)

13. Syaskyy A.O., Batyshkina Yu.V.: *Partial symmetric enforcement of curvilinear hole in the unbounded plate*. Herald of the Ternopil state technical university 2004, 9(2), P. 5–12.

ZESZYTY NAUKOWE POLITECHNIKI RZESZOWSKIEJ NR 274
Mechanika z. 81 2010

Victor SHABAYCOVITCH

Lutsk National Technical University, Ukraine

COMPETITIVENESS OF MANUFACTURE

In crisis, the competitiveness edge of a claimed produce acquired a special value. The paper considers the structure of competitiveness as a unity of quality, expenditure, profit and prices; describes method of forming competitiveness. It exemplifies an erroneous interpretation of competitiveness and methods of its "rapid determination". To analysis and synthesize an integral level of competitiveness, one may use the SADT method of detailed step-be-step hierarchy of the objects under study.

INTRODUCTION

In the conditions of crisis, the competitiveness of produce acquires a special significance, as only competitive products, equipment and processes will be claimed on the part of both consumer owing to a high quality and acceptable prices and producers in view with lower costs and a possibility of creating work places. In machine-building as ultimately in other industries of the national economy, the produce, technological processes and processing equipment a single complex providing competitiveness. Hereby, a temporary decrease in profit will be a must. Output of other produce will result in its non claiming, warehousing, stagnation of production and aggravating of the crisis. Competitiveness is favorably influences favourably, it is the unique index and recipient furthers the perfection. Competitiveness, as is generally known, is a property of objects that is characterized by a degree of real or potential satisfaction of a particular need as compared to analogous objects on a certain market [1]. Competitiveness is an integral value characterizing the attractiveness of products for the user and profitability for the produce. It is difficult to talk about the competitiveness of products with the a high cost of product output, but even at acceptable expenses, yet considerable operating expenditure or a high cost of produce competitiveness of produce can a become doubtful. A concept of competitiveness is a compromise between the producer and customer.

It is known that a competition (*lat*. *concurre* to be a rivals) is interpreted as a fight between the participants of market management for the most profitable conditions of production, purchase and sale of produce and services, as well as appropriation of maximum profits [1,2]. A competition is a self - regulator of economy with the functions of regulation, allocation, adaptation and controlling. The object of competition is the customer and producer, its subjects being enterprises, industries, regions, whole countries.

Statistics a note [2] that only 10% developed technologies and constructions are put into operation, others in of view of a low-level competitiveness are rejected. A

similar is the put situation with technological equipment, especially automatic. Most publications on this subject are concentrated on the establishment of ready made produce competitiveness, although a of greater importance is the forming competitiveness in the process.

STATEMENT OF PROBLEM

The method of determining the level of competitiveness consists in the following. The information for necessary determining the level competitiveness includes the indices of quality, all kinds of cost, profit and the price of sale (Fig. 1). Depending on whether this is produce, a process or major indices of quality (1) are set. Further on production (2) and operating (3) cost, profit (4) and price of sale (5) are calculated. These addends constitute the sun total these elements make necessary of the data necessary to the determine level of competitiveness (6). Following which, a reasonable choice of the prototype (7) results in developing the comparison index to determine competitiveness (8), cost (9), profit and the sale price (10) of the developed product, process or service (6) with the prototype (7) is it possible to get (11) partial integral levels of competitiveness (12) and comparison (13) as well as the integral level of the produce competitiveness (14). The presented factors and work with them are the well known points of determining a level competitiveness. The exclusion of any of the factors from consideration does not make it to estimate even approximately the level of competitiveness, let alone a whole group of factors, such as cost, price etc. The same goes for the absence of a prototype. For example, having a product with the complete list of both indices of quality and of cost, into fit and the price of sale, but for lack of the prototype it is impossible to judge about its competitiveness as at the market can offer to products-prototypes with both the better and the worse information, necessary for such determination.

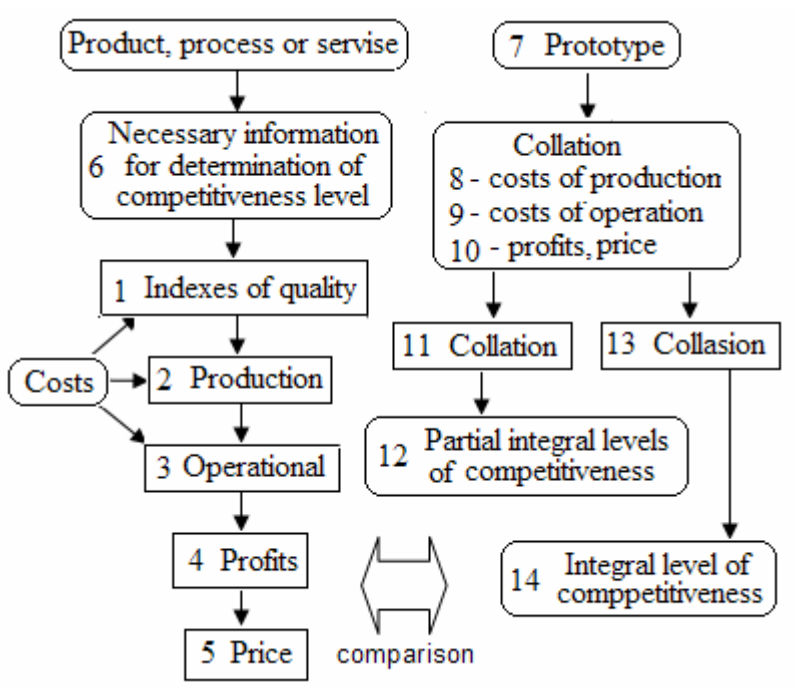

Fig. 1. Diagram of determination of level competitiveness

The mechanism of forming the competitiveness of products is to provide for revealing and determining the influence of all the factors of their production, sale and exploitation relatively combined in seven groups. Expenses, related to making the produce on design, technological and production levels, belong to the internal factors corresponding to the construction - technology - making and the quality. It is known

clan that the very design of the product is the basis for its competitiveness. Never once has any low quality and difficult to make produce been competitive. The mechanism of forming competitiveness is at that based on the application of the concept of virtual development, making and exploitation of the product, i.e. preliminary modeling of these processes on a computer and obtaining virtual constructions, technologies and exploitation and, on these grounds, - estimation of competitiveness. At positive results and further already real development it is possible to still more enhancing both the indices of quality and the level of competitiveness. The virtual planning and exploitation require special and costly programs rare as a complex so far.

INTRODUCED ERROR IN DETERMINATION OF COMPETITIVENESS

The method for advance estimation of quality and competitiveness of products was published in paper [3]. However, the process of competitiveness management is hampered by its misinterpretation as well as methods of estimation occasionally occurring in some publications. So, in works [4,5] published in *Poland* (2007) and *Slovakia* (2008) the *«rapid method»* of determining the competitiveness of flexible manufacturing systems (*FMS*) and technological processes on the proposed «criteria» whose values should be put in simple arithmetic formulas of the deformed averages and to obtain the result of the competitiveness level. Such a saluting to the problems is tempting. What is the point in exploiting the sophisticate familiar methods requiring numerous calculations, if the same result is arrived at quickly without the account of concomitant cost, basic indices of quality and even in the absence of the prototype?

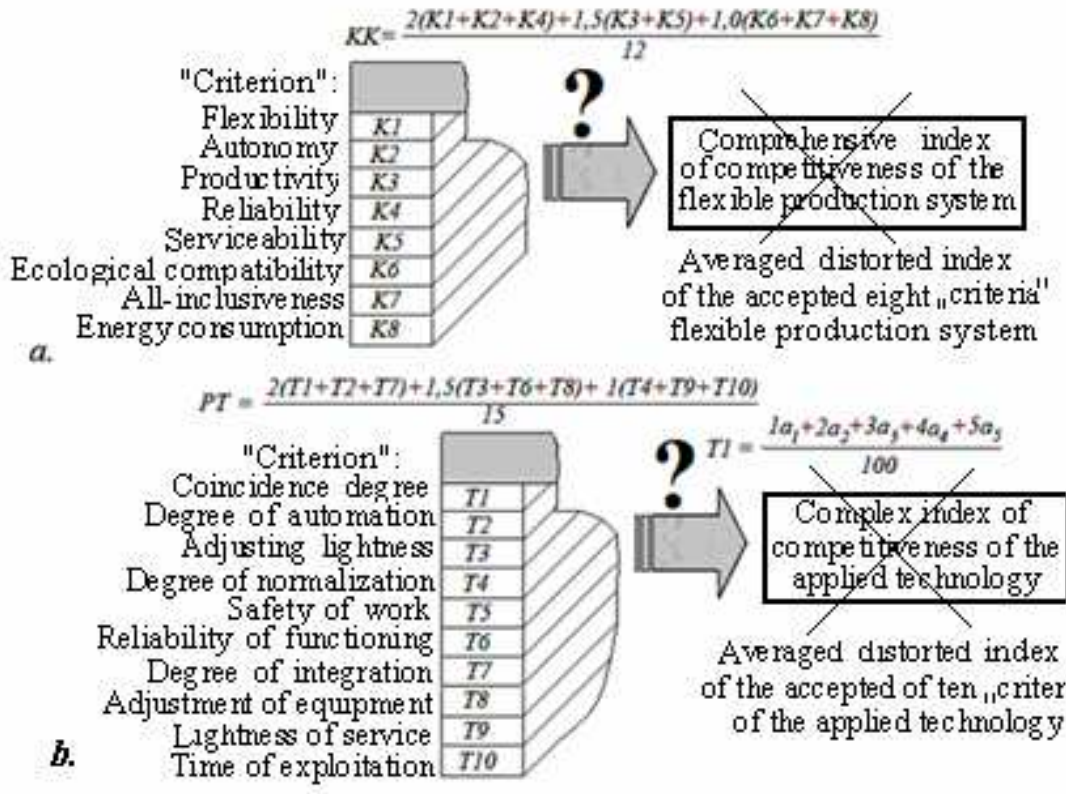

Fig. 2. Diagram of mistaken determination of «level competitiveness» on methods [4, 5]

The proposed «*rapid method*» consists in the following. On the strength of the row of «criteria», having pointage estimations within the limits of 1-5 and the averaged deformed formulas in which it is necessary to put them and values obtained, the «complex index of competitiveness» is determined. Distortion of average data is obtained due to the increase of the number of values in the denominator and the introduction of the coefficients of scales for two groups of the selected «criteria». The proposed formulas for the estimation of *FMS* competitiveness take into account eight «criteria» only: flexibility, autonomy, productivity, reliability, serviceability, ecological compatibility, and complexity and power consumption (Fig. 2*a*) which in any way can not be the criteria of competitiveness. At the sometime, the determinations of these «criteria» and their pointage estimations are erroneous, although these ore well-known determinations. For example, by flexibility an indirect index visa a degree of the use of time during the implemenfection of varies tasks, although it is common knowledge.

That flexibility is a possibility for purposeful change of technological actuality within the range of changing the regulative parameters, i.e. a possible number of the processed products or their nomenclature. An autonomy is for some reason defined as the time during which the *FMS* an operate unattended, although it's common knowledge, that an autonomy is independence, however, not of the maintenance staff. The productivity is not a correlation of the cost of the ready-made products for a certain period of time to the sum of the allocation costs related to the exploitation neither is reliability a correlation of the average time of shutdown to the useful fund of time [4] etc. Amusing is also the determination of ecological compatibility as a correlation of the mass of debris to that the ready-made products, although it is known that one should take into account not number of the debris, but their harmfulness for the environment. A most all of the «criteria» have the same illiterate definitions.

For the applied technology ten «criteria» are propose [5]: contemporaneity, automation possibility, simplicity of readjustment, degree of normalization, operating safety, reliability of functioning, extent of integration, adaptability of the equipment, easiness of service and term of use (Fig. 2*b*). By the way, many definitions of «criteria» are also erroneous, although these are long settled down terms. For the estimation of the applied technology for the productivity, accuracy, labor output ratio and other criteria are absent for some reason. Firstly, many factors determining competitiveness are not taken into account in these methods. Specialists know that competitiveness is determined by quality, production and operating costs, profits, price when compared to a prototype. For some reason, important indices without which on the whole it is impossible to fudge about competitiveness are not reflected here. These are, for example, technical level, accuracy, standardness, stability, material capacity, transportability, maintainability, efficiency, longevity, safety, diagnostic ability, controllability and also production and operating costs, price, terms of supply, after-sale service etc. Completely comparing absents to the prototype. Secondly, if in the given formulas for the weight of the «criteria», absurd results will be obtained. For example, a *FMS* variant with a good flexibility, autonomy, productivity and reliability is equivalent to a variant with useless «criteria» like these, but has a high serviceability, ecological compatibility, complexity and low energy consumption. Such a «rapid» result is proof of a total uselessness of the method. Such a «rapid method» helps only erroneous estimations for the competitiveness of products,

processes and equipment. The erroneousness of the «rapid method» is obvious from the comparison of Fig. 1 and 2.

DETERMINATION OF COMPETITIVENESS BY *SADT* - DIAGRAMS

With the purpose to optimize of providing the level of competitiveness at lowered costs can apply the method *of SADT* (*Structured Analysis and Design Technique*) of detailed the successive hierarchy of the objects under study. On these hierarchical levels, the analyzed object is examined greater in detail, equivalently to the previous level; functions and blocks of realizing the tasks set are determined. Influence of the environment is taken into account too. Simultaneously, the methods of dismemberment are wholly determined by the purpose set, and are not elated *SADT*-method. The application of this method is related to the realization of the multivariable process of determining the integral level of competitiveness on the accepted set of the operating factors with their optimization.

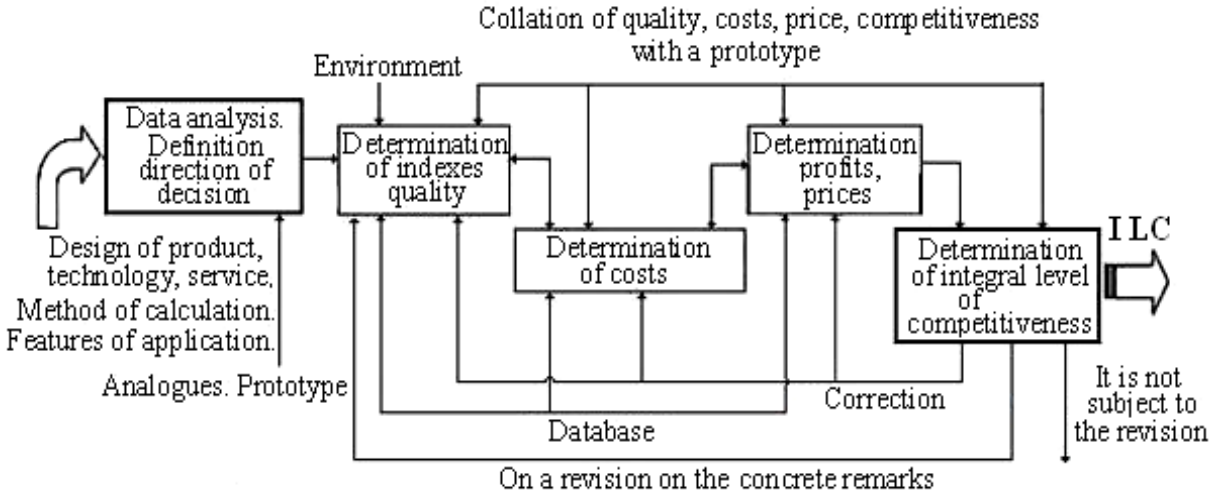

Fig. 3. *SADT*- diagram of initial stage of determination of level competitiveness (*ILC*)

The *SADT*- diagram of entry level (Fig. 3) takes into account the basic data, which are drafts of products, structure of the process or service, specificity of application, as well as analogues and the prototype, means of meeting the ands set and the output data. The method are supposes the use of four basic functions: determination of indices for the quality of product, process or service, concomitant costs, profit and the price of sale. On the basis of the input data, taking into account the influence of external environment, fundamental indices of quality are determined. Simultaneously, these indices are determined on the basis of operating requirements with due account of the analogical ones in the prototype which must be the best. Further calculated are production, extra-production and operating concomitant costs, income and the price of sale are determined. By the well known formulas [6] necessary data are calculated and comparison is made with the analogous ones in the prototype, whose basis the integral level of competitiveness of the object is determined. If the level appears to be somewhat lower, but can be made higher, the product, process or service are sent to revision or, in the opposite case, rejected.

SUMMARY

The generally accepted method of determining the level competitiveness envisages an obligatory taking into account of the indices for quality, development costs, introduction and exploitation, technological prime cost of the products made on it when compared to a prototype. Management of the competitiveness of products, technologies and equipment especially in the conditions of crisis except for marketing and application of the mechanism of directed forming envisages a reorganization of conducting of designer, technological and production works with the purpose of increase quality of indexes with at reduction of production costs due to the optimization of all links of the production chain, co-operation and specialization. The same goes for the reduction operating costs. Acceptability of the cost of products in the time of crisis must be provided due to marketing, management and diminishing of the expected profit. Nonproductive costs can be reduced by reorganizing of the infrastructure, deliveries, advertising etc, especially removals of unplanned expenses in the forms of bribes, recoils etc. Special place is occupied by the legal norms of enterprise, tax-reduction, profit regulation, legal assistance, inflation, sponsorship etc.

In this connection one can profit from the experience of the huge China and small Switzerland successfully reorganizing a productions, diminishing concomitant costs, reducing release prices, combating corruption, creating favorable conditions for production and business.

REFERENCES

1. Kuzmin O.S., Horbal N.I.: *Management of the Enterprise an International Competitiveness*. Lviv: KOMPAKT-LV, 2005. - 304c. (in Ukrainian).
2. Volchkevich L.I.: *Competitiveness of the Automatic Assembling in a Discrete Production.* Proceedines of the IV International conference «Module Technologies and Constructions in the Technology of Machines». - Rzeszow, 2006. P. 9-14, (in Russian).
3. Shabaykovich V.A., Grigorjeva N.S.: *Advance estimation of the Quality and Competitiveness of Products*. Proceedings of the 15-th International Conference. Vol 4. Donetsk, 2008. P. 3-6, (in Russian).
4. Lunarski E., Stadnicka D.: *Estimation of Competitiveness Level of the Applied Technology*. Technology and Automation of Assembling. Issues 2-3, - Warsaw, 2007. P.25-29, (in Polish).
5. Lunarski E.: *Determination of the Competitiveness of Flexible Manufacturing Systems*. Acta Mechanica, Slovakia 2-A, 2008. P. 381-386. (in Russian).

ZESZYTY NAUKOWE POLITECHNIKI RZESZOWSKIEJ NR 274
Mechanika z. 81 2010

Ján SLOTA
Ivan GAJDOŠ

Technical University of Košice, Slovakia

NUMERICAL SIMULATION OF THE HYDRAULIC BULGE TEST OF HSLA STEEL AND EXPERIMENTAL VERIFICATION OF RESULTS

In sheet metal forming operations the mechanical properties of the sheet metal (stress-strain curve, flow stress) greatly influence metal flow and product quality. Accurate determination of the stress-strain relationship is important in process simulation by finite element method. In this paper the sheet thickness gradation in different points of the hemisphere formed in the bulge test is analyzed, both by simulation and experimentally. A precise determination of sheet thickness at the pole is very important in the precise determination of stress-strain relationship. The aim of this paper is to show on some aspects of numerical simulation of hydraulic bulge test and experimental verification of obtained results.

1. Introduction

New vehicle structures should comply with severe crash requirements. To build a safe vehicle structure, it is necessary to select the optimum material for a given application. To do this requires a detailed understanding of dynamic material properties in both the as - rolled and formed condition. Advanced testing and CAE facilities are used in order to understand and improve the crashworthiness of it's materials. To understand the interactions between material, manufacturing process and design, authors uses impact facilities capable of testing some materials as well as real components [1].

The new microalloyed steels called also High Strength Low Alloy (HSLA) are becoming increasingly recognized as offering both cost savings and high performance for use in formed products. They find wide application in automotive, off-highway and similar original equipment industries. High-strength steel allows the user to increase the strength of the finished component or reduce the steel thickness, or both. The material plastic behaviour, joining and material failure (cracking) are included in impact research on vehicle sub-structures in automotive industry.

The paper deals with evaluation of mechanical and plastic properties of steel sheet with higher strength properties. To validate the application of material data in the engineering stage, authors use advanced CAE tools validated through experimental

testing. The results of the tests were used as the input data for simulation of deep drawing of drawn part with specified shape and dimensions. Simulation of bulge part by PamStamp software was realized. The results of simulation were verified by actual experiments. Tool design and forming process conditions were also verified by means of simulation with the aim of achieving the required quality.

2. Methods of experimental work

2.1. Experimental material

Steel sheet of new conception used in automotive industry were evaluated during experimental works, microalloyed steel H220PD with thickness a_0 = 0,80 mm.

Evaluated steel sheet was fully hot-dip galvanized, with amount of zinc of 100 g/cm^2.

The yield strengths exhibited with these materials range from 350 to 800 MPa without heat treatment. These strength capabilities make HSLA steels an economical alternative to quenched-and-tempered alloy steels. Microalloyed steels usually have carbon contents, manganese, silicon and either small amounts of vanadium, columbium (niobium), titanium or nickel and molybdenum in various combinations. Chemical composition of experimental materials is shown in Tab.1.

Tab. 1. Chemical composition of evaluated steels [%]

	C	Mn	P	S	Ti	Si	Al	Cr	Cu	Nb	Mo
A	0.004	0.415	0.042	0.004	0.037	0.1	0.035	0.031	0.011	0.026	0.005

2.2. Uniaxial tensile test

Evaluation of material formability of experimental material was realized by tensile test (STN EN 10002-1), test of planar anisotropy (STN 42 0437), test of normal anisotropy ratio (STN 42 0435) and test of strain hardening exponent (STN 42 0436). Significant directions of 0°, 45° and 90° against direction of rolling were tested during testing of drawability parameters. Tensile specimen according to STN EN 10002-1, L_0 = 80 mm was used for all mentioned tests. The tests were realized on the tensile machine TiraTEST 2300 with recording of the process. Interval of strain hardening exponent evaluation was within the range of uniform deformation of 5 – 20% for both tested sheets. Values of mechanical properties, degree of their planar anisotropy, coefficient of normal anisotropy and strain hardening exponent are shown in Tab.2. [2]

Tab. 2. Parameters of material drawability of microalloyed steel H220PD

	Direc-tion	$R_{P0.2}$ [MPa]	R_m [MPa]	A_{80} [%]	$PR_{P0.2}$ [%]	PR_m [%]	PA_{80} [%]	r	r_m	Δr	n	n_m	Δn
H220PD	0°	219	385	34.5				1.172	1.640	0.285	0.235	0.231	0.001
	45°	225	368	37.4	2.76	-4.29	8.24	1.782			0.231		
	90°	238	382	35.8	8.38	-0.69	3.67	1.823			0.229		

2.3. Biaxial bulge test

Bulge test (Fig. 1) was realized for the purpose of comparing the curves of hardening from uniaxial tensile test and biaxial tensile test. The hydraulic bulge test can better describe the plastic properties of a sheet metal at large strains (Fig. 3)[3,4].

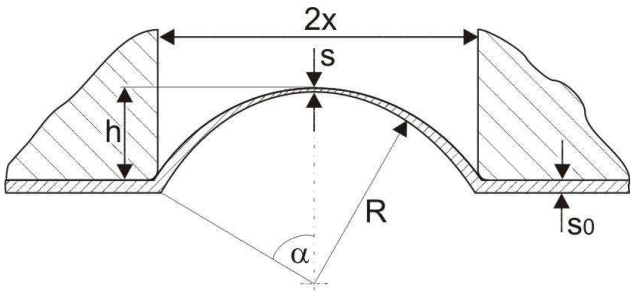

Fig. 1. Geometric parameters of hydraulic bulge test [5]. R- radius of curvature, s_0 – initial thickness, s- actual thickness, x-half of die aperture, h- bulge height

Fig. 2. Example tested specimens for HSLA H220PD steel sheet material (sample not burst)

To set the standards for material formability and expansion and to deliver reliable material data to the industry, the Department of Technologies and Materials at The Technical University of Kosice has developed and implemented the biaxial bulge test. This test can be used to determine the formability of various materials with thickness up to 1 mm.[5] Fig. 2 shows the tested sample of HSLA steel sheet material. Industrial pressure transmitter DMP 333 to measure the bulging pressure up to 250 MPa and linear gage to measure dome height were used for the test. Measuring devices were calibrated before the test to ensure accurate measurements.

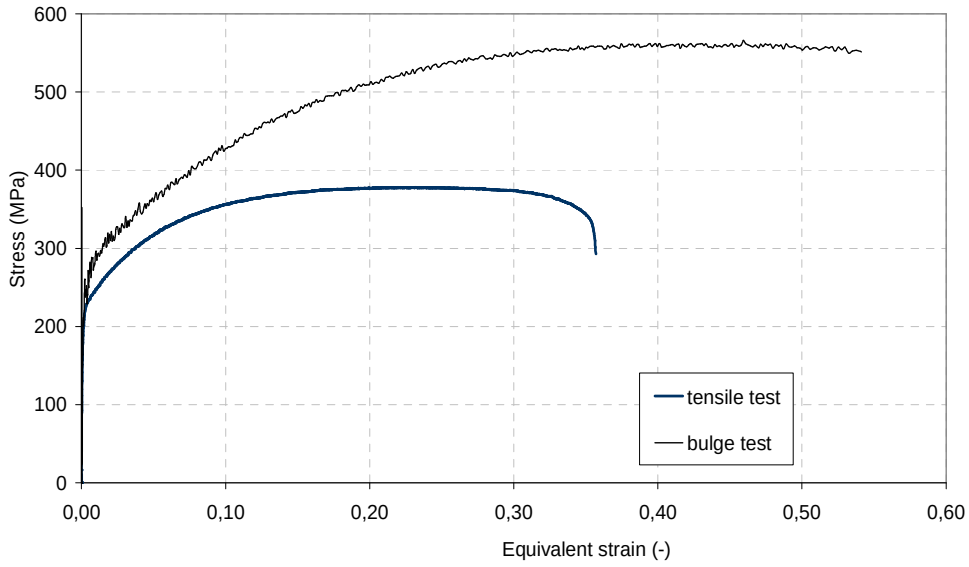

Fig. 3. Uniaxial and biaxial stress-strain curves of HSLA H220PD steel sheet material

2.4. Numerical simulation of the hydraulic bulge test

Hardening curve was estimated on the base of tensile test results. Simulation software PamStamp2G was used where specification of hardening curve model according to Krupkowsky was chosen:

$$\sigma = K.\left(\varepsilon_0 + \varepsilon_p\right)^n \tag{1}$$

where: σ is the stress, K is the strength index, ε_0 is the offset strain, ε_p is the plastic strain and n is the strain hardening index.

Isotropy model of strain hardening (the center of plasticity plane is constant and it is changing the size) was chosen for the calculation. The model is describing the change of plasticity plane (curve) in dependence on change of plastic deformation (or deformation rate). Hill48 material law for orthotropic materials was used for condition of plasticity, which determines curve form of plasticity in the main stresses area:

$$\sigma_{Hill48} = \sqrt{\frac{1}{2}\left(H\left(\sigma_{11}-\sigma_{22}\right)^2 + F\left(\sigma_{22}-\sigma_{33}\right)^2 + G\left(\sigma_{33}-\sigma_{11}\right)^2 + 2N\sigma_{12}^2\right)} \tag{2}$$

where: σ is the stress, F,G,N are Hill´s coefficients.

Fig. 4 shows a sample pressure vs. time curve for HSLA H220PD steel from which the burst pressure was obtained. The burst pressure was about 145 bar for tested specimens.

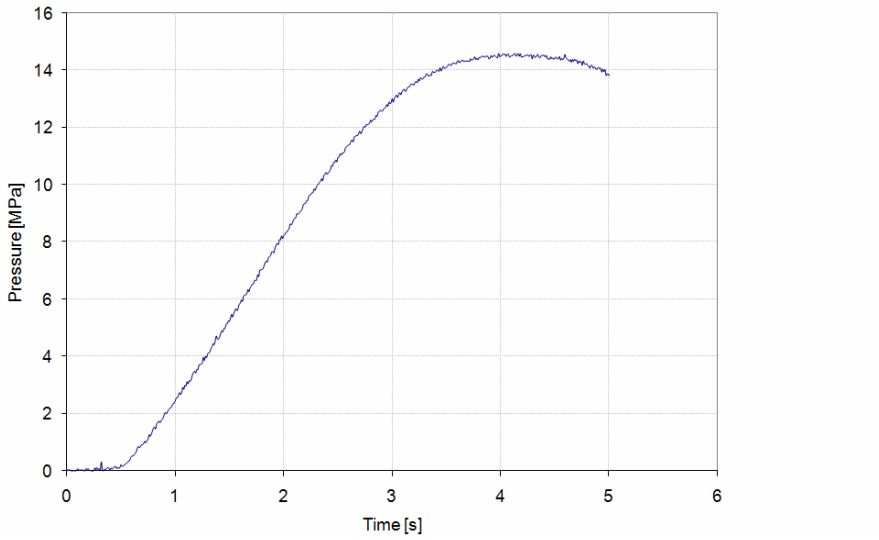

Fig. 4. Experimental pressure vs. time curve of HSLA H220PD steel sheet material

The numerical simulation of the hydraulic bulge process was performed. The material properties for determining of material model were obtained from uniaxial tensile test. FEM simulations and experiments have been performed in order to study the interrelationship of the geometric and material variables such as dome wall thinning, dome height and limit strains. From the study the limit strains and dome wall thinning under biaxial deformation conditions has been determined, both simulation (Fig. 5-6) and experimentally.

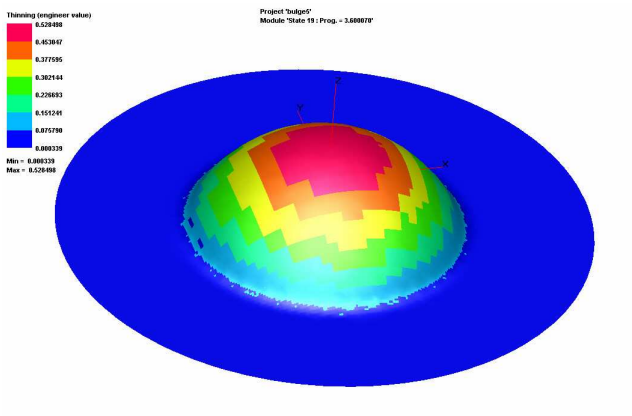

Fig. 5. Critical amount of thinning in a HSLA sheet metal before failure

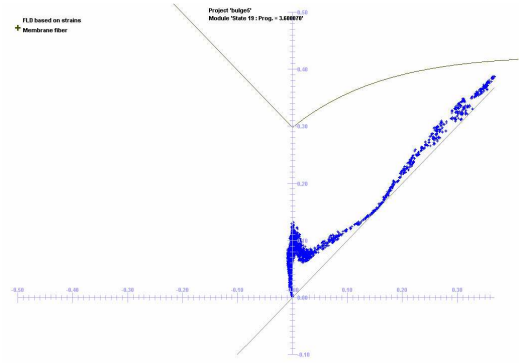

Fig. 6. Forming Limit Diagram (FLD) of HSLA steel sheets in same phase as show previous figure

3. Reached results and discussion

The results from numerical simulation with the experimental results from hydraulic bulge test were compared. Verification of simulation results mainly on local thinning of material was focused. Figs.7 -10 show a comparison of thickness distribution on dome of bulged profile obtained by hydraulic bulge test and from numerical simulation.

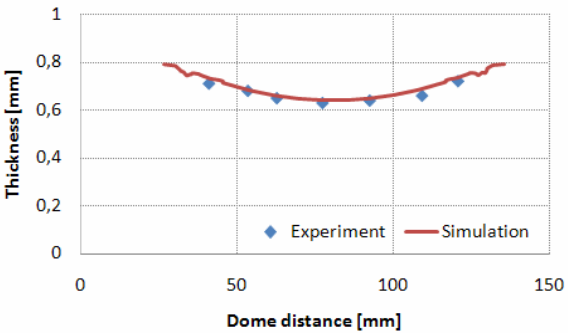

Fig. 7 Comparisom of numerical simulation with experiment, dome height h = 16 mm

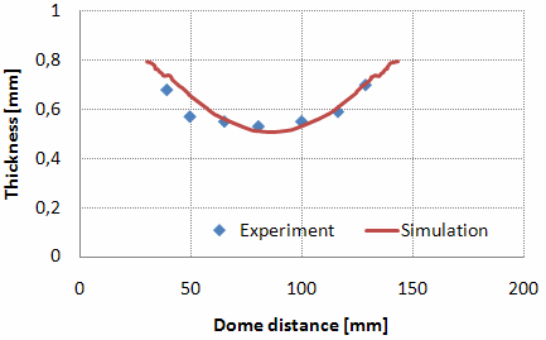

Fig. 8 Comparisom of numerical simulation with experiment, dome height h = 21 mm

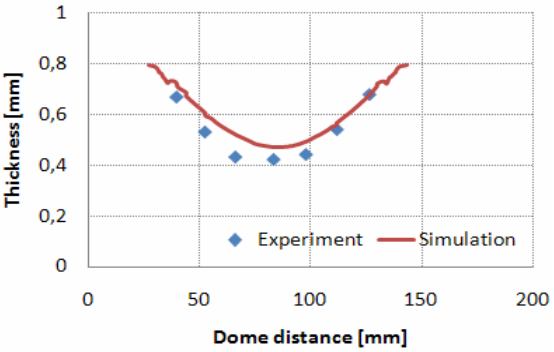

Fig. 9. Comparisom of numerical simulation with experiment, dome height h = 25 mm

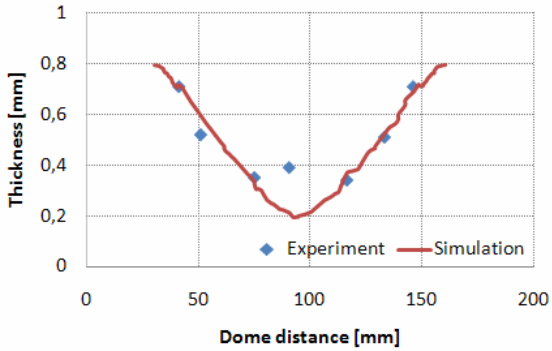

Fig. 10. Comparisom of numerical simulation with experiment, dome height h = 32 mm

No considerable variation of the thickness distribution between results from experiment and simulation, respectively, was observed. Material thinning from 1,5 to 3,9 % at lower strains was measured, while thinning in total range of deformation was up to 10 %. The results of simulation, which are shown in Fig. 7-10, mostly a few overestimate the results obtained from experiments.

Results comparison of simulation and actual experiment confirms results of simulation. Predicted thickness distribution of bulged profile from H220PD HSLA sheet material was observed. Thus, the material law and yield criterion used in simulation concept seems to be convenient.

4. Conclusions

On the base of realized experimental works, simulation and actual experiment, following conclusions can be formed:

1. The strain distributions of HSLA steel sheet on real bulged profile correspond with results from numerical simulation.

2. Deformation is localized in central area of bulged hemisphere, this result confirm known fact from literature.

3. The results from numerical simulation overestimate real thinning from 1 to 10 %, at lower strains only 1,5-3,9 %.

4. Variations between simulated and experimentally measured values can result from measurement inaccuracy.

5. Krupkowsky power law and Hill48 yield criteria provide strain predictions that seems to be convenient, the other material law and yield criteria needs to verify.

6. Verification of the numerical simulation of hydraulic bulge process of HSLA steel sheet by experiment is possibly to state, that prediction of bulge process by numerical simulation quite accurately showed possible issues at production.

REFERENCES

1. Kvačkaj T.: *Výskum progresívnej ocele nielen pre automobilový priemysel*. Strojárstvo č 5,6 (2006) p. 12-13
2. Hudák J., Tomáš M.: *Hodnotenie materiálovej tvárniteľnosti ocelí s vyššou pevnosťou pre automobilový priemysel*. Transfer inovácií 12/2008, s. 136-139.
3. Ranta-Escola A.: *Use of hydraulic bulge in biaxial tensile testing*. Int. J. Mech. Sci., 21, (1979), 457-465
4. Slota J., Spišák E., Stachowicz F.: *Investigation of biaxial stress-strain relationship of steel sheet metal*. Int. J. of Applied Mechanics and Engineering, vol. 9 No.1 (2004), pp. 161-168. ISSN 1425-1655
5. Slota J., Spišák E.: *Determination of flow stress by the hydraulic bulge test*. In: Metallurgy. vol. 47, no. 1 (2008), p. 13-17. ISSN 0543-5846.

Acknowledgement: This work was supported by the Slovak Research and Development Agency under the contract No. APVV-0629-06.

ZESZYTY NAUKOWE POLITECHNIKI RZESZOWSKIEJ NR 274
Mechanika z. 81 2010

Lýdia SOBOTOVÁ
Emil SPIŠÁK

Technical University in Košice, Slovakia

THERMAL DRILLING AS A PROGRESSIVE TECHNOLOGY OF CREATING OF BUSHINGS

The contribution deals with joining of materials and creating of bushings from aluminium materials, with using of new joining technology by thermal drilling, it means by Flowdrill method. This method is using at joining of materials such as sheets , pipes, hollow profile, where the thickness of material does not allow to make the drilling with enough number of threads. Also we can compare this thermal drilling technology with production of smooth cylindrical and conical bushings by forming technologies as hole burnishing. This paper was made with cooperation with firm Commerc Service spol.s.r.o., Prešov.

INTRODUCTION

With the development of automobile industry and using of new materials at the production of automobiles at present days arise the requirement of join of materials. At the production of automobile body usually joins metal coating sheets with non-metal-coating ones. In the same way there arise the requirements for join of ferrous and non-ferrous metals.

The classical joint of materials produced by spot welding or laser welding not always allow to provide for required quality of joints and necessity, therefore it is necessary to investigate the alternative methods of material join. The thermal friction method is using in joining of materials such as sheets, pipes, hollow profiles.

The contribution deals with the problem of material joins by method of thermal drilling - Flowdrill method. The experimental results presented in this contribution are the results of our cooperation with production firm in Prešov.

METHODS OF JOINS IN AUTOMOBILE INDUSTRY

The development of products in automobile industry, expansion of pipe industry, design of new machine products, utilisation of new materials, also the joint design in civil engineering, competition business in the world market force the producers to increase the production and to utilize new technologies. The force of automobile producers is the biggest from the economical and qualitative points. Therefore the producers try to simplify the production and to use the new progressive join methods of automobile components.

We differentiate in dependence of force transfer between point, linear and planar joint in the new material join methods. In the case of planar joint (for example glue-

joint), the transfer of loading of material is divided equally on the whole area, in the case of spot joint (for example joint is created by spot welding or riveting) loading is accumulated into particular points with local concentrate of stress.

We can divide material joints according to way of their production:

1. **mechanical joint**: join according to screw and matrix, stamps, rivets,
2. **welded joint:** laser beam welding, plasma welding, electro -contact welding, friction stir welding, spot friction stir welding,
3. **soldering joint**: contact soldering, diffusion soldering,
4. **glue joint**: with using of connecting mass, join by pouring.

At present days, it is often necessary to join one to another part and also sometimes is necessary to assembly or demount at reparation for example in automobile or machine industry. From this reason, producers begin to use progressive technologies:

- technology by using of drilling screws, joining by FDS® system at thin sheets,
- technology of thermal drilling by Flowdrill method in materials with greater thickness.

The technology of thermal drilling is used mainly in automobile industry. This join technology, consists in possibilities of smooth cylindrical respective conic bushings and threads in thin-walled materials, as the sheets, tubular profiles and pipes, but also for bearing length and shafts and also in the load-bearing parts of automobile body in the profiled steel constructions. The method of thermal drilling is shown in Fig. 1.

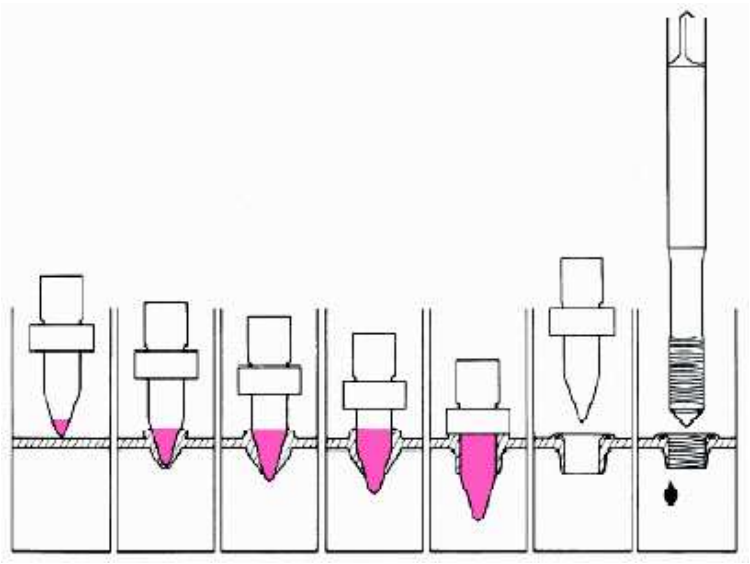

Fig. 1. Scheme of thermal drilling [1]

EXPERIMENTAL METHODS AND RESULTS OF TESTING

During the testing of thermal drilling technology, there were verified the suitability of mentioned technology for selected material, for evaluation of quality of produced holes, bushings and threads at various technological conditions and for observe the macro and microstructure of mentioned materials. For experimental aims, there were proposed for samples non-ferrous material aluminium, according to standard STN 42 4401.The dimension of tested material was jacket 30 x 30 x 2 mm.

The experiments were realized on pedestal drilling machine type Flott P 23 with hand control, in firm Commerc Service, spol.s.r.o in Prešov, Fig. 2.

The drill, type Flowdrill Short with diameter 7,3 mm and the drill, type Flowdrill Short/flat with diameter 7,3 mm with milling cutter and tapping tool were used in the experiments, Fig. 3.

Fig. 2. Drilling machine Flott P23

Fig. 3. The thermal drilling tool special holder of collet for heat removal, collet, drill Flowdrill, tapping tool

In the Table1 is shown the chemical compositions of testing material AlMgSi.

Table 1. The chemical composition of material - AlMgSi, standard STN 42 4401

Si	Fe	Cu	Mn	Mg	Zn	Ti	Cr	Ostatné
0,58 - 0,63 %	0,18 - 0,22 %	0,10 - 0,20 %	0,12 – 0,20 %	0,53 - 0,58 %	max - 0,02 %	max - 0,02 %	max - 0,08 %	max - 0,1 %

After realization of experiments, there were evaluated the shapes and quality of collars, bushings and threads from testing material at various technological conditions.

There were changed the drilling speeds in the range from 1470 sp.min^{-1} to 3420 sp. min^{-1}.In the Fig. 4 is shown the results from material aluminium, where we can see the collars and bushings and the original thickness of material.

Fig. 4. The collars and bushings from aluminium material, material thickness 2 mm

The bushing creates the enlarge possibilities of using of material thickness and areas, where the thickness of material can change more than twice. Also we can make threads into the bushings. For example we can use bushings for join of pipes as non-demountable join, Fig. 5 or for join with threads as demountable joins, Fig 6.

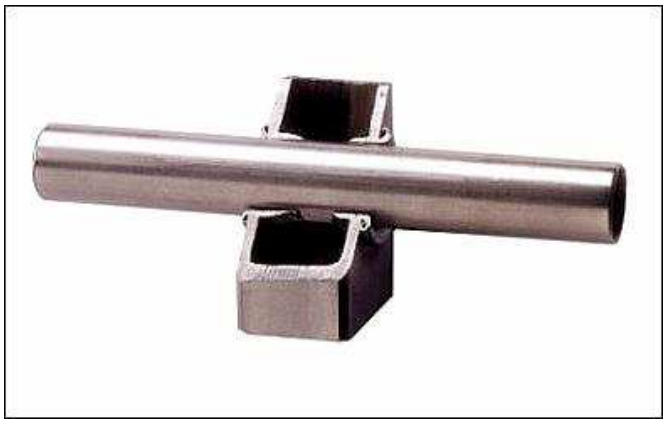

Fig. 5. The joint of pipe in bushings [2]

Fig. 6. The joint with bushing with threads [2]

In the Fig. 7, Fig. 8 and Fig. 9 are shown the results from technology of thermal drilling, it means collars from aluminium material at various technological conditions [3]. In the Fig. 10 and Fig. 11 are shown the bushing without collar made with long/flat drill.

Fig. 7. Al collar, 1470 sp min^{-1}

Fig. 8. Al collar, 2550 sp min^{-1}

Fig. 9. Al collar, 3 420 sp min^{-1}

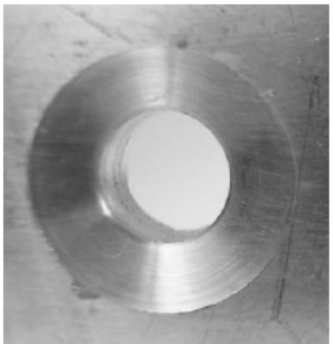

Fig. 10. Removed collar and bushing

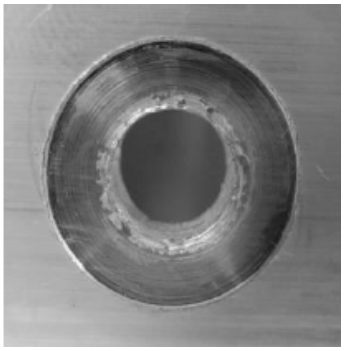

Fig. 11. Removed collar and bushing with threads

In the Fig. 12 is shown the shape of bushing from the bottom side. The shape of bushing is without cracks .The cross-section of aluminium bushing is in the Fig. 13 and bushing with threads is shown in the Fig. 14.

Fig. 12. Shape of Al busher

Fig. 13. Al busher, 2490 sp/min

Fig. 14. Rolled threads, aluminium

In the Fig. 15 is shown the detail of metallographic sample of collar tested from aluminium material at the operating speed 3420 $sp.min^{-1}$. The collar is not damaged and is round. In the Fig. 16 is shown the metallographic detail of formed thread in bushing.

Fig. 15. The detail of aluminium collar, m.50x

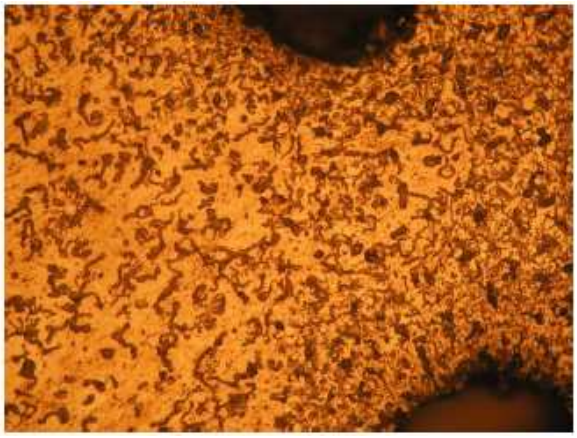

Fig. 16. Detail of microstructure- forming thread, material aluminium,m.200x

CONCLUSIONS

In the contribution was presented the view of nowadays progressive technology utilized in the join of various types of ferrous and non-ferrous materials, mainly in the automobile, pipe and civil industry.

The presented experiments were oriented to evaluation of material at various technological conditions on the created bushings and threads for mechanical thread joint.

In the frame of experiments were used aluminium sheets with thickness 2 mm .

We can make a conclusion from the results of the thermal drilling by Flowdrill method as from the metallographic samples, that the created bushing and thread can be used in joining technology. The bushings (with or without the threads) in material can

elongate the joining place and the joints will become more strong and safety. Also the bushings can be utilised as the helped parts in non-demount joints.

When we compare various materials from the point of shape quality, the part of joints from the aluminium material, it means the bushings and following created threads in bushings show the biggest variance from the requirement shape and in the many cases there occurred the damages of integrity in the bottom border of bushing, but the function of future joint is without changing and can be used in automobile industry.

REFERENCES

1. www.flowdrill.nl, [Online] February 2007,
2. *Thermal drilling*. [Online] May 2010,
   http://autospeed.com.au/cms/title_Thermal Drilling/A_110952/article.html
3. Sobotová L.: *Hodnotenie puzdier vytvorených metódou Flowdrill*. In: Transfer inovácií. č. 10 (2007), s. 144-148. Internet: <www.tuke.sk/sjf-icav/stranky/transfer/10-2007>. ISBN 978-80-8073-832-7
4. Sobotová L.: *Progressive technologies in joining of materials*. In: PRO-TECH-MA '09 : progressive technologies and materials : international scientific conference, Rzeszów-Bezmiechowa, Poland, 6th July - 8th July 2009. - Rzeszów : Politechnika Rzeszowska, 2009. - l . ISBN 978-83-7199-546-0. - P. 272-279.

The contribution was prepared in the frame of solving of grant scientific project VEGA č. 1/0725/08 - The research of conditions evaluated the limit deformation of thin surface modified steel sheets.

ZESZYTY NAUKOWE POLITECHNIKI RZESZOWSKIEJ NR 274
Mechanika z. 81 2010

Lýdia SOBOTOVÁ
Ľudmila DULEBOVÁ

Technical University in Košice, Slovakia

EVALUATION OF SOME MECHANICAL PROPERTIES OF STEEL SHEET

The requirement for reducing of weight of products urges the producers to reducing thickness of used materials. It means the reducing of thickness of products from sheet. The second requirement for product is its adequate stiffness. These requirements force product manufacturers from sheet material to ask for development of sheets with higher strength properties and formability from sheet producers. The properties of sheet must guarantee deep- drawing of stampings without problems, but with required qualitative and dimensional parameters. The contribution solves the problem of deep drawing of bath tubes and pressability of steel sheets used at the production of bath tubes. The thickness of used steel sheets were changed from 1,55 mm to presented 1,35 mm. This change had an influence on the required properties of steel sheets and also the changes of technological conditions of deep drawing. The next surface finishing of pressing - bath tube requires the roughness of surface in the defined boundary.

INTRODUCTION

Technological processing of new materials with new properties offers a number of problems, because in most cases there is reached a deterioration of indicator of their technological characteristics of pressability. Verification of material pressability is therefore often necessary.

Basic reviewing of pressability of steel sheets is carried out by using of characteristic values of the basic test of sheets (tensile test, compression, microhardness, metallographic evaluation). The test results can create an idea about the properties of materials and their possibility in practice use.

The deep drawing sheets are used with higher plastic properties. The formability of sheet metal, i.e. ability of the material to plastically deform without losing local stability, and without failure, the basic effect has:

- method of material production (materials cast by classic method, continuously or in a vacuum),
- chemical properties of the material (eg impurities, alloying elements),
- material structure ,
- material texture ,
- mechanical and plastic properties of materials,

• quality and quality of material surface,
• shape and size of intermediate.

Research, which results are presented in this paper, was made for the products of sanitary technique. The current trend in this production is to reduce the weight of the product. Sanitary products are now made of steel grade/mark KOSMALT 190, which is currently replacing with the new material quality suitable for deep drawing and enamelling, marked as KOSMALT 180 IF. The mentioned materials are used in the manufacture of sanitary technique, for example producing company is called FESTAP, a.s., Fiľakovo.

The basic mechanical and chemical properties of steel sheet suitable for enamelling, produced in USS Kosice, is shown in the Table 1 and Table 2.

Table 1. Chemical structure of steel sheets suitable for enamelling [1]

Quality according to EN 10209/96 U.S.Steel Košice, s.r.o.	Chemical analysis of melt analysis v %						
	C max.	Mn max.	Si max.	P max.	S max.	Al	Cu max.
KOSMALT 180 IF	0,005	0,35	0,01	-	0,015	min. 0,020	0,06
KOSMALT 190	0,04	0,19	0,01	0,015	0,012	0,02 0,06	0,060
KOSMALT 190 S	0,06	0,30	0,03	0,015	0,035	min. 0,020	0,060
KOSMALT 210	0,06	0,25	0,03	0,025	0,020	0,03 0,07	0,065

Table 2. Mechanical properties of steel sheets suitable for enamelling [1]

Quality according to EN 10209/96 U.S.Steel Košice,s.r.o.	Mechanical properties					Width [mm]
	$R_{p\,0.2}$ [MPa]	R_m [MPa]	A_{MIN} [%]	$r_{90\ min.}$ [-]	$n_{90\ min.}$ [-]	
KOSMALT 180 IF	180	270 - 350	42	I,80	0,22	0,40 – 2,00
KOSMALT 190	190	280 - 350	40	I,40	0,22	0,40 – 2,00
KOSMALT 190 S	190	270 - 350	40	I,80	0,20	0,40 – 2,00
KOSMALT 210	210	270 - 350	38	-	-	0,50 – 2,00
KOSMALT 240	240	270 - 390	32	-	-	0,50 – 2,00

In appreciate of the surface quality of the sheet there is evaluated the surface cleanliness, surface defects and surface micro geometry [1]. The surface quality for deep drawn steel sheets cold rolled prescribes the European standard EN 10130/91 + A1/98. The surface quality for deep drawn steel sheets hot rolled prescribes the European standard EN 10111/98.

The indicator evaluation of formability according to new criteria is listed in Table 3.

Tab. 3. Evaluation of formability of deep drawn steel sheets cold rolled [2]

Identification	Formula	Dimension	Evaluation of formability of cold forming
P	$P = R_m / R_{p0,2}$	[-]	The higher value of P the better the formability
k	$k = Ag / R_{p\,02}$	[% /MPa]	The higher value of k, the better the formability
Zp	$ZP = k´ . (R_m - R_{p\,02}) . A_g$	[MPa]	The higher value of ZP, the better the formability
KUT	$KUT = P . A_{50}$	[%]	The higher value of KUT, the better the formability
IT	$IT = 1000 . r_s . n_s$	[-]	The higher value of IT, the better the formability

EXPERIMENTAL METHODS AND RESULTS OF TESTING

Experimental tests were made on steel sheets of KOSMALT 190, with thickness 1,5 mm and KOSMALT 180 IF, with thickness 1,35 mm.

To determine the basic mechanical properties of metallic materials are used an uni-axial tensile test, which is one of the basic mechanical tests. The test was performed on a test machine, TIRA- test 2300, on the Department of Technology and materials, FME TU in Košice. Test samples for tensile test were taken in the directions 0 º, 45 º and 90 º with respect to the direction of rolling, according to STN EN 42 030.

For determination of the methodology for testing and evaluation of drawability of materials there have been designed following tests:

- a visual evaluation of tested materials according to standard STN 42 0108,
- preparation and implementation of metallographic analysis of the tested materials according to standard STN 42 0469.
- measured values of roughness of sheet, Ra, Rz, according to standard EN ISO 4287,
- sample preparation and implementation of a tensile test according to EN 10002-1,
- the test of normal anisotropy according to standard STN 42 0435;
- the test of the strain hardening exponent according to standard STN 42 0436;
- determination of the coefficients P, IT, KUT, Zp, according to the new criteria of formability.

On visual inspection of sheets KOSMALT there occur the most frequent errors such as scratches, corrosion, impressions after rolling. In Fig 1 is shown the corrosion on the sheet and in Fig. 2 is shown the impressions after rolling.

The fractographic evaluation, Fig. 3 and Fig. 4 , of test samples from steel sheet KOSMALT 190 were realised on the electron microscope JSM -35 CF JOEL, Japan.

Measurement of surface roughness was realised according to standard ISO 4287. To measure the surface roughness was used the equipment for roughness measuring Surfest MITUTOYO SJ – 301. The roughness values meet the requirements with delivery regulations and firm standard from Ra = 1,7 to 2,7 μm. The measured values of KOSMALT 190 ranged from Ra = 1,81 to 2,07 μm and KOSMALT 180 IF ranged from Ra = 1,74 to 1,96 μm.

Fig. 1. Visual evaluation –corrosion

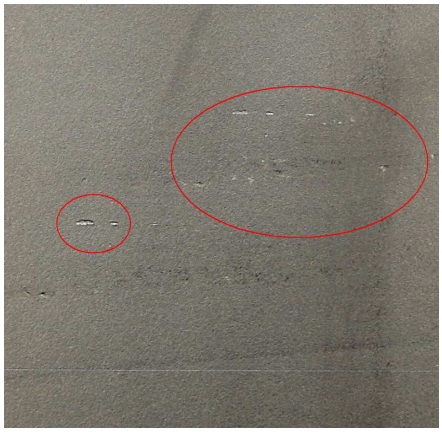

Fig. 2. Visual evaluation –impression after rolling

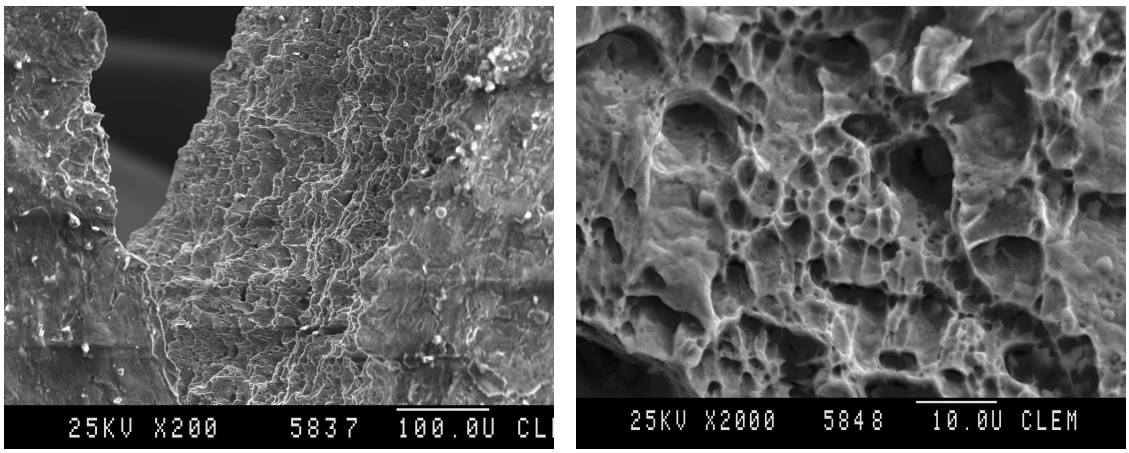

Fig. 3 The structure observed at the place of shear line: a) score with rough surface, b) structure with cavity failure

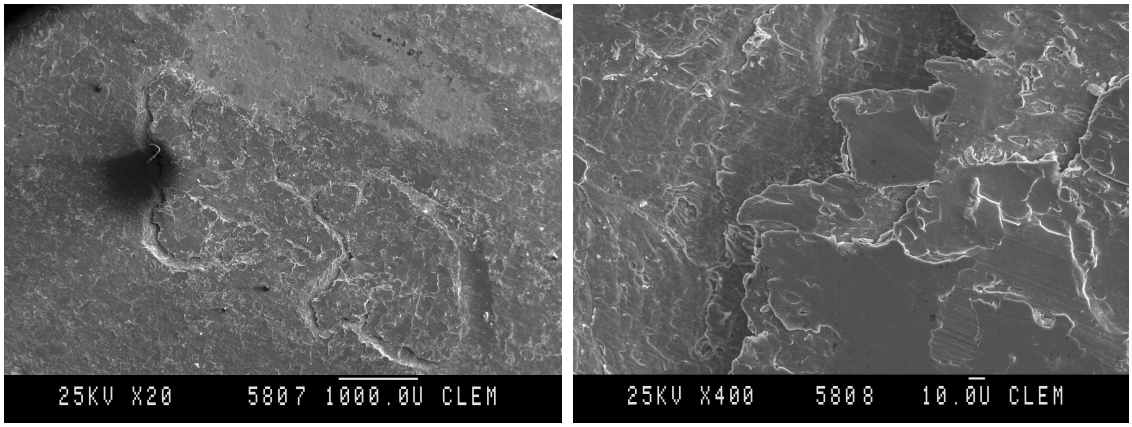

a)

b)

Fig. 4. The details of mill chips: Irregular shape of chip, b) separation of chips from basic material

Uni-axial tensile test was realised according to standard STN EN 10002-1, which provides the processing and evaluation of measured values. Tensile test was performed

on a certified tensile test machine TIRA-test 2300. There were used for experiments five samples from each of the rolling direction 0 º, 45 º, 90 º according to the rolling direction.

The measured mechanical properties are given in Table 4 for both tested materials.

Table 4. Mechanical properties of tested materials

Material	Measured values of mechanical properties			
	Rolling direction	$R_{p0,2}$ [MPa]	R_m [MPa]	A_{80} [%]
KOHAL 190	0°	189	300	44,2
	45°	202	317	40,8
	90°	198	306	44,6
KOHAL 180 IF	0°	173	317	46,0
	45°	180	322	44,1
	90°	179	315	46,3

In Table 5 are given the average values of strain hardening exponent and of normal anisotropy.

Table 5. The values of the strain hardening exponent and normal anisotropy

Material	Measured values of mechanical properties						
	Rolling direction	r [-]	r_m [-]	Δr [-]	n [-]	n_m [-]	Δn [-]
KOHAL 190	0°	1,498	1,327	0,608	0,201	0,199	0,004
	45°	1,023			0,197		
	90°	1,764			0,202		
KOHAL 180 IF	0°	1,630	1,721	0,404	0,244	0,239	0,006
	45°	1,519			0,236		
	90°	2,217			0,240		

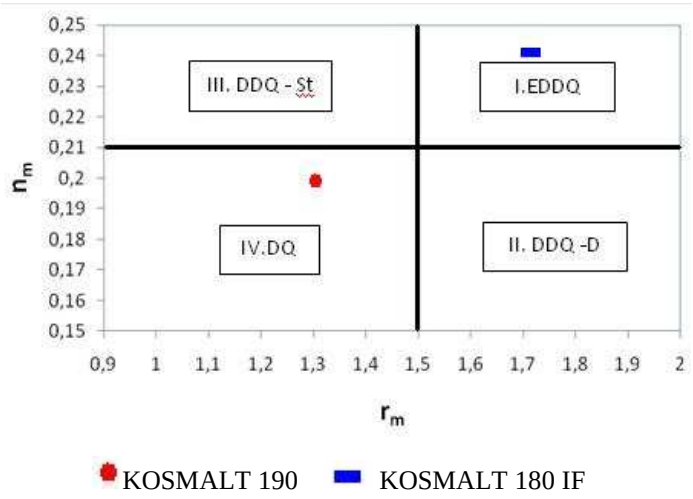

Fig. 5. Evaluation of formability according to r_m, n_m

The complex evaluation of the average coefficient of normal anisotropy and strain hardening exponent is indicated in the diagram in Fig. 5.

The criteria, based on measured values by tensile test for examination of the formability of cold-rolled sheets, are shown in Tab. 6

Table 6. The average values of new criteria of formability

Material	Criteria of formability					
	Rolling direction	P [-]	KUT [-]	Zp [-]	k [-]	IT [-]
KOHAL 190	0°	1,587	70,145	1148,05	0,234	2640,73
	45°	1,569	64,015	947,78	0,202	
	90°	1,545	68,907	1083,78	0,225	
KOHAL 180 IF	0°	1,832	84,272	1761,98	0,266	4113,19
	45°	1,789	78,895	1534,24	0,245	
	90°	1,760	81,488	1630,87	0,259	

CONCLUSIONS

The paper deals with the solving of problem of expertise evaluation of the functional characteristics of the determined material for special use and for deep drawing.

On this basis, it can be concluded that the obtained results and experimental measurements can be used for the evaluation of the sheet application of type KOSMALT 190 with a thickness of 1,5 mm and KOSMALT 180 IF with a thickness of 1,35 mm in the production of new and innovative products and can be recommend them as an input materials for the production of large pressings. The obtained experimental results show that mainly the tested steel sheets KOSMALT 180 IF with a thickness of 1,35 mm have a high ability of strain (the values of n, A_{80}) and less suitability for the drawing from the flange (low values of r).

Introduction into production of new materials with improved of deep-drawn properties, with less thickness, by the introduction of new advanced technologies, with ongoing study, by training and control can be achieved the desired results and, ultimately, the competitiveness of companies in global markets.

REFERENCES

1. U .S. Steel Košice, s.r.o. – výrobné produkty. [Online] www. usske.sk/products
2. Spišák E.*: Matematické modelovanie a simulácia technologických procesov – ťahanie*. TYPO Press Košice, Košice 2000, ISBN 80-7099-530-0
3. Sobotová L., Dulebová Ľ.*: Materiálová tvárniteľnosť plechov*. In. PRO TECH-MA 2008. Acta Mechanica Slovaca 2008, roč.12,3-A/2008, pp. 429-434.
4. Stachowicz F., Trzepieciński T.: *Finite element analysis of the deep pressing of rectangular drawpieces*. PRO TECH-MA 2006. Acta Mechanica Slovaca 2006, roč.10,2B/2006, pp. 405-410.

The contribution was processed in the framework of Grant Project VEGA 1/0725/08

Emil SPIŠÁK
Jana MAJERNÍKOVÁ

Technical University in Košice, Slovakia

ANNEALING PROCESS AND ITS INFLUENCE ON MECHANICAL PROPERTIES OF PACKAGING SHEETS

In the contribution sheets made by single rolling and double reduction, batch and continual annealed have been compared. The comparison has been done based on two tests, by uniaxial tensile test and earring test.

INTRODUCTION

Thin steel tinned sheet for the production of metal packaging is made from low-carbon, deep-drawing, aluminum killed steel, casting on equipment for continuous slabs bloom casting. Slab casting is followed by hot rolling on wide-strip mill. Hot rolling is followed by treatment at Cold Rolling Mill. During the Cold rolling treatment increased strength, hardness and decrease of plastic properties of rolled materials is achieved as a result of material plastic strain and strength increase. To eliminate these negative changes in material, recrystallization annealing is included in the sheet production process. Annealing is made by continuous process (CA – Continual Annealing) or by batched process (BA – Batch Annealing).

Continual annealing takes about 2-3 minutes. In this process the belt is indirectly warmed up. This heat process is especially suitable for harder qualities of tinned sheets. This new method of annealing process includes temper hardening with temperatures around 450ºC, which allows to produce practically non-ageing material.

Batch annealing introduces a multi-hour process for the recovery of crystalline structure which was deformed by cold rolling. The advantage of these furnaces is in achieving structure recovery and considerable softening of the annealed material as a result of long annealing and very slow cooling. The disadvantage of this process is in its long time and unequal temperature in the whole annealing batch content in comparison with continual annealing in coil.

As for very thin tinplates, the second reduction of thickness by cold rolling at intervals 10 – 36 % is made after annealing. The resulting product has higher hardness and strength after double reduction compared to a single reduced material. The finalization of packaging sheet production is the process of double side electrolytic tinning. The tin layer fulfills anticorrosive function of this sheet.

In the contribution sheets made by single rolling and double reduction, batch and continual annealed have been compared. The comparison has been made based on two tests, by uniaxial tensile test and earring test. The uniaxial tensile test has been chosen in order to compare the achieved strength and plastic properties of thin batch and continual annealed packaging sheets of different thicknesses in rolling direction and perpendicular in respect of rolling direction. The compressibility of batch and conti-

nual annealed packaging sheets has been examined by earring test, as well. This test includes the influence of material properties as well as technological conditions and geometry of the active parts of drawing tool for drawing process. The anisotropy properties of tinplates demonstrated by earring creation have been evaluated on cup from earring test.

The results of these tests should lead to the optimization of testing method for setting the objective sheet properties and that way creating conditions for their troublefree drawing processing.

Two types of materials produced by different processes have been chosen for the verification of annealing influence on anisotropic properties of tinplates and from each one two different thicknesses have been tested.

SHEETS ANISOTROPY

Directional values of mechanical properties (anisotropy) have great importance during sheet treatment by drawing. The main reason of anisotropy lies both in the rolling process and sheet annealing after rolling. Heterogeneous ingredients of structure are being plastically transformed by rolling and therefore changes of shape and grain orientation appear. Rolling is characterized by significant grain elongation in the rolling direction, whereas deformations in perpendicular direction are much smaller. Structural or crystallographic texture participates on the total anisotropy, too.

The sheets show two types of anisotropy: surface and normal.

The **surface anisotropy** expresses inequality of mechanical properties in different directions of sheet plane. To detect surface anisotropy we need the results from tensile tests taken from sheets in various angles in respect to rolling direction. The surface anisotropy has adverse influence during the process of symmetrical cup drawing not only on the creation of earrings needed to be removed, but it can also cause thinning of cup wall thickness and cause circularity deviations of cylindrical cups.

The **normal anisotropy** expresses the inequality of properties obtained in sheet plane in respect to properties in perpendicular direction to sheet plane (in thickness direction). So it expresses sheet resistance to thinning at deep drawing.

EVALUATION OF PROPERTIES BY UNIAXIAL TENSILE TEST

Nowadays the uniaxial tensile test is the most frequently used test for obtaining basic mechanical properties of sheet. The goal of this test, which has its conditions and test sample shape indicated in the specifications STN EN 10002-1+AC1 and STN 42 0321, is to obtain the values of yield point, ultimate tensile strength and elongation. For tinned sheets that show sharp cup stress at uniaxial tensile test it is problematic to determine the value of maximum uniform deformation. Lüders strain is followed by sharp cup stress with values between 4 – 10 % achieved by the former one. On tested sample it is manifested in jumps of strain creation in specific sample sections. It starts in one place, suddenly stops in it and passes on to a completely different sample place.

To determine the anisotropic material properties for the uniaxial tensile test samples in rolling direction 0° and perpendicular direction 90° in respect of rolling direction have been taken. From the uniaxial tensile test the following have been evaluated: the cup stress, the ultimate tensile strength and total elongation. The measured values are shown in Table 1.

Tab. 1. Measured and calculated values of cup stress, ultimate tensile strength and elongation achieved by uniaxial tensile test in rolling direction 0° and perpendicular direction 90° in respect of rolling direction

Material	Sample number	Sample thickness [mm]	$R_{p0,2}$ - 0° [MPa]	$R_{p0,2}$ - 90° [MPa]	R_m - 0° [MPa]	R_m - 90° [MPa]	A_{50} - 0° [%]	A_{50} - 90° [%]
TS 550 BA	13	0,14	564	674	552	663	2,78	1,04
	23	0,17	429	442	420	434	5,71	3,66
TH 550 CA	1	0,17	579	538	591	563	4,48	10,5
	58	0,27	548	550	562	576	2,27	7,71

From the measured results we can conclude that as for batch annealed sheets lower values of cup stress and ultimate tensile strength in rolling direction and higher values in perpendicular direction in respect of rolling direction have been measured. Higher cup stress than ultimate tensile strength in both of tested directions have been measured with both samples of batch annealed sheets. The measured elongation in rolling direction has been higher than in perpendicular direction in respect of rolling direction.

Lower values of cup stress than ultimate tensile strength in both tested directions have been measured at both samples with continual annealed sheets. Measured elongation in rolling direction is likewise lower for both samples than in perpendicular direction in respect of rolling direction.

This strangeness stems from material structure that is shown in Fig. 1 and 2.

For both annealing processes of tested packaging sheets material rupture shown in Figures 3 and 4 was characteristic. The reason of higher obtained elongation for continual annealed sheets in perpendicular direction in respect of rolling direction was the fact that plastic strain deformation expanded at first uniformly in the whole section of measured length of tested bar. As for batch annealed sheets there have been ruptures in all samples during local sheet strain without any expansion of strain in the whole measured length of tested sample (see Fig. 3 and 4).

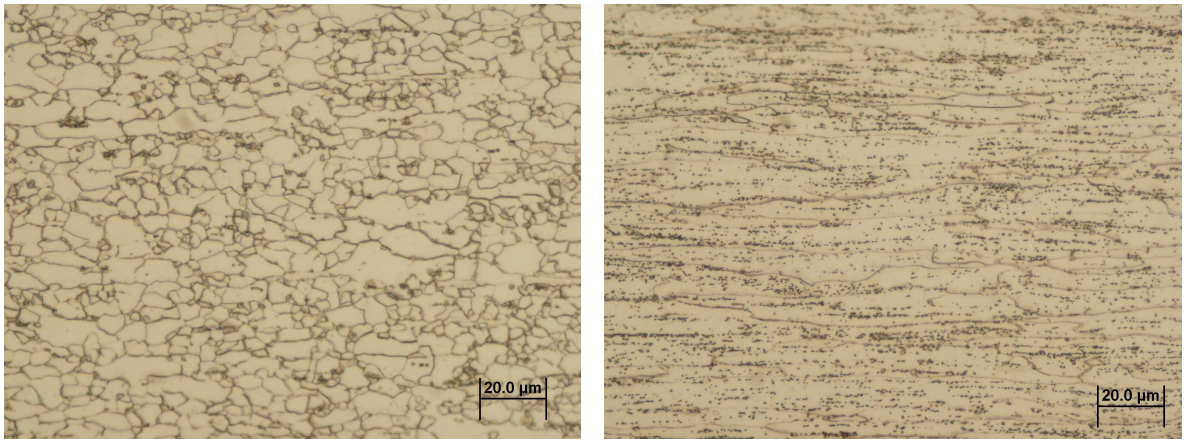

Fig. 1. Microstructure of continual annealed (left) and double reduced batch annealed material (right) of samples taken in rolling direction

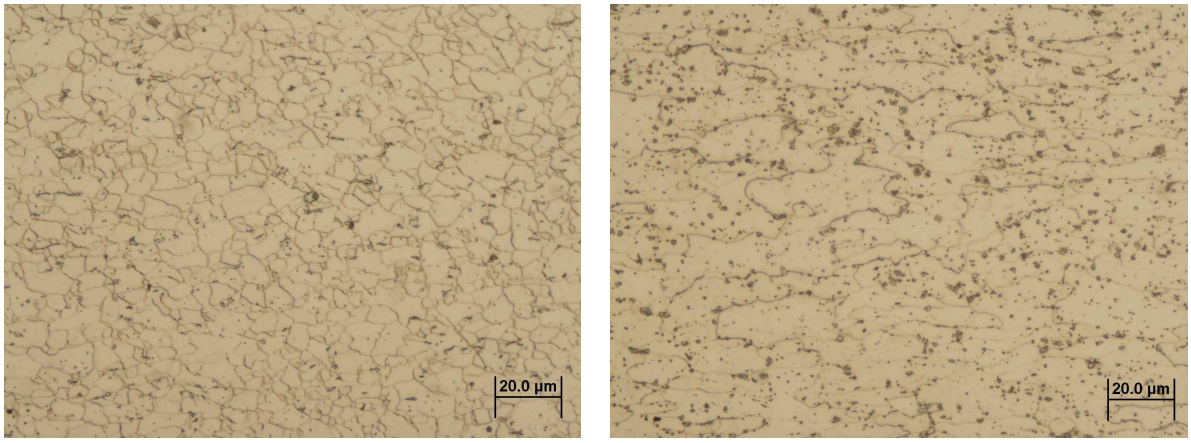

Fig. 2. Microstructure of continual annealed (left) and double reduced batch annealed material (right) of samples taken in perpendicular direction in respect of rolling direction

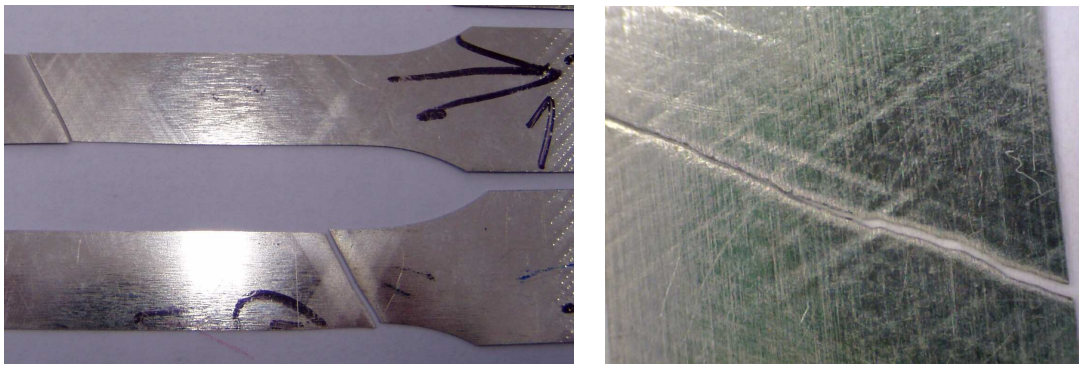

Fig. 3. Rupture of sample after uniaxial tensile test with significant slip planes

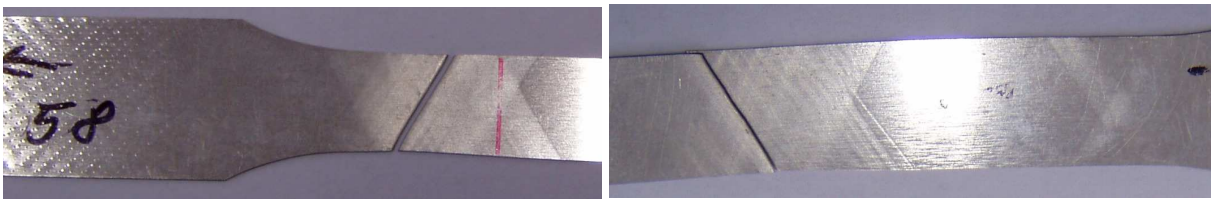

Fig. 4. Significant slip planes in two directions in respect of loading direction of tested sample

In Figures 5 and 6 surface ruptures of tested samples are shown. From Fig. 5a) we can expressly conclude that except primary slip planes where the rupture of tested samples appeared, also the so called secondary slip planes appeared in their proximity. Local thinning of tested sheet has occurred in these places, as well. In the rest of measured part the tested sample has not been plastically deformed. The rupture surface in Fig. 5a), but also the detail in Fig. 5b) and in Fig. 6 show, that in the place of sample rupture a sharp contraction (necking) has occurred. It points at the fact that the material itself has better plastic properties than the plastic properties measured by method of elongation at uniaxial tensile test.

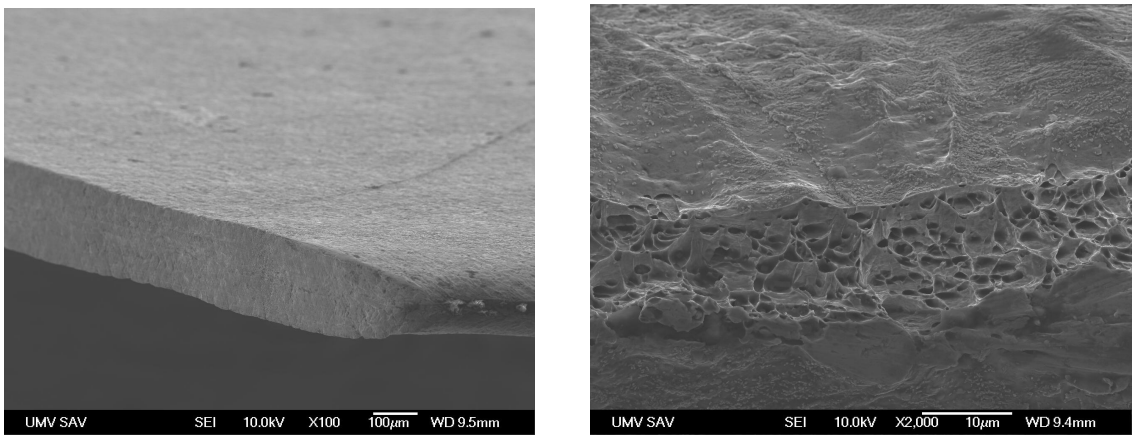

a) b)

Fig. 5. Rupture surface and her detail

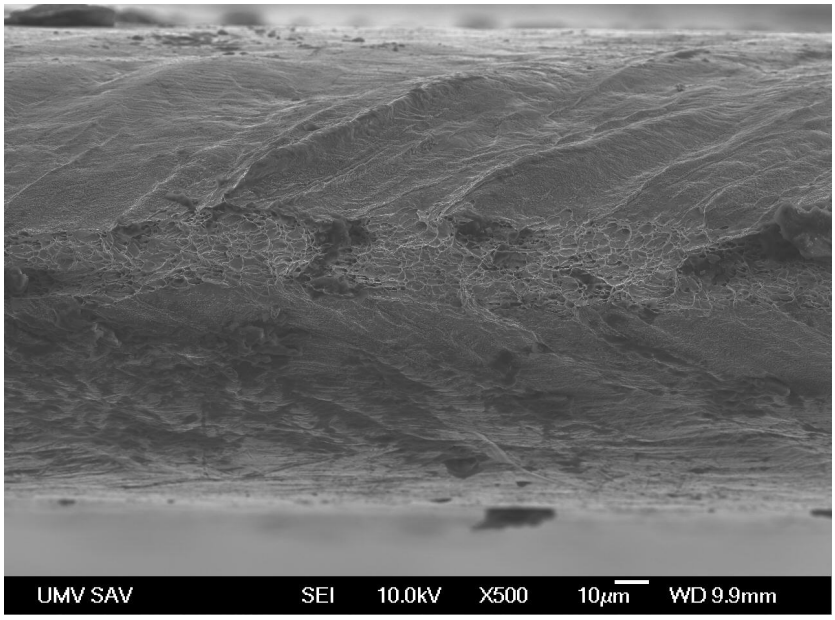

Fig. 6. Perpendicular view of rupture surface and slip planes

From the details of rupture surface in Fig. 5b), but mainly from Fig. 6, we can expressly see the slip planes which are manifested on the surface of the sheet in the nearness of the rupture as waves. Exactly these sharp “wavings” induce considerable reduction of cross-section at small thicknesses of tested sheet. This cross-section is not able to transfer the strength necessary for the strain of another section of testes sample. The rupture shows characteristic signs of plastic intercrystalline fracture expanding along grain boundaries where inclusions can be found.

ANISOTROPY EVALUATION BY EARRING TEST

Earring test has been carried out for cylindrical cups. A cup of diameter d has been drawn from circular blank of diameter D from flange. Circular tested samples of diameter 55 mm produced by turning have been used. The test has been evaluated from three tested samples of every kind of packaging sheet.

The anisotropy of sheets is manifested during cup drawing without flange is manifested by nonequivalent height of cups in different directions in respect of sheet rolling direction. Its expression can be made in multiple forms. Following processes have been used for the evaluation:

- Degree of earring $\Delta h = \frac{h_0 - 2h_{45} + h_{90}}{2}$
- Coefficient of earring $Z = \frac{h_{max} - h_{min}}{h_{min}} * 100$ [%]
- Maximal difference of height cup $= h_{max} - h_{min}$

There are recommend criteria for earring evaluation of DR tinplates shown in Table 2. Measured and calculated values are shown in Table 3.

Tab. 2. Criteria for evaluation of DR tinplates earring according to SEFEL

Sample thickness [mm]	Maximal difference of height cup [mm]	Middle height cup [mm]	Earring [%]
0,140	< 0,85	16,2 ± 0,1	< 2,5
0,155	< 0,85	16,2 ± 0,1	< 2,5
0,170	< 0,90	16,2 ± 0,1	< 3
0,180	< 0,90	16,2 ± 0,1	< 3

Fig. 7. Cups after earring test

Tab. 3. Measured and calculated values of earring coefficient, earring degree and maximum difference of height cup obtained by earring test

Material	Sample number	Nominal thickness [mm]	Z [%]	Δh [mm]	Max. difference of height cup [mm]
TS 550 BA	13	0,14	4,06	-0,38	0,66
	23	0,17	3,35	-0,37	0,55
TH 550 CA	1	0,17	3,47	-0,24	0,56
	58	0,27	2,83	-0,22	0,48

In spite of very low elongation values from all tested sheets we had no problems with drawing cups (Fig. 7) of the abovementioned size and shape. Their measured earring is the result of anisotropy properties of tinplates. The highest earring indicators have been measured with batch annealed sheet of thickness 0,14 mm. The sheet continually annealed of thickness 0,27 mm fulfills two criteria for earring evaluation, but none of the tested tinplates succeeds in all three criteria for earring evaluation of tinplates at the same time.

Considering significant difference in the shape of grain at single and double reduced sheets, we supposed that as for double reduced sheets the measured values characterizing anisotropy properties would be considerably more significant than for single reduced sheets. Considering higher strength of double reduced sheets, the anisotropy during cup drawing has not been manifested in such a significant earring way as it was supposed.

CONCLUSIONS

Within this contribution tinplates produced by different processes of rolling and annealing have been evaluated. From the measured results we can conclude that elongation of tested sheets obtained by uniaxial tensile test does not correspond with real plastic properties of tested sheets. The values of cup stress at double reduced sheets have been higher than the values of ultimate tensile strength. This fact is the cause of strain localization at uniaxial tensile test and subsequent rupture of tested sample without uniform expanding of strain on the whole section of measured length.

As for earring test, in spite of very low values of tested material elongation obtained by uniaxial tensile test there have not appeared any problems by drawing of cups. The measured values of anisotropy from drawn cups do not comply with all the three criteria at the same time, but the earring of all tested sheets is rather insignificant.

From the measured results it possible to conclude that the uniaxial tensile test for very thin double reduced tinplates does not give relevant results especially about their plastic properties.

This work was supported by the Slovak Research and Development Agency under the contract No. APVV-0629-06

REFERENCES

1. Spišák E., Majerníková J.: Plastic deformation of tin coated steel sheet under different stress-strain states. In: Progressive technologies and materials. 3-B: Materials. Rzeszów, Oficyna Wydawnica Politechniki Rzeszowskiej, 2009. ISBN 978- 83-7199-550-7. pp. 25-35.
2. Majerníková J., Spišák E.: Limiting states analyze of stress and strain of tinplates by different stress-strain states. In: PRO-TECH-MA '09 : Progressive technologies and materials: International scientific conference, Rzeszów - Bezmiechowa, Poland, 6th July 8th July 2009. Rzeszów : Politechnika Rzeszowska, 2009. ISBN 978-83-7199-546-0. P. 151-160.
3. Slota J., Spišák E.: Determination of flow stress by the hydraulic bulge test. In: Metalurgija. Vol. 47, no. 1 (2008). ISSN 0543-5846. P. 13-17.
4. Spišák E., Majerníková J.: Properties evaluation of progressive wrapping materials. In: Mechanical Engineering SI 2008: 12th International Conference: proceedings of papers. Bratislava STU, 2008. ISBN 978-80-227-2982-6. S. 1-8.

5. Spišák E., Majerníková J.: Porovnanie vlastností jedenkrát a dvakrát redukovaných obalových plechov skúškou jednoosovým ťahom a dvojosovou skúškou. In: Acta Mechanica Slovaca. Roč. 12, č. 3-A PRO-TECH-MA (2008). ISSN 1335-2393. S. 453, 458.
6. Spišák E., Slota J., Majerníková J.: Modelovanie medzných deformácií pri ťahaní tenkých obalových plechov. In: Mechanical Engineering 2007, Bratislava, November 29, 30, 2007. Bratislava, STU, 2007. ISBN 978-80-227-2768-6. 9 s.

ZESZYTY NAUKOWE POLITECHNIKI RZESZOWSKIEJ NR 274
Mechanika z. 81 2010

Emília SPIŠÁKOVÁ

Technical University of Košice, Slovak Republic

THE COMPARISON OF INNOVATION ACTIVITY OF SLOVAK AND POLISH ENTERPRISES

The article deals with the evaluation and comparison of innovation activities of Slovak and Polish enterprises. It is focused on the number of innovative enterprises according to their size (small, medium, large enterprises) and according to the sector of their operation (industry, services, construction). The attention is also paid to the cooperation of enterprise in the innovation's creation and development, i.e. to the cooperation from the perspective of countries of partner operation, from the perspective of the type of cooperating subject or institutions and from the perspective of those who participated in the creation of new or significantly improved product or process (either the enterprises itself or enterprise in cooperation with other enterprises, respectively new products or processes are developed by other enterprises).

INTRODUCTION

In the recent years the innovation are considered as a driver force of economic growth in the economies of advanced industrial countries. In 2000 the European Council met in Lisbon and it has identified the innovation as the most important factor of the competitiveness of European enterprises. At a present, the innovation and new knowledge are considered as a starting point from the current financial and economic crisis. As the European Union lags in innovation performance behind the U.S. and Japan, the V4 countries lags in innovation performance behind the EU average. Slovak Republic and Poland (together with Hungary) are in the last group of countries according to the Summary Innovation Index, called catching-up countries. These countries are characterized by the lack of innovation activity, situated well below the average EU 27. Therefore, the article presents results from the analyze of innovation activity of Slovak and Polish enterprises and compares this two countries.

THE INNOVATION ACTIVITY OF SLOVAK ENTERPRISES

Slovak republic is the smallest country of V4 countries not only by its extent, but also by the number of the population. Together with the Poland and Hungary belongs country to the group of catching-up countries, whereby its innovation activity, which is evaluated by the Summary Innovation Index, is higher then the innovation activity of two mentioned countries from this group.

The size of country is also reflected in the number of enterprises in Slovak republic (the lowest number of enterprises in comparison with the other V4 countries). From the number of 6 465 enterprises only ¼ of enterprises decided to create and implement

some type of innovation (Tab. 1). The most of enterprises still regard this activity as expensive and very risky; therefore they prefer a simple way without the innovation. The most of product and process innovation were in the year 2006 implemented in the large enterprises, the least in small enterprises with the number of staffs from 10 to 49. Regardless of the size of enterprise, in the country predominated and still dominate the enterprises without the innovation activity.

Table 1. The enterprises with innovation activity according to the size and the type of implemented innovation in Slovak republic

Size of enterprise/type of innovation	Total enterprises	Enterprises with innovation activity					Enterprises without innovation activity
		Total	Product and process innovation	Product innovation	Process innovation	Establish innovators, ongoing and/or abandoned only	
Small enterprises	4 575	874	257	218	342	57	3 701
Medium enterprises	1 459	492	217	113	147	16	967
Large enterprises	431	242	148	29	57	7	189

Source: self elaboration according to the data from Eurostat on 13.1.2010

According to the analyze of innovation activity of enterprises by the sector of their operation we can state, that in the year 2006 had the highest share the industrial enterprises, nearly 27% of enterprises innovated their production by the implementation of product, process or both product and process innovation. From the total number of enterprises, 2 828 enterprises didn't realized any innovation activity [6].

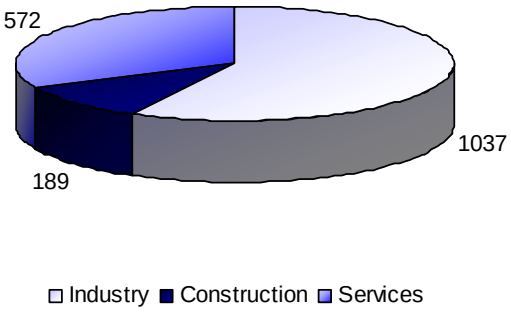

Fig. 1. The number of enterprises with innovation activity according to the sector in Slovakia

The highest innovation activity was recorded in the industrial enterprises in the area of Manufacture of office machinery and computers, where exactly half of the enterprises in the year 2006 introduced some type of innovation. Less than half of innovative enterprises were from all other areas of industry, for example from the area of Manufacture of medical, precision and optical instruments, watches and clocks and Manufacture of electrical machinery and apparatus with the 43% share of enterprises with innovation activity on the total number of enterprises in this area.

On the other hand, the lowest innovation activity was observed in enterprises deals with the Collection, purification and distribution of water (5,88% of enterprises), the Manufacture of wearing apparel, dressing, dyeing of fur clothing production, processing and dyeing of fur, the Manufacture of textiles and textile products, leather and leather products with around 10% share of innovative enterprises on the total number of enterprises in this area [6].

In the service sector has decided to improve their services or to improve the level of services supplying about half of the number of industrial enterprises (Figure 1), but their share on the total number of enterprises providing services was almost 22%. These enterprises preferred process innovation, not product innovation.

The most of innovative services were provided by the enterprises in the area of Financial intermediation, except insurance and pension funding (62,22% of these enterprises provided new or improved service), also in the area of Research and development, with the 61,36% share of innovative enterprise on the total number of enterprises in this area, and in the area of Post and Telecommunications, where exactly 60% of enterprises decided to innovate providing services.

The lowest innovation activity, but not so much low than in the industrial sector, was in enterprises that realized Supporting and auxiliary transport activities, activities of travel agencies with the 13,48% share of innovative enterprises on the total number of enterprises in this area [6].

In the year 2006, enterprises in the construction sector were showed the lowest innovation activity. From the total of 1 526 construction enterprises, only 12,39% of enterprises innovated their production mainly by introducing new or significantly improved processes.

According to the analyze of innovation activity of enterprises operating in the different sectors according to their size we can state, that both in industrial and in service sector were the most numerous small enterprises, but the share of small innovative enterprises on the total number of small enterprises in industrial and service sector was the lowest (Figure 2). By contrast to this, the least numerous were large enterprises, of which over half enterprises decided to introduce the innovation in the year 2006.

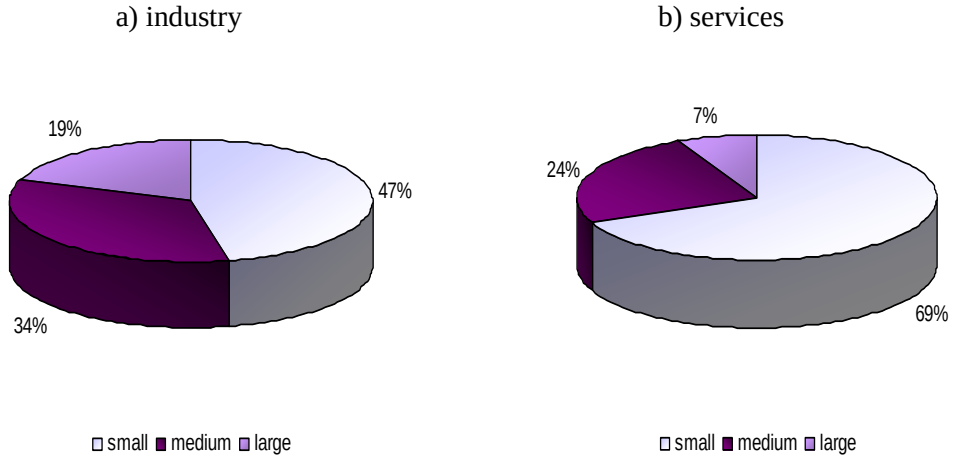

Fig. 2. The enterprises with the innovation activity according to their size in Slovak Republic

THE COOPERATION IN CREATING AND IMPLEMENTING INNOVATION IN SLOVAK REPUBLIC

The development of new or significantly improved product and process may be involved in various enterprises, institutions. Innovation may be the result of the enterprise's activity or the activity of the group of enterprises that introduce it, the result of cooperation of particular enterprise with the other enterprises or may be fully developed by other companies, institutions.

According to data available from Eurostat for the period 2004 - 2006 it can be state that the most of Slovak enterprises, either alone or in cooperation with the group of enterprises developed product or process innovation. The new product was developed by 733 enterprises and the new process by 580 enterprises. We can also say that in this period were dominant industrial enterprises above the enterprises from the service and construction sector (Tab. 2).

In the development of new product 243 enterprises cooperated with other enterprises or institutions and in the development of new process that was nearly double number of enterprises. Again, the industrial enterprises dominated in cooperating during the development of new product or process, not enterprises from the sector of services or construction.

In the analyzed period, the enterprises used at least the possibility to develop new product or process entirely by another institution or company.

Table 2. Product and process innovation according to the developing organization and the sector of their operation in Slovak Republic

Sector of enterprise's operation / developing organization of new products or processes	Product developed			Process developed		
	mainly by other enterprises or institutions	by enterprise or the group of enterprises	in cooperation with the other enterprises or institutions	mainly by other enterprises or institutions	by enterprise or the group of enterprises	in cooperation with the other enterprises or institutions
Number of enterprises in:						
industry	57	441	138	145	311	282
construction	17	55	7	65	59	30
services	35	237	98	94	210	146
Total in all sectors	109	733	243	304	580	458

Source: self elaboration according to the data from Eurostat on 13.1.2010

During the period 2004 – 2006, 574 of Slovak enterprises had decided to cooperate by creation and implementation of innovation with some of institutions or subjects operating in the country. The most important partners were suppliers of equipment, materials, components or software, i.e. 278 of enterprises cooperated with this partner (Tab. 3). The greatest interest in cooperation had small enterprises and their share on the total small innovative enterprises was 20,48%.

For the cooperation with other enterprises within the group of enterprises had decided 128 enterprises. In this case, mainly large and medium-sized enterprises cooperate. Several enterprises also had an interest to work with a very important group, with clients and customers.

The smallest interest had Slovak enterprises in cooperation with the government or public research institutions, where only one medium-sized enterprise, two large and six small enterprises preferred this type of cooperation.

Table 3. Number of enterprises in Slovak republic cooperating with other institutions in creation and implementation of innovation

Cooperative institution / size of enterprises	Total number of cooperative enterprises	Number of cooperative enterprises according to their size		
		small	medium	large
The cooperation of enterprises with:				
consultants, commercial labs, or private R&D institutes	37	7	16	13
government or public research institutes	9	6	1	2
universities or other higher education institutions	20	7	6	7
suppliers of equipment, materials, components or software	278	179	61	38
clients or customers	89	31	38	20
competitors or other enterprises of the same sector	12	2	6	4
other enterprises within your enterprise group	128	26	49	53

Source: self elaboration according to the data from Eurostat on 13.1.2010

If we want to evaluate the cooperation of Slovak enterprises in the period 2004 - 2006 with other enterprises by the country of their operation we find out that unlike the other V4 countries, Slovak enterprises preferred the cooperation with enterprises operating in various European countries. But the difference is not significant (Tab. 4). During this period the cooperation with European countries was preferred by 489 enterprises and the cooperation with enterprises operating in the Slovak Republic was preferred by 478 enterprises. The greatest interest in these two types of partners had the large enterprises (about 50% share of large cooperating enterprises on the total number of innovative enterprises), followed medium-sized enterprises with approximately 30,5% share and small businesses with an average 24% share.

The cooperation with the enterprises in USA or in other countries was preferred by 143 Slovak enterprises, whereby dominated large enterprises.

Table 4. Number of enterprises in Slovak republic cooperating in creation and implementation of innovation according to the country of partner operation

Cooperative institution / size of enterprises	Total number of cooperative enterprises	Number of cooperative enterprises according to their size		
		small	medium	large
Enterprise engaged in any type of innovation cooperation:				
within United States and other countries	143	42	39	63
national	478	205	152	121
within other Europe	489	214	151	125

Source: self elaboration according to the data from Eurostat on 13.1.2010

THE INNOVATION ACTIVITY OF POLISH ENTERPRISES

Poland is according to its area and population the largest country of V4 countries, what corresponds to the number of enterprises operating in this country. In 2006 were in Poland multiple numbers of enterprises in comparison with the Slovak republic. But from the total of 44 480 enterprises in Poland, only 23% of enterprises had decided to innovate their activities. The most innovative active were large enterprises (36,16%), but this group of enterprises was the least numerous group of enterprises in Poland (Tab. 5). In 2006, only 15,45% of small businesses decided to introduce innovation, either product, process innovation or both, product and process innovation [6].

The prevailing type of innovation introduced in this country was the combination of product and process innovation, but in contrast to the most countries, the enterprises didn't preferred product innovation, but process innovation.

Table 5. The enterprises with innovation activity according to the size and the type of implemented innovation in Poland

Size of enterprises/type of innovation	Total enterprises	Enterprises with innovation activity					Enterprises without innovation activity
		Total	Product and process innovation	Product innovation	Process innovation	Establish innovators, ongoing and/or abandoned only	
Small enterprises	31 951	4 937	2 182	945	1 713	98	27 014
Medium enterprises	10 339	3 895	1 862	639	1 289	105	6 445
Large enterprises	2 190	1 403	792	172	407	31	787

Source: self elaboration according to the data from Eurostat on 13.1.2010

In 2006 were dominated in Poland the industrial enterprises above the enterprises providing services (Figure 3). From the total of 27 874 enterprises in the industry, 6672, i.e. 23,94% of enterprises, had decided to invest money in the some type of innovation.

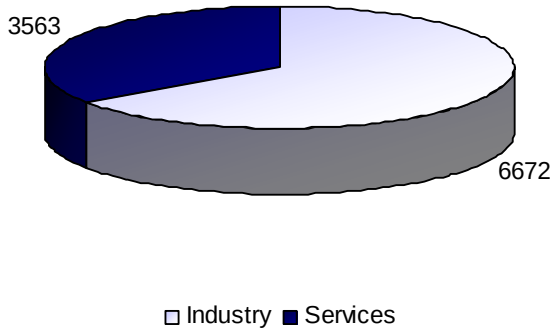

Fig. 3. The number of enterprises with innovation activity according to the sector in Poland

The highest activity was recorded in the innovative enterprises from the area of Manufacture of tobacco products, where even 90,91% of enterprises innovated their production. The second highest innovation activity was recorded in the industry of

coke, refined petroleum products and nuclear fuel production, with nearly 60% share of innovative enterprises in the total number of industrial enterprises.

On the other hand, the enterprises from the area of the Manufacture of garments, processing, dyeing of fur, consider innovating their production as a very risky, which is also reflected in their innovation activity. In 2006, only 7,24% of these enterprises had introduced some type of innovation. To the group of enterprises with the lowest innovation activity in Poland were also included enterprises from the area of Textile production and Manufacture of leather goods [6].

In the service sector even 78,55% of enterprises decided to introduce any innovation. The least innovative enterprises were enterprises providing services in the area of Land and pipeline transport, water transport, air transport with about 14% share of innovative enterprises in the total number of enterprises in this area.

The highest innovative activity (but in comparison with other V4 countries this activity was not very high) was recorded in enterprises providing Insurance and pension funds, except compulsory social security, where 68,35% of enterprises innovated their services and in enterprises providing Financial intermediation, except insurance and pension funds with 60,96% share of innovating enterprises in the total number of enterprises in this area.

In terms of the size of innovation active enterprises operating in various sectors, in 2006 dominated in the industry medium-sized enterprises with the number of employees between 50 and 249 and in the service sector dominated small enterprises. The number of large enterprises in both sectors was the lowest (Figure 4).

It is not possible to do the analysis of the data in the construction because the data for this area in Poland are unavailable.

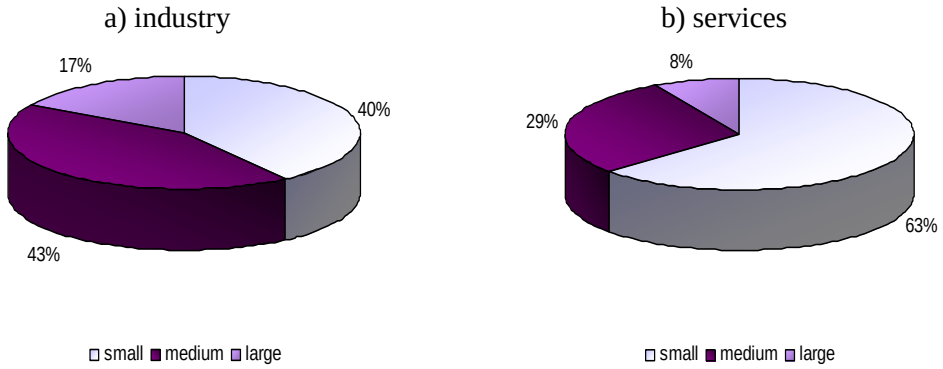

Fig. 4. The enterprises with the innovation activity according to their size in Poland

THE COOPERATION IN CREATING AND IMPLEMENTING INNOVATION IN POLAND

In Poland new products and processes were developed either in the enterprises themselves, or were developed by the group of enterprises or the enterprises cooperated with other enterprises, respectively they maintained these innovation activities to another company or institution. During the period 2004 - 2006, up 5 041 enterprises decided alone, respectively in cooperation with a group of enterprises to which they belong, to develop innovative products, while 70% of them were enter-

prises from the industry sector. Also the development of new process using this type of cooperation dominated in industrial enterprises, not in the enterprises providing services (Tab. 6).

Table 6. Product and process innovation according to the developing organization and the sector of their operation in Poland

Sector of enterprise's operation / developing organization of new products or processes	Product developed			Process developed		
	mainly by other enterprises or institutions	by enterprise or the group of enterprises	in cooperation with the other enterprises or institutions	mainly by other enterprises or institutions	by enterprise or the group of enterprises	in cooperation with the other enterprises or institutions
Number of enterprises in:						
industry	190	3 578	613	755	3 388	1 257
construction	n.a.	n.a.	n.a.	n.a.	n.a.	n.a.
services	392	1 463	356	790	1 425	630
Total in all sectors	582	5 041	969	1 545	4 813	1 887

Source: self elaboration according to the data from Eurostat on 13.1.2010

During the period 2004 - 2006 were in Poland 4 930 enterprises that had decided to develop and introduce new or significantly improved products and processes by using the cooperation with companies or institutions operating in this country (Tab. 7). The Polish enterprises were considered the most important collaborators in their innovation activities just suppliers of equipment, materials, components or software. From the number of 2 194 cooperating enterprises was the most numerous group of small enterprises with the 20,17% share of total number in innovative small enterprises. The least numerous was the group of large enterprises, but the share of cooperating large enterprises in the total number of innovation active enterprises was the highest, i.e. 24%.

Table 7. Number of enterprises in Poland cooperating with other institutions in creation and implementation of innovation

Cooperative institution / size of enterprises	Total number of cooperative enterprises	Number of cooperative enterprises according to their size		
		small	medium	large
The cooperation of enterprises with:				
consultants, commercial labs, or private R&D institutes	274	108	109	57
government or public research institutes	312	75	155	81
universities or other higher education institutions	195	51	100	44
suppliers of equipment, materials, components or software	2 194	996	862	337
clients or customers	897	417	317	163
competitors or other enterprises of the same sector	194	95	78	22
other enterprises within your enterprise group	864	230	361	272

Source: self elaboration according to the data from Eurostat on 13.1.2010

897 Polish enterprises had decided to cooperate with major groups, i.e. clients and customers, which significantly affected the demand for innovative products or processes. Then followed the cooperation with other enterprises within the group of enterprises and the cooperation with the government or public research institutions. This cooperation was preferred mostly by medium-sized enterprises.

The smallest interest had Polish enterprises in cooperation with universities or other higher education institutions and also with the competitors or other enterprises in the same sector with 1,90% share of the cooperating enterprises in the total number of innovating enterprises during the period.

According to the countries in which the partner operates, also in Poland the enterprises preferred the cooperation with domestic enterprises to the cooperation with foreign countries. During the period 2004 – 2006, 4 418 enterprises had decided to cooperate in developing and implementing the innovation at national level, whereby dominated the cooperation between the medium or small enterprises with other enterprises in the country (Tab. 8).

Again, the smallest interest had the Polish enterprises in cooperation with the United States and other countries in the world, where only 688 enterprises during the period had decided for this type of cooperation. The share of large enterprises using this type of cooperation in the total number of large innovative active enterprises was 16,54%, the share of medium-sized enterprises in the total number of innovating medium-sized enterprises was 5,65%. This type of cooperation was also preferred by 237 small enterprises, but their share in the total number of innovative small enterprises was only 4,80%.

Table 8. Number of enterprises in Poland cooperating in creation and implementation of innovation according to the country of partner operation

Cooperative institution / size of enterprises	Total number of cooperative enterprises	Number of cooperative enterprises according to their size		
		small	medium	large
Enterprise engaged in any type of innovation cooperation:				
within United States and other countries	688	237	220	232
National	4418	1789	1794	834
within other Europe	2231	696	907	627

Source: self elaboration according to the data from Eurostat on 13.1.2010

CONCLUSIONS

The article compares the innovation activity of Slovak and Polish enterprises. On the basis of the analysis we can state, that in both countries during the year 2006 dominated the interest of enterprises to introduce either product and process innovation, not only product or process innovation. The largest group of enterprises introducing some type of innovation were small enterprises, the least numerous were large enterprises. Looking at the sector of operating the innovative enterprises we can state that the most innovative active were industrial enterprises and the least were construction enterprises.

New or significantly improved product or process can by developed by various institutions from different countries. The enterprises in all three sectors during the period 2004 - 2006 preferred the development of new products or processes in their own enterprise or within the group of enterprises before the cooperation with other enterprises or institutions. The enterprises also preferred the cooperation with suppliers of equipment, materials, components or software, also with the clients or customers and other businesses within the group.

The article also includes the analysis of cooperation of domestic enterprises in the innovation's creation and development with other enterprises located in different countries. During the period 2004 - 2006 preferred the Polish enterprises the cooperation with domestic enterprises operating in the country, before the cooperation with enterprises or institutions operating in other European countries or in U.S. and other countries in the world. But Slovak enterprises mostly preferred the cooperation with other European countries.

REFERENCES

1. European Commission: *European innovation scoreboard 2007*. Comparative analysis of innovation performance, [online] February, 2008. Available on: <http://www.proinno-europe.eu/admin/uploaded_documents/European_Innovation_Scoreboard_2007.pdf>.
2. European Commission: *European innovation scoreboard 2008*. [online] February, 2009. Available on: <http://www.proinno-europe.eu/node/19299>.
3. European Commission: *INNO-Policy TrendChart – Innovation Policy Progress Report*. Slovak Republic 2009, January, 2010. Available on: <http://www.proinno-europe.eu/node/extranet/upload/countryreports/Country_Report_Slovakia_2009.pdf>.
4. European Commission: *Innovation Tomorrow: Innovation policy and the regulatory framework: Making innovation an integral part of the broader structural agenda.* France, 2002. 221 s. ISBN 92-894-4549-1
5. European Commission: *Communication from the commission on the European Competitiveness Report 2008*. [online] November, 2008. Available on: <http://ec.europa.eu/enterprise/enterprise_policy/competitiveness/doc/compet_rep_2008/com_2008_0774.pdf>.
6. Suhányi L.: *Inovatívny prístup k zabezpečeniu verejných služieb - verejno-súkromné partnerstvá*. In: Transfer inovácií, Košice: SjF, TU v Košiciach, 2009, č. 13, s. 61 – 64, ISSN 1337-7094
7. http://epp.eurostat.ec.europa.eu/portal/page/portal/science_technology_innovation/data/database
8. http://www.stat.gov.pl/cps/rde/xchg/gus
9. http://www.statistics.sk

ZESZYTY NAUKOWE POLITECHNIKI RZESZOWSKIEJ NR 274
Mechanika z. 81 2010

Marko TODOROV
Ivo DRAGANOV

Ruse University "Angel Kanchev", Bulgaria

EQUATIONS OF ELASTICITY THEORY IN A HELICAL COORDINATE SYSTEM

The present research provides working out the equations of solid elastic continuum in non-orthogonal helical coordinate system. A comparison has been drawn with regard to known equations of static, geometry and physics in a cylindrical coordinate system. Some examples have been provided solution to.

INTRODUCTION

Helical bodies have been known since ancient times [12]. The applications they were subject to have enjoyed a wide variety: transportation of liquids and cargo in-bulk, joining elements, transformation of rotation into translation, tools etc.

Various mathematical forms of describing, hence, understandings of the term "helical body" exist. According to [9] a helical body is formed when a cross-section of a particular shape having a normal helical line is set to motion. According to [2], the latter comes to exist when a spot moves round a circle keeping constant speed velocity while the circle oscillates keeping constant speed velocity into a direction which is normal to the plain it lies onto. This definition is quite suitable to use in defining helical coil springs since the cross-section mentioned afore disposes of a simple shape - most often circular or rectangular. According to [10] helical bodies are formed up when a cylinder has been taken off a section following a helical line but situated onto a plane that is defined by the rotation axis and the cylinder radius, pointing to the current position along the helical line.

In this present research a helical body is conceived of as one that has been formed up through simultaneous rotation along a constant axis and a translation in the direction which is normal to the plain it lies onto: Figure 1. It is possible that the rotation axis does not coincide with the weight centre of the cross-section, as is in cases with helical coil springs and screw of odd number of strokes.

The description of a stress-deformed state of the helical body in a helical coordinate system allows for an easier setting of boundary conditions.

Introduction of helical coordinate system has been adopted when solving some problems in domains of physics as well.

In [6] a beam having piezoelectric qualities has been regarded that allow for controlling the twisting of the beam itself. A tri-dimensional coordinate system has been introduced possessing straight axes whose orientation in relation to the initial coordinate system changes along the longitudinal axis thus drawing a helical line. The coordinate system being so defined represents an orthogonal one.

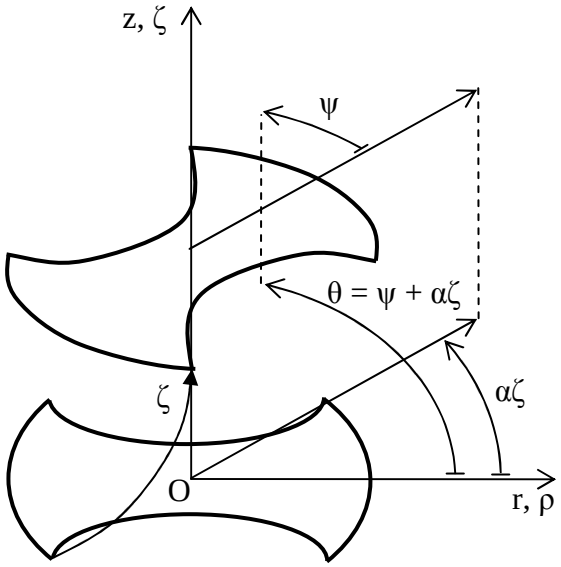

Figure 1. Formation of a helical body

In his dissertation [3] equations by Navier–Stokes have been worked out pertaining to laminar stream of non-Newtonian fluids in a helical tube and an orthogonal helical coordinate system has been defined

In the work of [1] a helical coil spring comes under regard having arbitrary length and a constant cross-section, loaded with a self-balanced system of forces at the one end. It has been proven that the principle of Saint-Venant is valid, and in order to manage calculations there has been introduced a helical coordinate system having straight lined axes and is non-orthogonal.

In [8] a modeling of a fluid stream passing through an extruder consisting of two jointly operating screws. For the purpose proper a Yu and Hu helical coordinate system has been introduced with one straight-line axis ζ, one radial axis ρ and a rotation angle ψ: Fig. 1. The coordinate system being so introduced is a non–orthogonal one. The link between the Cartesian and the so introduced coordinate system is as follows:

$$\begin{aligned} x^1 &= \xi^1 \cos(\xi^2 + \alpha\xi^3), \\ x^2 &= \xi^1 \sin(\xi^2 + \alpha\xi^3), \\ x^3 &= \xi^3. \end{aligned} \tag{1}$$

The inverse relation is:

$$\begin{aligned}
\xi^1 &= \sqrt{\left(x^1\right)^2 + \left(x^2\right)^2}\,, \\
\xi^2 &= -\alpha x^3 + arctg(\frac{x^2}{x^1})\,, \\
\xi^3 &= x^3\,.
\end{aligned} \tag{2}$$

Another research areas where the helical coordinate systems is in use - image recognition in geodesy [5], study of microorganisms' motion [4], modeling and research in laminar and turbulent stream [13].

EQUATION OF ELASTICITY THEORY IN HELICAL COORDINATE SYSTEM

1. Basis vectors, metric tensors and Christoffel symbols in a natural (covariant) and a dual (contravariant) helical coordinate systems.

A helical coordinate system has been defined in accordance with [8], with links between Cartesian and the new system provided through formulas (1) and (2). Denotes of coordinates in different coordinate systems are given in table 1.

Table 1: Denote coordinates

Cartesian coordinate system	Cartesian coordinate system – index record	Cylindrical coordinate system	Cylindrical coordinate system – index notation	Helical Coordinate system	Helical Coordinate System - index notation
x [m]	x^1 [m]	r [m]	y^1[m]	ρ [m]	ξ^1 [m]
y [m]	x^2 [m]	θ [-]	y^2[-]	ψ [-]	ξ^2 [-]
z [m]	x^3 [m]	z [m]	y^3[m]	ζ [m]	ξ^3 [m]

Basis vectors in the natural coordinate system have are as follows:

$$\begin{aligned}
\mathbf{g}_1 &= \cos\left(\xi^2 + \alpha\xi^3\right)\mathbf{e}_1 + \sin\left(\xi^2 + \alpha\xi^3\right)\mathbf{e}_2 = \mathbf{e}_1^* \text{ [-]}, \\
\mathbf{g}_2 &= -\xi^1 \sin\left(\xi^2 + \alpha\xi^3\right)\mathbf{e}_1 + \xi^1 \cos\left(\xi^2 + \alpha\xi^3\right)\mathbf{e}_2 = \rho\mathbf{e}_2^* \textbf{ [m]}, \\
\mathbf{g}_3 &= -\xi^1\alpha \sin\left(\xi^2 + \alpha\xi^3\right)\mathbf{e}_1 + \xi^1\alpha \cos\left(\xi^2 + \alpha\xi^3\right)\mathbf{e}_2 + \mathbf{e}_3 = \alpha\rho\mathbf{e}_2^* + \mathbf{e}_3^* \text{ [-]},
\end{aligned} \tag{3}$$

and in the dual one:

$$\begin{aligned}
\mathbf{g}^1 &= \mathbf{g}_1 = \mathbf{e}_1^* \text{ [-]}, \\
\mathbf{g}^2 &= B\mathbf{g}_2 - \alpha\mathbf{g}_3 = \frac{1}{\xi^1}\mathbf{e}_2^* - \alpha\mathbf{e}_3^* \textbf{ [1/m]}, \\
\mathbf{g}^3 &= -\alpha\mathbf{g}_2 + \mathbf{g}_3 = \mathbf{e}_3^* \text{ [-]},
\end{aligned} \tag{4}$$

where by $\mathbf{e}_i$ there have been marked single basis vectors in a Cartesian coordinate system, and by $\mathbf{e}_i^*$ there have been marked basis vectors in a cylindrical coordinate system.

The metric tensors in the natural and dual helical coordinate system are, accordingly:

$$\left[g_{ij}\right]=\left[\mathbf{g}_i\mathbf{g}_j\right]=\begin{bmatrix}1 & 0 & 0\\ 0 & \left(\xi^1\right)^2 & \alpha\left(\xi^1\right)^2\\ 0 & \alpha\left(\xi^1\right)^2 & \left(\alpha\xi^1\right)^2+1\end{bmatrix} \textbf{ and } [g^{ij}]=\begin{bmatrix}1 & 0 & 0\\ 0 & B & -\alpha\\ 0 & -\alpha & 1\end{bmatrix} \tag{5}$$

where $B=\dfrac{1+\left(\alpha\xi^1\right)^2}{\left(\xi^1\right)^2}$ [m^{-2}].

Metric tensors possess values other than zero out of the main diagonal due to the fact that the coordinate system is a non-orthogonal one.

Christoffel symbols of first order have been defined according to the following subordination:

$$\Gamma_{ijk}=\frac{1}{2}\left(g_{jk,i}+g_{ki,j}+g_{ij,k}\right) \tag{6}$$

and represent the following:

$$\Gamma_{ij1}=\begin{bmatrix}0 & 0 & 0\\ 0 & -\xi^1 & -\xi^1\alpha\\ 0 & -\xi^1\alpha & -\xi^1\alpha^2\end{bmatrix},\ \Gamma_{ij2}=\begin{bmatrix}0 & \xi^1 & \xi^1\alpha\\ \xi^1 & 0 & 0\\ \xi^1\alpha & 0 & 0\end{bmatrix},\ \Gamma_{ij3}=\begin{bmatrix}0 & \xi^1\alpha & \xi^1\alpha^2\\ \xi^1\alpha & 0 & 0\\ \xi^1\alpha^2 & 0 & 0\end{bmatrix}, \tag{7}$$

and those of second order according to the following subordination:

$$\Gamma_{ij}^{l}=g^{lk}\Gamma_{ijk} \tag{8}$$

and come in as follows:

$$\Gamma_{ij}^{1}=\begin{bmatrix}0 & 0 & 0\\ 0 & -\xi^{1} & -\xi^{1}\alpha\\ 0 & -\xi^{1}\alpha & -\xi^{1}\alpha^{2}\end{bmatrix},\ \Gamma_{ij}^{2}=\begin{bmatrix}0 & \frac{1}{\xi^{1}} & \frac{\alpha}{\xi^{1}}\\ \frac{1}{\xi^{1}} & 0 & 0\\ \frac{\alpha}{\xi^{1}} & 0 & 0\end{bmatrix},\ \Gamma_{ij}^{3}=\begin{bmatrix}0 & 0 & 0\\ 0 & 0 & 0\\ 0 & 0 & 0\end{bmatrix}. \qquad (9)$$

Since the coordinate axes are not straight linear, Christoffel symbols are other than zero.

The physical components of a vector go defined according to the following subordinations:

$\underline{v}^{i}=v^{i}\cdot\sqrt{g_{(ii)}}$ - covariant components and (10)

$\underline{v}_{i}=v_{i}\cdot\sqrt{g^{(ii)}}$ - as per contravariant components. (11)

In a helical coordinate system the physical components of a vector are defined according the following subordinations:

$$\underline{v}^{1}=v^{1};\ \underline{v}^{2}=\xi^{1}v^{2};\ \underline{v}^{3}=v^{3}\sqrt{\left(\alpha\xi^{1}\right)^{2}+1}\ \text{and} \qquad (12)$$

$$\underline{v}_{1}=v_{1};\ \underline{v}_{2}\frac{\sqrt{(\alpha\xi^{1})^{2}+1}}{\xi^{1}}v_{2};\ \underline{v}_{3}=v_{3}. \qquad (13)$$

2. Working out the equations of elasticity theory in a helical coordinate system.

The equations of elasticity theory in a general manner are known (arbitrary coordinate system) [7]:

The equations of static (equations of equilibrium) are as follows:

$$\tau^{ji}\big|_{j}+p^{i}=0, \qquad (14)$$

where with τ^{ji} there have been marked the stresses, and by p^{i} the volume forces.

Covariant derivative of tensor is:

$$\tau^{ij}\big|_{k}=\tau_{,k}^{ij}+\Gamma_{km}^{i}\tau^{mj}+\Gamma_{km}^{j}\tau^{im} \qquad (15)$$

Using equations (9) and (15) for helical coordinate system equilibrium equations we get:

$$\tau_{,1}^{11}+\tau_{,2}^{12}+\tau_{,3}^{31}+\frac{1}{\xi^{1}}\tau^{11}-\xi^{1}\tau^{22}-\xi^{1}\alpha^{2}\tau^{33}-2\xi^{1}\alpha\tau^{23}+p^{1}=0\ \ [\text{N/m}^{3}]$$

$$\tau^{12}_{,1} + \tau^{22}_{,2} + \tau^{23}_{,3} + \frac{3}{\xi^1}\tau^{12} + \frac{2\alpha}{\xi^1}\tau^{31} + p^2 = 0 \text{ [N/m}^4\text{]}$$
$$\tau^{31}_{,1} + \tau^{23}_{,2} + \tau^{33}_{,3} + \frac{1}{\xi^1}\tau^{31} + p^3 = 0 \text{ [N/m}^3\text{]} \quad (16)$$

Geometry equations go as follows:

$$\gamma_{ij} = \frac{1}{2}\left(v_i\big|_j + v_j\big|_i\right) = \frac{1}{2}\left(v_{i,j} + v_{j,i}\right) - \Gamma^k_{ij} v_k \,, \quad (17)$$

where γ_{ij} represent the strains and v_i represent displacements.

Using (9) we obtain as follows:

$$\gamma_{11} = v_{1,1} \text{ [-]}, \ \gamma_{22} = v_{2,2} + \xi^1 v_1 \text{ [m}^2\text{]}, \ \gamma_{33} = v_{3,3} + \alpha^2 \xi^1 v_1 \text{ [-]},$$
$$\gamma_{12} = \gamma_{21} = \frac{1}{2}(v_{1,2} + v_{2,1}) - \frac{1}{\xi^1} v_2 \text{ [m]}, \ \gamma_{23} = \gamma_{32} = \frac{1}{2}(v_{2,3} + v_{3,2}) + \alpha\xi^1 v_1 \text{ [m]}, \quad (18)$$
$$\gamma_{31} = \gamma_{13} = \frac{1}{2}(v_{3,1} + v_{1,3}) - \frac{\alpha}{\xi^1} v_2 \text{ [-]}.$$

Physics equations (Hook's law) go like this:

$$\tau^{ij} = C^{ijkl}\gamma_{kl} \,, \quad (19)$$

where C^{ijkl} is a tensor bearing material characteristics that may be represented as follows:

$$C^{ijkl} = G\left(g^{ik}g^{jl} + g^{il}g^{jk} + \frac{2\nu}{1-2\nu} g^{ij}g^{kl}\right). \quad (20)$$

In the last equation G is the marking of a second order elasticity module, and g^{ij} comes to be the mark of the metric covariant tensor.

If the additional subordinations be introduced:

$$\mu = G = \frac{E}{2(1+\nu)} \text{ [Pa]}, \ \lambda = \frac{E\nu}{(1+\nu)(1-2\nu)} \text{ [Pa]}, \ \nu = \frac{\lambda}{2(\lambda+\mu)} \text{ [-]},$$
$$E = \frac{\mu(3\lambda+2\mu)}{\lambda+\mu} \text{ [Pa]}, \quad (21)$$

where E comes to denote the first order elasticity module and ν be the mark Poisson's ratio then Hook's law comes to be:

$$\tau^{im} = 2\mu\gamma^{im} + \lambda g^{jm}\gamma^{i}_{j}\,. \tag{22}$$

Taking into account (5), (21) and the last equation what we get as per the helical coordinate system physics equations come to be the following:

$$\begin{aligned}
&\tau^{11} = \frac{2G}{1-2\nu}\left[(1-\nu)\gamma_{11} + \nu\left(B\gamma_{22} + \gamma_{33} - 2\alpha\gamma_{23}\right)\right],\ [\mathrm{N/m^2}],\\
&\tau^{22} = \frac{2G}{1-2\nu}\left[\nu B\gamma_{11} + (1-\nu)B^2\gamma_{22} + \left(\alpha^2 + \nu C\right)\gamma_{33} - 2\alpha B(1-\nu)\gamma_{23}\right],\ [\mathrm{N/m^4}],\\
&\tau^{33} = \frac{2G}{1-2\nu}\left[\nu\gamma_{11} + \left(\alpha^2 + \nu C\right)\gamma_{22} + (1-\nu)\gamma_{33} - 2\alpha(1-\nu)\gamma_{23}\right],\ [\mathrm{N/m^2}],\\
&\tau^{12} = \tau^{21} = 2G\left(B\gamma_{12} - \alpha\gamma_{31}\right),\ [\mathrm{N/m^3}],\\
&\tau^{23} = \tau^{32} = \frac{2G}{1-2\nu}\left\{\left[B(1-2\nu) + \alpha^2\right]\gamma_{23} - \alpha\left[\nu\gamma_{11} + B(1-\nu)\gamma_{22} + (1-\nu)\gamma_{33}\right]\right\}\ [\mathrm{N/m^3}],\\
&\tau^{31} = \tau^{13} = 2G\left(B\gamma_{31} - \alpha\gamma_{12}\right),\ [\mathrm{N/m^2}].
\end{aligned} \tag{23}$$

In equations (23) the following denotation has been introduced: $C = \dfrac{1-\left(\alpha\xi^1\right)^2}{\left(\xi^1\right)^2}$.

In order to define the physical components of a strain tensor there has been used the subordination [14]:

$$\underline{\tau}^{ij} = \tau^{ij}\sqrt{\frac{g_{jj}}{g^{ii}}} \tag{24}$$

In a helical coordinate system the physical components of stress tensor acquire the following representation:

$$\begin{aligned}
&\underline{\tau}^{11} = \tau^{11};\ \underline{\tau}^{22} = \frac{(\xi^1)^2}{\sqrt{(\alpha\xi^1)^2+1}}\tau^{22};\ \underline{\tau}^{33} = \sqrt{(\alpha\xi^1)^2+1}\,\tau^{33},\\
&\underline{\tau}^{12} = \xi^1\tau^{12};\ \underline{\tau}^{21} = \frac{\xi^1}{\sqrt{(\alpha\xi^1)^2+1}}\tau^{21};\ \underline{\tau}^{12} \neq \underline{\tau}^{21},\ \underline{\tau}^{23} = \xi^1\tau^{23};\ \underline{\tau}^{32} = \xi^1\tau^{32},\\
&\underline{\tau}^{31} = \tau^{31};\ \underline{\tau}^{13} = \sqrt{(\alpha\xi^1)^2+1}\,\tau^{13};\ \underline{\tau}^{13} \neq \underline{\tau}^{31}.
\end{aligned} \tag{25}$$

How it sees the tensor of physical components is non-symmetric.

Conditions of surface (Cauchy's equations). The full stress vector $\mathbf{t}^n$ in a plane with normal vector $\boldsymbol{n}$ will by express by the covariant basis vectors:

$$\mathbf{t}^n = t^{k(n)}\mathbf{g}_k\,, \tag{26}$$

Figure 2 provides the single normal vectors to coordinate surfaces. They are collinear by contravariant basis vectors.

The physical components of normal stresses to coordinate surfaces are:

$$\underline{\sigma}^{\rho} = t^{1(\rho)} = \tau^{11};\ \underline{\sigma}^{\psi} = \sqrt{\frac{1}{g^{(22)}}}\, t^{2(\psi)} = \frac{1}{B}\tau^{22} = \frac{(\xi^1)^2}{(\alpha\xi^1)^2+1}\tau^{22};\ \underline{\sigma}^{\zeta} = t^{i(\zeta)} = \tau^{33}, \tag{27}$$

and tangential ones are:

$$\begin{aligned}
&\underline{\tau}^{(\rho)} = \sqrt{(\xi^1\tau^{12})^2 + (\tau^{13})^2[(\alpha\xi^1)^2+1] + 2\tau^{12}\tau^{13}\alpha(\xi^1)^2}\,,\\
&\underline{\tau}^{(\psi)} = \\
&\sqrt{\frac{(\xi^1)^2}{(\alpha\xi^1)^2+1}\{(\tau^{21})^2 + (\tau^{22})^2\frac{\alpha^2(\xi^1)^4}{(\alpha\xi^1)^2+1} + 2\tau^{22}\tau^{23}\alpha(\xi^1)^2 + (\tau^{23})^2[(\alpha\xi^1)^2+1]\}}\,,\\
&\underline{\tau}^{(\zeta)} = \sqrt{(\tau^{31})^2 + (\xi^1\tau^{32})^2 + (\tau^{33})^2(\alpha\xi^1)^2 + 2\tau^{32}\tau^{33}\alpha(\xi^1)^2}\,.
\end{aligned} \tag{28}$$

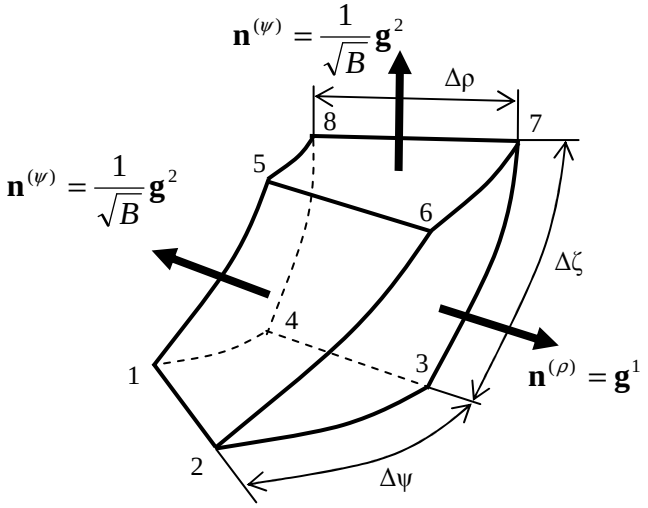

Figure 2. Single normal vectors to coordinate surfaces

3. Comparison of results to a cylindrical coordinate system

If in equations of elasticity theory in helical coordinate system we replace α = 0, the following expressions come out:

Equations of static:

$$\begin{aligned}
&\tau^{11}_{,1} + \tau^{21}_{,2} + \tau^{31}_{,3} + \frac{1}{y^1}\tau^{11} - y^1\tau^{22} + p^1 = 0 \ \text{[N/m}^3\text{]}\\
&\tau^{12}_{,1} + \tau^{22}_{,2} + \tau^{32}_{,3} + \frac{3}{y^1}\tau^{12} + p^2 = 0 \ \text{[N/m}^4\text{]}\\
&\tau^{13}_{,1} + \tau^{23}_{,2} + \tau^{33}_{,3} + \frac{1}{y^1}\tau^{31} + p^3 = 0 \ \text{[N/m}^3\text{]}
\end{aligned} \tag{29}$$

Equations of geometry:

$$\gamma_{11} = v_{1,1}\ [-],\ \gamma_{22} = v_{2,2} + y^1 v_1\ [m^2],\ \gamma_{33} = v_{3,3}\ [-],\ \gamma_{12} = \gamma_{21} = \frac{1}{2}(v_{1,2} + v_{2,1}) - \frac{1}{y^1} v_2 \quad (30)$$

$$[m],\ \gamma_{23} = \gamma_{32} = \frac{1}{2}(v_{2,3} + v_{3,2})\ [m],\ \gamma_{31} = \gamma_{13} = \frac{1}{2}(v_{3,1} + v_{1,3})\ [-].$$

Equations of physics:

$$\begin{aligned}
\tau^{11} &= \frac{2G}{1-2\nu}[(1-\nu)\gamma_{11} + \nu(\frac{\gamma_{22}}{(y^1)^2} + \gamma_{33})]\ [N/m^2], \\
\tau^{22} &= \frac{2G}{(1-2\nu)(y^1)^2}\ [(1-\nu)\frac{\gamma_{22}}{(y^1)^2} + \nu(\gamma_{11} + \gamma_{33})]\ [N/m^4], \\
\tau^{33} &= \frac{2G}{1-2\nu}\ [(1-\nu)\gamma_{33} + \nu(\gamma_{11} + \frac{\gamma_{22}}{(y^1)^2})]\ [N/m^2],
\end{aligned} \quad (31)$$

$$\tau^{12} = \tau^{21} = 2G\frac{\gamma_{12}}{(y^1)^2}\ [N/m^3],\ \tau^{23}\ \tau^{32} = 2G\frac{\gamma_{23}}{(y^1)^2}\ [N/m^3],\ \tau^{31} = \tau^{13} = 2G\gamma_{31}$$

$[N/m^2]$.

Those are the equations of elastic continuum in a cylindrical coordinate system equations worked out in [11], to which corresponds the helical one in view of the replacement introduced.

4. Examples

Example A. Let there be a displacement vector in a helical coordinate system:

$$\begin{Bmatrix} v_1 \\ v_2 \\ v_3 \end{Bmatrix} = \begin{Bmatrix} a\xi^1 \\ b\xi^1 \\ \alpha b\xi^1 + c\xi^3 \end{Bmatrix}.$$

Using equations (18) the deformation tensor comes to be:

$$\begin{bmatrix} \gamma_{11} & \gamma_{21} & \gamma_{31} \\ \gamma_{12} & \gamma_{22} & \gamma_{32} \\ \gamma_{13} & \gamma_{23} & \gamma_{33} \end{bmatrix} = \begin{bmatrix} a & -\frac{b}{2} & -\frac{b\alpha}{2} \\ -\frac{b}{2} & a(\xi^1)^2 & a\alpha(\xi^1)^2 \\ -\frac{b\alpha}{2} & a\alpha(\xi^1)^2 & c + a(\alpha\xi^1)^2 \end{bmatrix}.$$

Using equations (23) for the stress tensor we obtain:

$$\begin{bmatrix} \tau_{11} & \tau_{21} & \tau_{31} \\ \tau_{12} & \tau_{22} & \tau_{32} \\ \tau_{13} & \tau_{23} & \tau_{33} \end{bmatrix} = 2G \begin{bmatrix} \dfrac{(a+\nu c)}{(1-2\nu)} & -\dfrac{b}{2\left(\xi^1\right)^2} & 0 \\ -\dfrac{b}{2\left(\xi^1\right)^2} & \dfrac{\dfrac{a+\nu c}{\left(\xi^1\right)^2}+\alpha^2[c+\nu(2a-c)]}{(1-2\nu)} & -\dfrac{\alpha[c+\nu(2a-c)]}{(1-2\nu)} \\ 0 & -\dfrac{\alpha[c+\nu(2a-c)]}{(1-2\nu)} & \dfrac{[c+\nu(2a-c)]}{(1-2\nu)} \end{bmatrix}.$$

Volume forces vector comes to be the following:

$$\begin{Bmatrix} p^1 \\ p^2 \\ p^3 \end{Bmatrix} = \begin{Bmatrix} 0 \\ -2G\dfrac{b}{2\left(\xi^1\right)^3} \\ 0 \end{Bmatrix}.$$

Example B. If helical coordinate system displacement functions be provided as follows:

$$u_1 = a.\cos\left(\xi^2+\alpha.\xi^3\right)+b.\sin\left(\xi^2+\alpha.\xi^3\right),\ u_2 = -a.\xi^1.\cos\left(\xi^2+\alpha.\xi^3\right)+b.\xi^1.\sin\left(\xi^2+\alpha.\xi^3\right)$$
$$u_3 = -a.\alpha.\xi^1.\cos\left(\xi^2+\alpha.\xi^3\right)+b.\alpha.\xi^1.\sin\left(\xi^2+\alpha.\xi^3\right)+c$$

when using equations (18) what is obtained concerning deformations is as follows:

$$\gamma_{11} = \gamma_{22} = \gamma_{33} = \gamma_{12} = \gamma_{23} = \gamma_{31} \equiv 0\,.$$

Indeed, that corresponds to displacement of a rigid helical body.

Example C. Tension-compression of a cylindrical body.

Let displacements be provided in the following manner:

$$u_1 = \cos\left(\xi^2+\alpha\xi^3\right)\left[-\frac{\mu.F.\xi^1\cos\left(\xi^2+\alpha\xi^3\right)}{E.S}+C.\xi^1.\sin\left(\xi^2+\alpha\xi^3\right)-A.\xi^3+a_0\right]+$$
$$+\sin\left(\xi^2+\alpha\xi^3\right)\left[-\frac{\mu.F.\xi^1\sin\left(\xi^2+\alpha\xi^3\right)}{E.S}+B\xi^3-C\xi^1.\cos\left(\xi^2+\alpha\xi^3\right)+b_0\right],$$
$$u_2 = -\xi^1.\sin\left(\xi^2+\alpha\xi^3\right)\left[-\frac{\mu.F.\xi^1\cos\left(\xi^2+\alpha\xi^3\right)}{E.S}+C.\xi^1.\sin\left(\xi^2+\alpha\xi^3\right)-A.\xi^3+a_0\right]+$$
$$+\xi^1.\cos\left(\xi^2+\alpha\xi^3\right)\left[-\frac{\mu.F.\xi^1\sin\left(\xi^2+\alpha\xi^3\right)}{E.S}+B\xi^3-C\xi^1.\cos\left(\xi^2+\alpha\xi^3\right)+b_0\right],$$
$$u_2 = -\xi^1.\alpha.\sin\left(\xi^2+\alpha\xi^3\right)\left[-\frac{\mu.F.\xi^1\cos\left(\xi^2+\alpha\xi^3\right)}{E.S}+C.\xi^1.\sin\left(\xi^2+\alpha\xi^3\right)-A.\xi^3+a_0\right]+$$

$$+\xi^1.\alpha.\cos\left(\xi^2+\alpha\xi^3\right)\left[-\frac{\mu.F.\xi^1\sin\left(\xi^2+\alpha\xi^3\right)}{E.S}+B\xi^3-C\xi^1.\cos\left(\xi^2+\alpha\xi^3\right)+b_0\right]+$$

$$+\frac{F.\xi^3}{E.S}+A.\xi^1.\cos\left(\xi^2+\alpha\xi^3\right)-B.\xi^1.\sin\left(\xi^2+\alpha\xi^3\right)+c_0.$$

Strains in lieu of equation (18) are:

$$\gamma_{11}=-\frac{\mu F}{ES},\ \gamma_{22}=-\frac{\left(\xi^1\right)^2\mu F}{ES},\ \gamma_{33}=-\frac{F\left[\left(\xi^1\right)^2\alpha^2\mu-1\right]}{E.S},\ \gamma_{23}=-\frac{\left(\xi^1\right)^2\alpha\mu F}{ES},$$
$$\gamma_{12}=\gamma_{31}=0.$$

Stresses from (23) are:

$$\tau^{22}=\frac{\alpha^2F}{S},\ \tau^{33}=\frac{F}{S},\ \tau^{23}=-\frac{\alpha F}{S},\qquad(32)$$
$$\tau^{11}=\tau^{12}=\tau^{31}=0.$$

Boundary conditions from equations (27) and (28) are:

$$\underline{\sigma}^{\rho}=\tau^{11}=0,\ \underline{\sigma}^{\psi}=\frac{\left(\xi^1\right)^2}{\left(\alpha\xi^1\right)^2+1}\tau^{22}=\frac{\left(\alpha\xi^1\right)^2}{\left(\alpha\xi^1\right)^2+1}\frac{F}{S},\ \underline{\sigma}^{\zeta}=\tau^{33}=\frac{F}{S},$$

$$\underline{\tau}^{\rho\psi}=\xi^1\left(\tau^{12}+\alpha\tau^{13}\right)=0,\ \underline{\tau}^{\psi\rho}=\frac{1}{\sqrt{B}}\tau^{21}=0,$$

$$\underline{\tau}^{\psi\zeta}=\frac{\alpha\left(\xi^1\right)^3}{1+\left(\alpha\xi^1\right)^2}\tau^{22}+\xi^1\tau^{23}=-\frac{\alpha\xi^1}{\left(\alpha\xi^1\right)^2+1}\frac{F}{S},\ \underline{\tau}^{\zeta\psi}=\xi^1\left(\tau^{32}+\alpha\tau^{33}\right)=0,$$

$$\underline{\tau}^{\rho\zeta}=\frac{\alpha\left(\xi^1\right)^2}{\sqrt{1+\left(\alpha\xi^1\right)^2}}\tau^{12}+\sqrt{1+\left(\alpha\xi^1\right)^2}\tau^{13}=0,\ \underline{\tau}^{\zeta\rho}=\tau^{31}=0.$$

If we transform equations (32) into a Cartesian coordinate system using the transformation matrix:

$$\begin{bmatrix}\cos\left(\xi^2+\alpha.\xi^3\right) & \sin\left(\xi^2+\alpha.\xi^3\right) & 0\\ -\xi^1\sin\left(\xi^2+\alpha.\xi^3\right) & \xi^1\cos\left(\xi^2+\alpha.\xi^3\right) & 0\\ -\xi^1\alpha\sin\left(\xi^2+\alpha.\xi^3\right) & \xi^1\alpha\cos\left(\xi^2+\alpha.\xi^3\right) & 1\end{bmatrix},$$

what we get is:

$\sigma_z = \frac{F}{S}$, $\sigma_x = \sigma_y = \tau_{xy} = \tau_{yz} = \tau_{zx} = 0$, which corresponds to tension-compression.

CONCLUSION

The equations worked out describe the qualities of an elastic continuum in a helical coordinate system. They allow for provision of boundary conditions of a helix shaped body in a fairly simple manner. Comparison of obtained equations to known ones in a cylindrical coordinate system indicates that when replacing parameter $\alpha = 0$, they coincide. Examples solved illustrate the link between displacements, strains and stresses in a helical coordinate system. The task remains left ajar as per tension-compression and torsion of a helical body.

REFERENCES

1. Batra R.: *Saint-Venant's Principle for a Helical Spring*. Journal of applied mechanics, Vol. 45, No. 2, 297 - 301, June 1978.
2. Bermant A., Aramanovich I.: *Short course mathematical analysis*. Nauka, Moscow, 1966.
3. Cheng L.: *Mathematical Modeling of Laminar and Turbulent Single-phase and Two-phase Flows in Straight and Helical Ducts*. North Carolina State University, 2004.
4. Chwang A.: *Helical movements of flagellated propelling microorganisms*. California Institute of Technology Pasadena, California, 1971.
5. Claerbout J.: *Image Estimation by Example*: Geophysical soundings image construction Multidimensional autoregression. Stanford University, 2008.
6. Dienerowitz F.: *Dar Helixaktor Zum Konzept eines vorverwundenen Biegeaktors*. Universität Kalstuhe, 2008.
7. Eschenauer H., Schnell W.: *Elastizitätstheorie Grundlagen, Flächentragwerke, Strukturoptimie_-ung*. Wissenschaftsverlag, 1995.
8. Esley J.: *Dynamic Modelling Measuremant and Control of Co-rotating Twin-Screw Extruders*. Department of Chemical Engineering, University of Sydney, 2002.
9. Feodosiev V.: *Strength of materials*. Technica, Sofia, 1965.
10. Hristov D., Nachev S.: *Calculating and constructing of machine elements*. Technica, Sofia, 1963.
11. Koltunov M., Vasilev Y.: *Elasticity and strength of cylindrical bodies*. Vyssha shcola, Moscow, 1975.
12. Rorres C.: *The Turn of the Screw: Optimal Design of an Archimedes Screw*. Journal of hydraulic engineering, January, 72-80, 2000.
13. Toyokura T., Kurokawa J., Kumoto Y.: *Three-dimensional Boundary Layer Flow on Rotating Blades*. Bulletin of the JSME, Vol. 25, No. 202, 513-520, 1982.
14. Truesdell C.: *The physical components of vectors and tensors*. A.angew. Math Mech. Bd. 33 Nr. 10/11 Okt./Nov., 345-356, 1953.
15. Trusdell C.: *Primary course in rational continuum mechanics*. Mir, Moscow, 1975.

ZESZYTY NAUKOWE POLITECHNIKI RZESZOWSKIEJ NR 274
Mechanika z. 81 2010

Ján VARGA
František GREŠKOVIČ

Technical Univerzity in Košice, Slovakia

THE INFLUENCE OF RADIATION CROSSLINKING ON MECHANICAL PROPERTIES OF PLASTICS

The presented article deals by the application area of radiation cross-linking of plastics, which follows after the processing (injection moulding, extrusion or blow moulding). The main objective of the presented article is investigation of influence irradiation dosage on mechanical properties of materials: PP filled by 15 % of mineral filler – talc. Mechanical properties - tensile strength were examined in dependence on absorbed dose of the beta rays on various conditions and were compared with non-irradiated samples

INTRODUCTION

The cross-linking of plastics is a chemical process, in which particular molecules of plastics are connected together. In an ideal case, all the molecules will be integrated into the above mentioned grid and the process can be activated by radiation in case of many plastics.

Cross linking will be initiated by irradiating with high energy electron beams or gamma rays. The energy resulting from the irradiation is absorbed by the plastic. The main difference between beta and gamma rays lies in their abilities of penetrating the irradiated material. Gamma rays have a high penetration capacity. The penetration capacity of electron rays depends on the energy of the accelerated electrons [1].

Radiation of plastics is a way to crosslink them and to improve considerably their properties. The most important properties of cross-linking systems are tensibility and elasticity, which also remain under long-time temperature and mechanical loading.

For cross-linking, no other ingredients are necessary with using the radiation and the main advantage is that the process of cross-linking starts after the process of injection, extrusion or blow moulding. Radiation cross-linking takes place in room temperature without additional loading of the product. Another advantage is the possibility of changing the level of cross-linking in radiated parts by changing the radiation parameters. Irradiated products are not radioactive [2].

MATERIAL AND TREATMENT

For experiments was used material Hostacom CR 250 F G61330. The choice of material was made in view application by plastic parts product for automotive industry.

Material Hostacom CR 250 F G61330 – is a material, which is filled by 15 % mineral filler – talc. Its good mechanical properties, good scratch resistance and can be processing by different of technology – injection moulding, blow moulding, or extrusion. The using find in automotive, electronics, engineering and consumer industries. The manufacturer of the material is a company Basell Polyolefins.

Tab. 1 Mechanical properties of tested material

Hostacom CR 250 F G61330	Unit	Value
Tensile strength	MPa	18
Relation elongation	%	9
Modulus of elasticity	MPa	1900
IZOD impact test (23˚C)	kJ/m²	16

The test samples without cross-linking agent were produced on the injection moulding machine DEMAG ERGOTECH PRO 25 – 80 (Fig. 1) and on the injection moulding machine ARBURG 370 S 800 – 350 (Fig. 2) were produced test samples, which were scilicet by cross-linking agent.

It was used injection mould with replaceable mould boards. The processing conditions during the injection moulding were according to the recommendation of the producers.

Fig. 1. Injection moulding machine - DEMAG

Fig. 2. Injection moulding machine - ARBURG

To prepare of test samples for the irradiation was necessary to mix granulate materials with different cross-linking agent. It was the type of cross-linking agent. TAIC - Tryallyloxy-1 ,3,5-triazine. The manufacturer is a company Sigma Aldrich.

For evaluation of tensile properties of plastics was made according to EN ISO 527-1, 2 and was used sample type 1A for testing.

The test samples were controlled after injection moulding process and after the conditioning time. Tensile test was carried out on tensile machine TIRA- test 2300. It

was tested in 5 samples of each type of materials in standard ambient and after UV exposure chamber.

The artificial aging test by fluorescent UV lamps were made in the UV chamber according to EN ISO 4892-3, exposure time 28 days at 12 hour cycles for all test materials. The test samples after removal of UV chambers were conditioned according to ISO 291:2008. Afterwards, was performed tensile test to detect changes in the properties of the materials after artificial aging by UV fluorescent lamps according to above-mentioned methodology.

EXPERIMENTAL RESULTS

The graphic dependence of the measured average values of tensile strength of test samples in a standard ambient and degradation in UV chamber in Fig. 4.

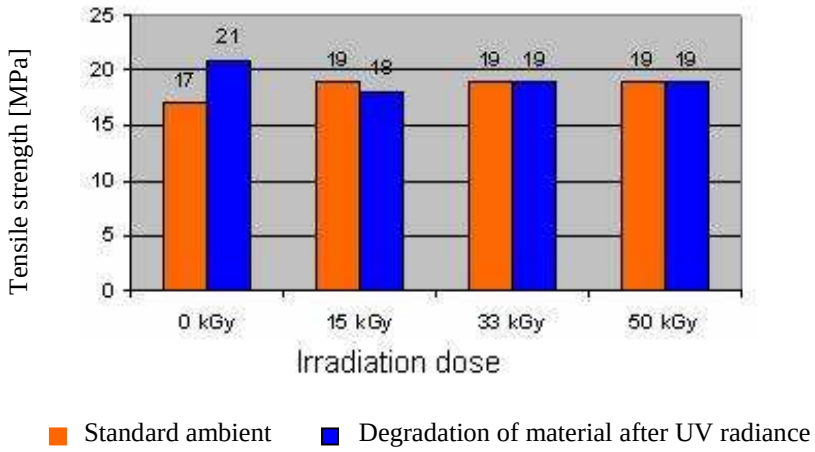

Fig. 3. Comparisons of tensile strength of tested materials

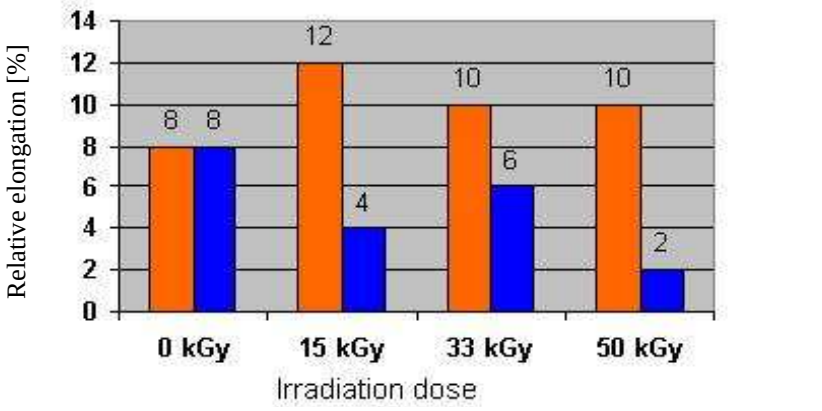

Fig. 4. Comparisons of relative elongation of tested materiale

The fracture areas of test samples after tensile test were observed on scanning electron microscope JEOL JSM - 7000F, Japan.

The fracture areas of test samples of non irradiated and irradiated materials with different of radiation dose in standard ambient after tensile test are in Figs. 5 to 8.

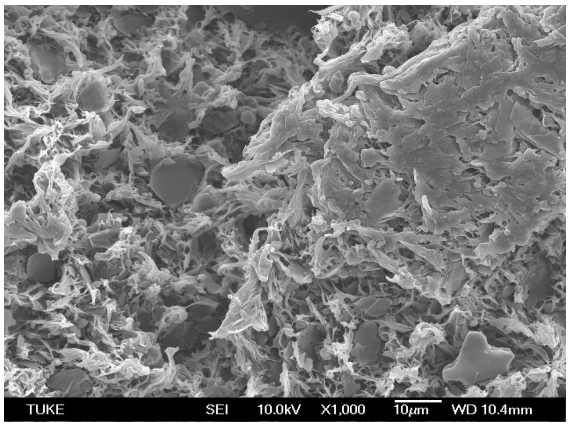

Fig. 5. The fracture area – non irradiated

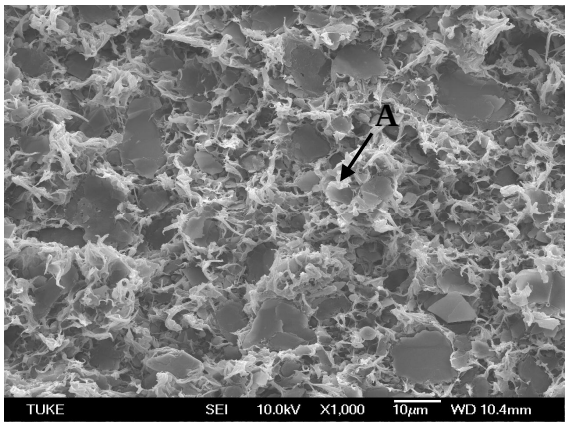

Fig. 6. The fracture area – irradiated 15 kGy

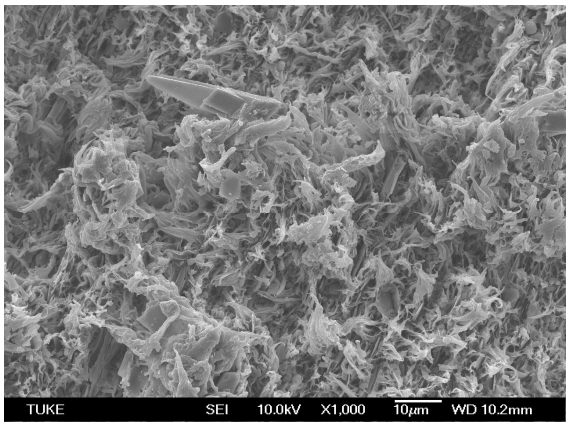

Fig. 7. The fracture area irradiated 33 kGy

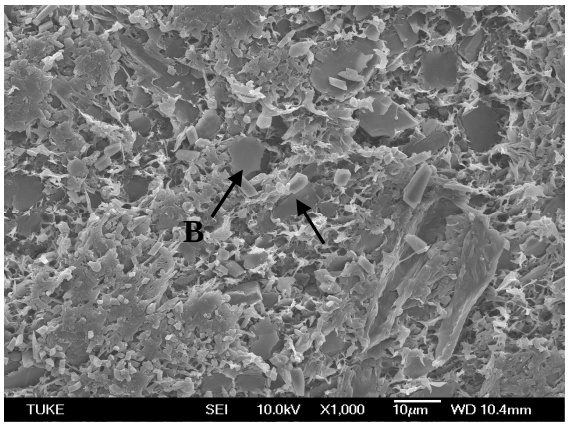

Fig. 8. The fracture area irradiated 50 kGy

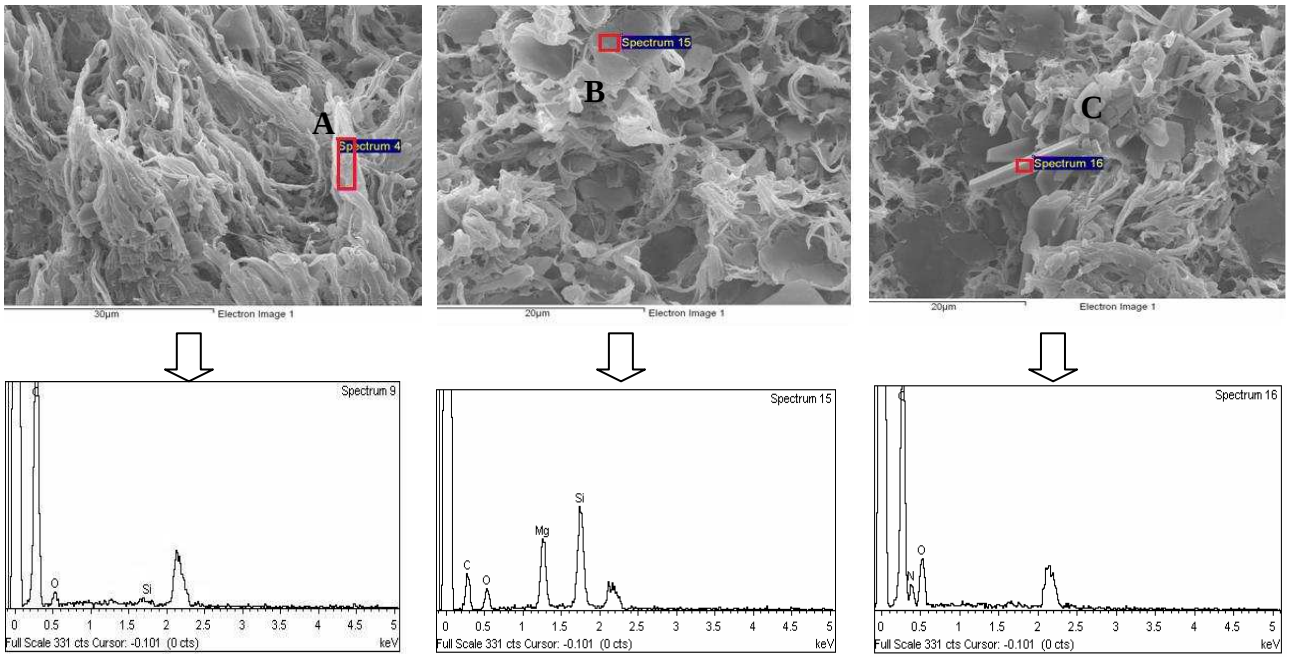

Fig. 9. The spectrum of the chemical composition of tested material

The spectrum of the by cross–linked can be seen increasing density of crosslink-king, a sufficient number of cross-linked areas. For all test samples there has been a brittle fracture of testing samples [3].

The spectrum of the chemical composition shown in Fig. 9 confirmed for scanning images of test samples in standard ambient the presence of chemical elements. These were the elements of the polymer - A label, the elements of filler - B label and the elements of cross-linking agent (TAIC) - label C.

The fracture areas of test samples of non irradiated and irradiated materials with different of radiation dose after degradation in UV chamber after tensile test are in Fig. 10 to Fig. 13 [3].

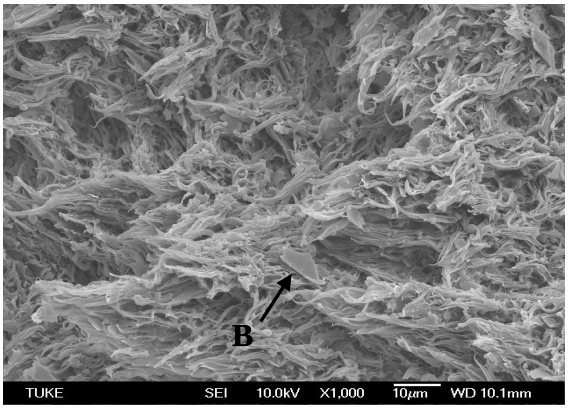

Fig. 10. The fracture area – non irradiated

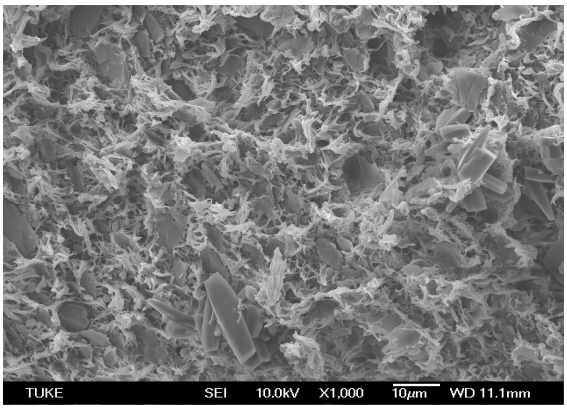

Fig. 11. The fracture area – irradiated 15 kGy

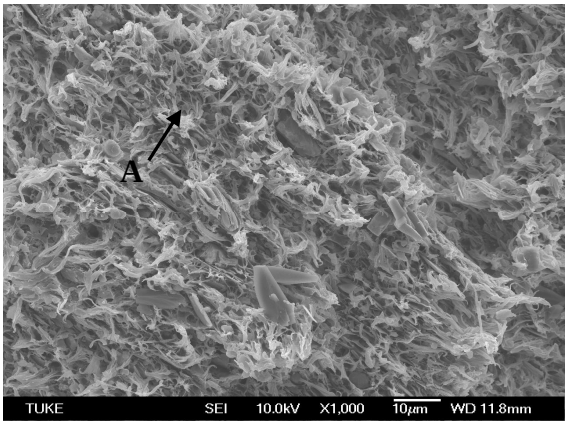

Fig. 12. The fracture area – irradiated 33 kGy

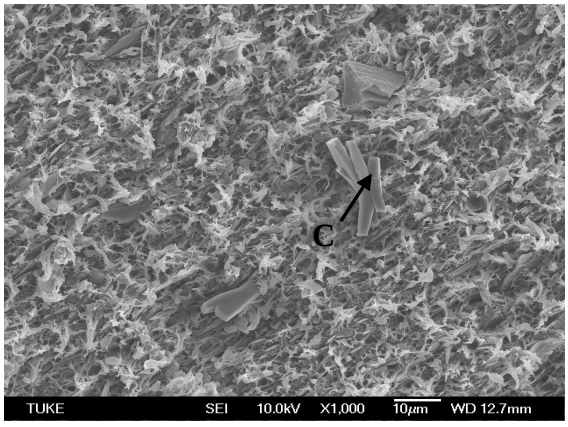

Fig. 13. The fracture area – irradiated 50 kGy

DISCUSSION

On the basis of the experimental results of mechanical tests the following conclusions could be formulated:

- After tensile test with material Hostacom CR G61330 250 F G61330 by test samples in standard ambient was found increasing tendency of tensile strength and relation elongation. We can state, that the values of tensile strength and relation elongation were influenced by irradiation dose – Fig. 3.
- The value of tensile strength achieved increasing tendency by irradiated test samples in standard ambient against the base material about 10%. By irradiated test

samples after degradation in UV chamber were achieved the values of tensile strength decreasing tendency. These values were influenced by irradiation dose about 10 – 15%.

- Irradiated test samples in standard ambient had against non irradiated material progressive tendency of relative elongation. These values were influenced by irradiation dose about 25 – 50%. Irradiated test samples after degradation in UV chamber had against non irradiated material decreasing tendency of relative elongation. These values were influenced by irradiation dose about 25 – 75%.

The final properties of composites filled with fillers depend on many parameters such as properties of matrix and reinforcement, configuration and consistence of the surface with a filler matrix. The consistence of matrix with filler has a high influence on the resulting tension transfer on the reinforcement and also on final mechanical properties.

CONCLUSIONS

Obtained knowledge in this paper are only parts of the general problem of possible applications of plastics cross-linking.

As the automotive industry using a wide range of plastics, it would be suitable to extend the experiments to other materials and monitoring of other properties such as:

- bonding – gluing and coating (adhesion improvement),
- the influence on welding property, change of colours,
- thermo-analyses,
- recycling of cross-linked plastics.

REFERENCES

1. Gamma irradiatiors for radiation processing, International atomic energy agency. Vienna, Austria 1 – 40 s.

2. Brocka Z: *Strahlenvernetzte Kunstoffe Verarbeitung, Eigenschaften, Anwendung*. Springer VDI Verlag, Düsseldorf 2006. ISBN 3-935065-30-2.

3. Varga J.: *Vplyv radiačného sieťovania na mechanické vlastnosti výliskov*. Doktorandská dizertačná práca, TU v Košiciach, Strojnícka fakulta. 2009.

ZESZYTY NAUKOWE POLITECHNIKI RZESZOWSKIEJ NR 274
Mechanika z. 81 2010

Ján VIŇÁŠ
Janette BREZINOVÁ
Anna GUZANOVÁ

Technical University of Košice, Slovakia

TRIBOLOGICAL PROPERTIES OF SELECTED CERAMIC COATINGS

The contribution deals with methods of plasma sprayed ceramic materials evaluation. There were evaluated ceramic coatings A 99, Cr_2O_3 and Cr_2O_3 + 5% TiO_2. Influence of the interlayer NiCr on the functional properties of sprayed coatings was also studied. There were determined thickness, microhardness and adhesion of particular coatings together with their resistance to abrasive wear and thermal cyclic loading.

INTRODUCTION

One way to improve the functional properties of machine parts is the using of the protective coatings with improved properties relative to the base material. Therefore, there is intensive development of new material combinations that enable new, qualitatively higher concept of products. One possibility of coating deposition is thermal spraying methods. Another utilization of thermal spraying is the renovation of worn surfaces of the parts, machinery and tools. [1-4, 6-8]

MATERIALS AND METHODS

The test samples for coatings deposition were made of low carbon steel S235JRG1. Surface pre-treatment of test samples was realised by abrasive blasting using brown corundum. Granularity of blasting medium was characterized by mean particle size d_z = 0.75 mm. Blasting medium was accelerated by compressed air, air pressure was 0.4 MPa.

Microgeometry of the blasted surfaces and applied coatings was evaluated according to STN ISO 4287 by stylus roughness tester Surftest SJ – 301, Mitutoyo. For the thermal spraying of coatings equipment with the gas stabilization of the arc Sulzer METCAL 9MCE was used.

Before deposition of all studied types of ceramic materials interlayer of composite NiCr (83% Ni +17% Cr, particle size 45±5 μm) by flame spraying using the torch NPK2 on pretreated substrate was applied. NiCr is often used as an interlayer under refractory materials such as Al_2O_3, ZrO_2 and ZrSiO4. NiCr interlayer provides better adhesion to the base material, balances the CTE substrate and ceramic layers.

The materials used to coatings formation:

1) A 99 - corundum (αAl_2O_3 ρ = 3.97 g.cm^{-3}, melting point 2040°C, evaporation temperature of 2980 °C, $CTE_{(200–800)}$ = 7.8x10^{-6}K^{-1}).

2) Chromium oxide Cr_2O_3 (melting point 2265°C, density ρ = 5.2 g.cm^{-3} and the value of open porosity (OP) of 6.2 %, $CT_{E(20–500)}$ = 7.2x10^{-6}K^{-1}).

3) Cr_2O_3 + 5% TiO_2 (titanium dioxide: ρ = 4.22 g.cm^{-3}, melting point 2125°C, $CTE_{(20-950)}$ = 7.5x10^{-6}K^{-1}), the additive of TiO_2 is used to reduce the coating porosity and to increase the resistance to abrasive wear.

The quality of the thermal sprayed coatings was evaluated by abrasive wear test [9] by wading in bulk abrasive agent on laboratory test device Di – 1. As abrasive agent brown corundum (d_z = 0.75 mm) was used. The parameters of the test are shown in Table 1.

Table 1 Abrasive wear test conditions [5]

Abrasive agent	corundum grit d_z = 0.75 mm
Abrasive impact angle	75°
Immersion depth of samples into abrasive	60 mm
Wading speed of sample in abrasive	1.74 m.s^{-1}
Duration of the test	6 hrs

Abrasive wear was determined by gravimetric method on the basis of mass loss. Relative wear resistance is expressed by:

$$\psi = \frac{W_{h,et}}{W_{h,vz}} . \frac{\rho_{vz}}{\rho_{et}}$$

where: $W_{h, et}$ – weight loss of reference material [g], $W_{h, vz}$ – weight loss of the coating [g], ρ_{vz} – specific weight of coating [g.cm^{-3}], ρ_{et} – specific weight of reference material [g.cm^{-3}]

The quality of the coatings was also evaluated on the basis of determining their microhardness in the cross-section according to ISO 4516 using M1C 100 device with a load of 10 grams for base material and 30 grams for coatings.

Applied coatings were evaluated also in conditions of cyclic thermal loading. Heating was performed in a chamber electric furnace TS-PCS-31.

The regime of thermal cycles:

1. Heating the sample at 1000 °C,
2. Remaining in the furnace for 20 minutes,
3. Cooling the samples to the room temperature in water (cooling rate = 28°C.s^{-1}).

Resistance to thermal cycles was evaluated on the basis of changes of the adhesion of coating in the process of thermal cyclic loading.

Adhesion of the applied coatings was evaluated by pull-off test according to the STN EN 582. Test samples and mate was hold together by epoxy glue for the determination of adhesion, see Fig. 1.

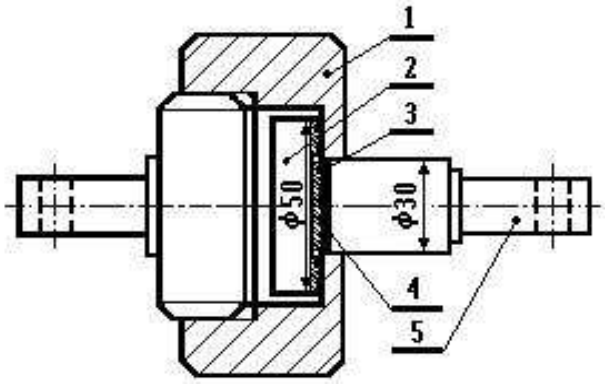

Fig. 1. Test piece arrangement for pull-off test [5, 8]: 1 – fixture with holder, 2 – test sample, 3 – coating, 4 – glued bond, 5 – mate

RESULTS

The roughness of the base material pretreated by blasting was Ra 9.3 μm, Rz 63.2 μm. The roughness of the interlayer NiCr surface was Ra 18.2 μm a Rz 109.1 μm. Thickness of the particular coatings before and after the abrasive wear test are shown in Fig. 2. Substantial change in thickness of the coatings after abrasive wear test was observed in coatings Al_2O_3 and Cr_2O_3+5%TiO_2. The smallest change in thickness was reached in Cr_2O_3 coating. After the addition of TiO_2 to the matrix of Cr_2O_3, the anticipated improvement in resistance to abrasive wear was not observed. Relative abrasive wear resistance for particular coatings is shown in Fig. 3.

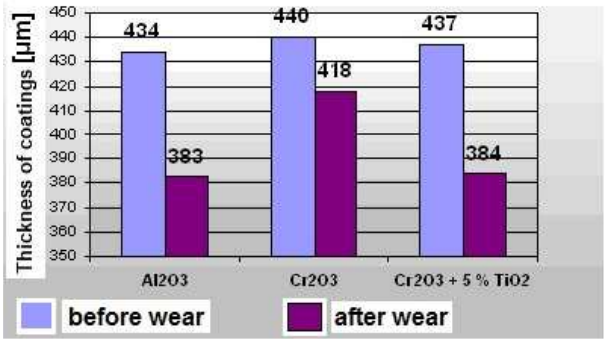

Fig. 2. Thickness of coatings before and after wear [5]

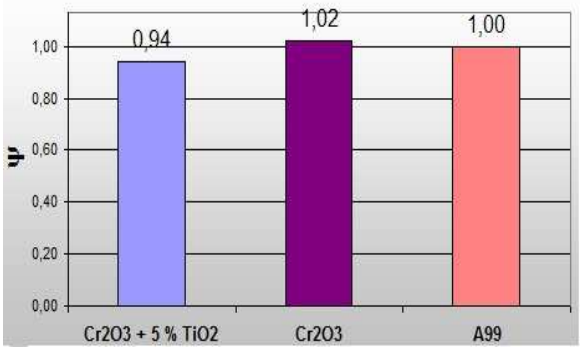

Fig. 3. Relative resistance of particular coatings to abrasive wear [5]

The highest relative abrasive wear resistance was showed by the coating Cr_2O_3 (ψ = 1.02). The stated dependence shows that all three tested materials reach around the same resistance to abrasive wear.

The highest values of microhardness showed Cr_2O_3 coating (1268 HV0.3), lower showed his doped modification (1218 HV0.3) and the lowest values of the microhardness showed Al_2O_3 coating (1062 HV0.3).

Resistance to thermal cycles was evaluated by changing the initial coatings adhesion in the process of the heat cyclic loading. Samples where both coated parts withstood an agreed number of cycles (10), underwent adhesion test. The obtained results are showed in Figs. 4 and 5.

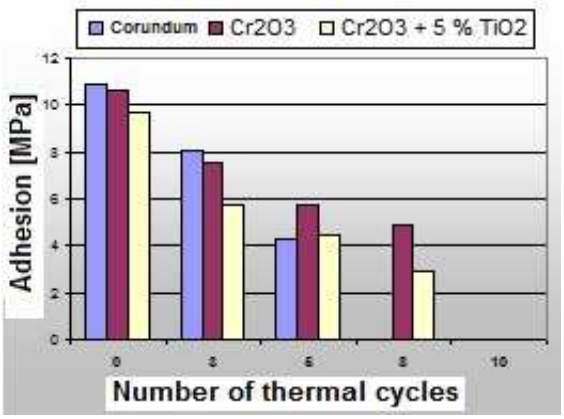

Fig. 4. Coating adhesion without interlayer NiCr [5]

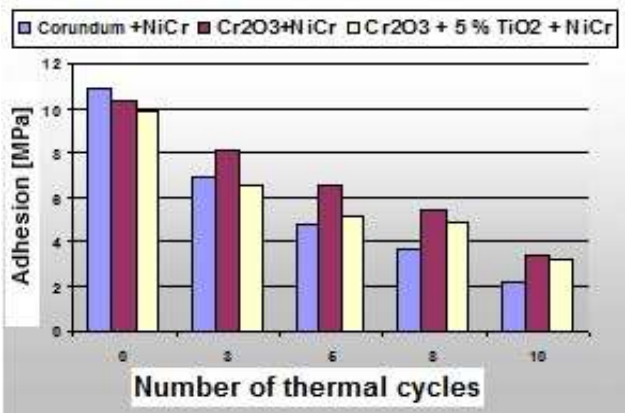

Fig. 5. Coating adhesion with interlayer NiCr [5]

Effect of interlayers applied was reflected in the evaluation of the coatings in the conditions of cyclic thermal loading. The value of the adhesion after mentioned test was higher in all evaluated coatings. Only for the Al_2O_3 coating in the early stages of the experiment, the adhesion was higher for coating without the interlayer. However, after five thermal cycles adhesion of these coatings decreased and higher levels of adhesion were reached in coatings with NiCr interlayer. Coating on the basis of Al_2O_3 without the interlayer withstood up to five thermal cycles. Similarly, other evaluated coatings withstood without breaking the integrity lower number of cycles and in the early stages of the experiment, lower values of adhesion could be observed. During the cyclic loading in coatings applied without the interlayer NiCr, given the different CTE value of base material and ceramic coating, local and then a total subversion and separation of coating from the base could be observed, Fig. 6.

Fig. 6. Appearance of evaluated coatings after thermal cyclic loading

All studied coatings can be marked as suitable for the purpose of the heat loading of up to 1000°C using the interlayer to reduce the differences in coefficients of thermal expansion.

CONCLUSION

The addition of TiO_2 to the Cr_2O_3 material increases the coating density, but does not substantially reduce its hardness, which was confirmed by measuring of micro-

hardness. Despite the stated, this doped material in the conditions of abrasive test (wading in the abrasive) showed the lowest abrasive wear resistance among the tested materials.

- At evaluating the thickness of the selected coatings in the process of the abrasive wear test the lowest loss of material thickness were shown by Cr_2O_3; Al_2O_3 and Cr_2O_3 + 5% TiO_2 materials showed higher losses, about the same size.
- Microgeometry of the test samples surfaces was evaluated by arithmetical mean deviation of the profile - Ra. Blasted surface met the conditions for perfect anchoring of the applied coating, the surface of the applied interlayer showed approximately twice the value of roughness. Assuming a perfect connection of base material with interlayer material, the higher roughness provides better conditions for the creation of so-called "wedge" connections of the ceramic coating with the interlayer material and increase of the share of the mechanical method of anchoring the coating.
- In the observation of the abrasive wear of selected coatings knowledge about the durability of coatings was gained, on the basis of their mutual comparison. Among the studies coatings, relatively higher values of the abrasive wear resistance were, compared to reference material, shown by Cr_2O_3 coating, the coating on the basis of Cr_2O_3 + 5% TiO_2 showed slightly lower values of the wear resistance, which is contrary to the assumption of higher density and lower porosity of the coating due to the dopant, but consistent with the measurement of microhardness of the coatings.
- The highest microhardness values were measured in material Cr_2O_3. The obtained results are consistent with the assumptions and justify the dominance of oxide ceramics in general as materials suitable for application in the loading conditions, requiring the hardness of the sprayed coatings. It is assumed that the variance of the individual microhardness values for each studied material is caused by the inhomogenity of the coating ingredients.
- In the evaluation of high temperature fatigue of selected ceramic coatings in the used mode of thermal cycles it was concluded, that the interlayer NiCr has the appropriate surface microgeometry and allows for at least such an anchoring of the ceramic coating as the base steel material pre-treated by blasting. In all three coatings, using metal interlayers, the increase in their resistance to thermal shock could be observed. All studied coatings can be evaluated as suitable for the purpose of the thermal loading of up to 1000°C using the interlayer to reduce differences in coefficients of thermal expansion.

REFERENCES

1. Jones R. L.: *Methods and devices for thermal coating*. Journal of thermal spray technology, (6) 1997, pp. 77-84.
2. Reignier C., Sturgeon A., Lee D., Wet D.D.: *HVOF sprayed WC-Co-Cr as a generic coating type for replacement of hard chrome plating*. ITSC 2002, Essen 2002.
3. Matejka D., Benko B.: *Plazmové striekanie kovových a keramických práškov*. Alfa, Bratislava 1988.
4. Blaškovič P., Čomaj M.: *Renovácia naváraním a žiarovým striekaním*. ZSVTS, Žilina 1991
5. Jakubov M.: *Hodnotenie úžitkových charakteristík žiarovo nanášaných keramických povlakov*. Diplomová práca, KTaM, SjF TU v Košiciach, 2008
6. Bačová V.: *Nové poznatky o vlastnostiach keramických povlakov*. Kandidátska dizertačná práca. VŠT SjF, Košice 1984

7. ISO/R 2063-1971 (B): *Metal spraying of zinc and aluminum for the protection of iron and steel against corrosion*. May 1971
8. Jakubov M.: *Analýza procesov tvorby keramických povlakov technológiou žiarového striekania plazmou.* Kandidátska dizertačná práca. SjF TU, Košice 2003
9. Kovaříková Sukubová I., et al.: *Study and characteristic of abrasive wear mechanisms*. In: Materials Science and Technology [online]. - ISSN 1335-9053. - Roč. 9, č. 1 (2009)

Contribution was processed within the frame of Grant Scientific Project VEGA No. 1/0144/2008 and 1/0510/2010.

Ján VIŇÁŠ
Janette BREZINOVÁ
Anna GUZANOVÁ
Denisa LORINCOVÁ

Technical University of Košice, Slovakia

HARD SURFACING REPAIRING LAYERS IN EROSIVE WEAR PROCESS

The contribution deals with evaluation of tribological properties of two types three-layer hard surfacing claddings with various structural bases. There were used samples made out from S235JRG2 EN10025-94 as reference material. Within the frame of experimental works there was realised metallographic analysis, measuring of hardness and micro-hardness of claddings before and after erosive wear loading. Erosive wear was evaluated by simulation of erosive action. Aim of research was to determine influence of erosive particle impact angle and structural composition of claddings on their wear resistance.

INTRODUCTION

Economic reasons of maximal exploitation of materials in mechanical production are actual topics of scientific research nowadays. Shortage of raw materials in world market and its more difficult and more expensive procuring raises efforts to increase products' lifetime and saving of raw materials and energy. Industrial development is connected mainly with development of material-technical basis with its technology and technical modernization and with substantial advance in labour productivity.

The most frequent causes of parts and construction failures are tribology processes occurring on functional surfaces. Tribological characteristics of used materials are of great importance for correct operation of parts and construction nodes. Interaction of functional surfaces during their mutual motion causes undesirable changes on surface layers giving birth to wear. In term of material loss prevention, the most important concern should be active surface protection technology in friction nodes. [1-3] Renovation was established as a financially advantageous way of maintenance of machinery and operating equipment. In the renovation, there are used a variety of different technologies that allow the recovery machine parts or prolong their life. Welding-on technology allows not only the restoration of worn surfaces geometry, but gives them new, often better properties than the original material.

One of the determining factors for erosion wear intensity of cladding metals is their hardness. Hardness of claddings is a function of their chemical composition and the thermal mode during and after cladding making. These factors directly affect the structure of claddings.

The contribution deals with evaluation of tribological properties of two types three-layer hard surfacing claddings with various structural bases. There were used samples made of S235JRG2 EN10025-94 as reference material. Within the frame of experimental works there was realised metallographic analysis, measuring of hardness and microhardness of claddings before and after erosive wear test. Erosive wear was evaluated by simulation of erosive action. Aim of research was to determine influence of erosive particle impact angle and structural composition of claddings on their wear resistance.

MATERIALS AND METHODS

The test samples with size of 35x20x8 mm were made of base material - steel S235JRG1 EN 10025-94. Chemical composition and mechanical properties of base material are shown in Tables 1 and 2. This is conventional carbon steel with 0.17% C and guaranteed weldability. For cladding making there were used following hard surfacing welding wires (covered electrodes): E 508 B (E 6-UM-55-GT DIN 8555) and E 518 B (E 10-UM-60-CGP DIN 8555) made in VUZ Bratislava. Cladding was realised by 111 method according to EN ISO 4063 - MMA (manual metal arc welding) at welding unit marked WTU 400. Chemical composition of these wires meets the requirements for structural heterogeneity of claddings. Table 3 and 4 shows chemical composition of used welding wires. To eliminate the effect of mixing of basic and additional surfacing material claddings were carried out as a three-layer.

Table 1. Chemical composition of the base material S235JRG1 EN 10025-94 steel [wt.%]

C	N	S	P	Fe
0.17%	0.005%	0.03%	0.03%	balance

Table 2. Mechanical properties of the base material S235JRG1 EN 10025-94 steel

Hardness HV	Impact strength K [kJ/m^2]	Ultimate elongation A_5 [%]	Tensile strength R_m [MPa]
140	$\geq$ 27	$\geq$ 26	340 - 470

Table 3. Chemical composition of hard surfacing welding wire E508B [wt.%]

C	Mn	Si	Cr	Mo	Fe
0.4	0.7	0.4	6	0.6	balance

Table 4. Chemical composition of hard surfacing welding wire E 518 B [wt.%]

C	Mn	Si	Cr	Fe
3.5	0.8	0.8	27.5	balance

Used welding parameters are shown in Tables 5 and 6. Welding technology used required preheating of base material. Preheating temperature for E 508 B welding wire

was 200°C and for E 518 B was 400°C, what is consistent with recommendations of producer. Preheating temperature was verified by thermochalk.

Table 5. Welding parameters used for welding wire E 508 B (E 6-UM-55-GT DIN 8555)

Layer	Process EN ISO 4063	Welding wire	Ø [mm]	Welding position ISO 6947	Current [A]	Voltage [V]	Current Type Polarity
1 (the first layer)	111	E 508 B	3.2	PA	95 - 110	26	DC +
2 (the second layer)	111	E 508 B	3.2	PA	100 - 120	26	DC +
3 (cover layer)	111	E 508 B	3.2	PA	100 - 120	26	DC +

Table 6. Welding parameters used for welding wire E 518 B (E 10-UM-60-CGPDIN 8555)

Layer	Process EN ISO 4063	Welding wire	Ø [mm]	Welding position ISO 6947	Current [A]	Voltage [V]	Current Type Polarity
1 (the first layer)	111	E 518 B	3.2	PA	95 - 110	26	DC +
2 (the second layer)	111	E 518 B	3.2	PA	100 - 110	26	DC +
3 (cover layer)	111	E 518 B	3.2	PA	100 - 110	26	DC +

The surface of the welds was cut in planar grinding machine. Erosive wear test was realised on laboratory mechanical blasting equipment KP-1. Principle of the test consists in high-speed impact of the abrasive blasting medium on the surface of the samples. Blasting medium is supplied to the centre of a rotating blasting wheel with blades using circular conveyor. Blasting medium gains high blasting speed at the exit of the blades and impinges on surface of test samples placed around the blasting chamber.

Test conditions:

- blasting medium – steel grit G_B 8 (STN 42 9823),
- grain size 0.71 mm, hardness 600 - 700 HV,
- blasting wheel speed 7000 min^{-1}
- blasting media velocity v_{TP} = 70.98 mps
- blasting angles α = 30, 45, 75, 90 [°],
- weight loss was evaluated after 25, 50, 100, 300, 500 and 1000 blasting cycles.

Wear intensity was determined using direct method based on weight loss in particular test phases with measurement accuracy of 10^{-4} g. Hardness course in claddings cross sections was found by Vickers hardness method at measurement load 30N. Hardness of particular structural phases was found by microhardness measurement HV 0,05 according to ISO 4516, measuring unit used SHIMADZU – DUH 202. Metallographic analysis was realised with help of light microscope ZEISS NEOPHOT II and SEM TESLA BS-301 [4].

EXPERIMENTAL RESULTS

Hardness measurement of E 508 B claddings showed mixing of cladding and base material. Hardness in melted area of the first deposited layer hardly increased and reached maximal value 550 HV. Hardness in the second deposited layer was in average 615 HV, and in the third layer about 648 HV. Hardness measurement

confirmed here theoretical and practical assumptions that effect of the mixing base material and cladding metal is lost to the third layer. Similar hardness course showed also E 518 B claddings, but in the first layer already was reached hardness value given by welding wire producer - 660 HV. Measured hardness values in particular layers didn't markedly differ and in the third layer reached even 770 HV. Considering high content of C and Cr less mixing with base material occurred. In term of reached hardness it is possible to assume higher wear resistance in claddings made of E 518 B. Average hardness value of reference material was 120 HV.

Results of wear tests of reference material and claddings are shown in Fig. 1, 2 and 3. Graphs present significant dependence of weight loss on particles impact angle. Wear intensity of reference material decreased with increasing impact angle of particles. For E 508 B claddings minimal wear appears at impact angles 30° and 45°. At impact angles 75° and 90° weight loss achieved almost triple value. Minimal wear of E 518 B claddings appeared at impact angle 30°, maximal at 45°. Comparison of both cladding types showed substantial difference in impact angles 90° and 45°. Overall, however, the claddings 508 E B achieved significantly higher wear values than welds E 518 B with the exception of the angle of 45°.

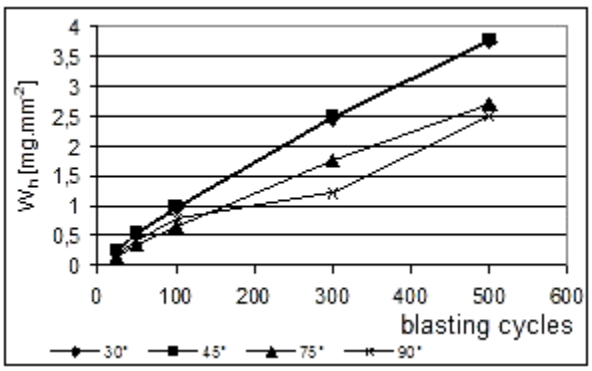

Fig. 1. Wear of reference material

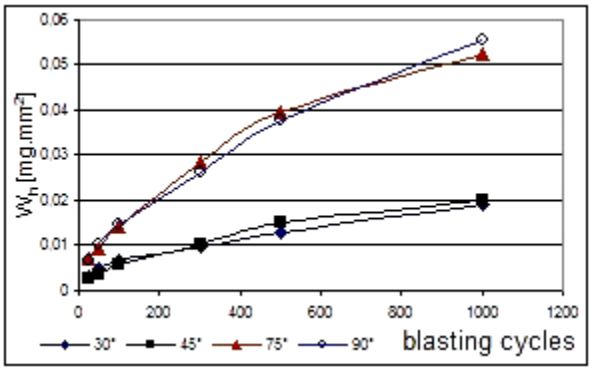

Fig. 2. Wear of E 508 B cladding

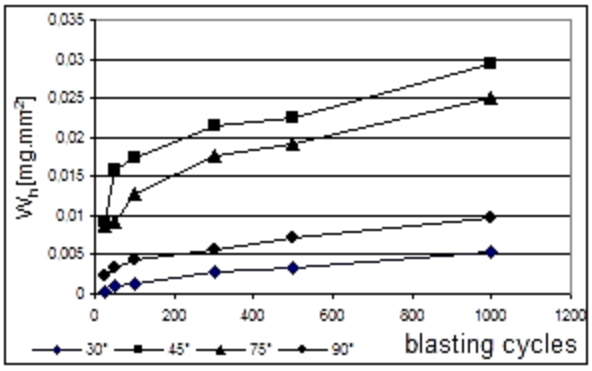

Fig. 3. Wear of E 518 B cladding

Influence of impact angle of particles on the wear course of reference material and tested claddings after 500 cycles are shown in Fig. 4 and 5. High wear intensity of reference material at low impact angles of particles with higher hardness is caused by removal of material in the form of microchips [5].

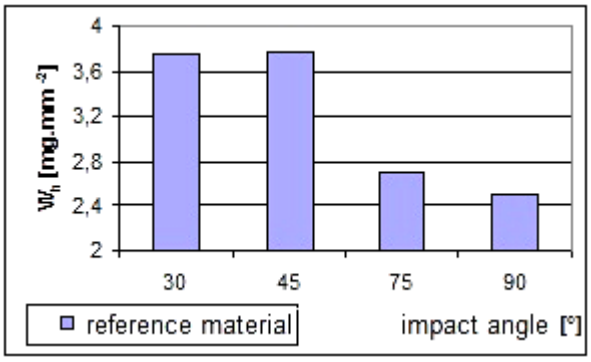

Fig. 4. Wear of reference material after 500 blasting cycles

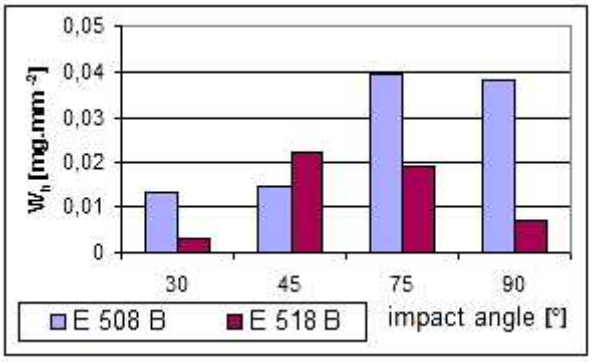

Fig. 5. Wear of investigated claddings after 500 blasting cycles

At higher impact angles surface hardening appears by forging effect of impinged particles. This is reflected by lower values of wear. Evaluated claddings markedly differ each other by their structural composition. Welding wire E 508 B represents cladding based on medium-alloyed steel with carbon content up to 0.4 %. Structure of cladding E 508 B is formed by bainite with fine segregated carbidic phase, Fig. 6. The structure has a high state of dislocations, whose movement is intensive braked by dispersive phase. Plastic deformation, therefore, requires high strength for realisation the movement of dislocations. The highest wear values for this cladding appears at impact angle of particles 75°and 90°. At mentioned angles impact energy of particles is the highest and causes hardening of matrix and shelling of carbide particles. Impact energy of impinged particles at impact angle 30° is low and it can load surface only in terms of elastic deformations. Results of wear of reference material and cladding E 508 B consist with literature references. Soft and ductile materials reach maximal wear at the impact angles from 10° to 45°, at large impact angles less wear appears. For hard and brittle materials intense erosive wear appears at high impact angles. [2,6,7]. Although the hardness of 518 E B cladding is not significantly different from E 508 B cladding, wear course at higher angles is not consistent with the literature data and suggests the complexity of the wear process. It follows that, in addition to hardness the structure of welds plays also an important role in the wear process [9, 10].

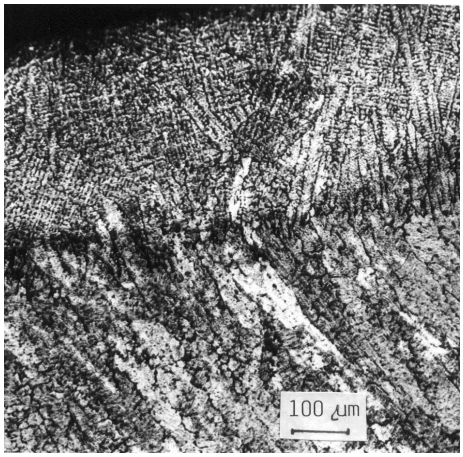

Fig. 6. Structure of cover layer E 508 B

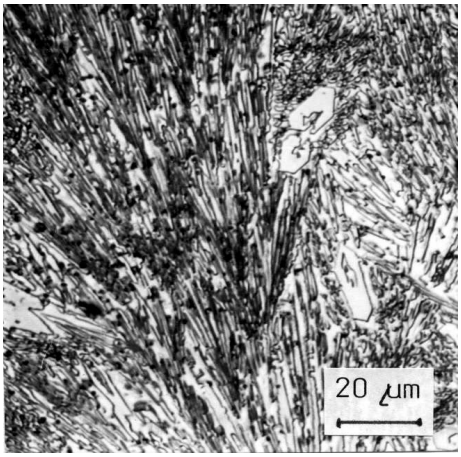

Fig. 7. Structure of cover layer E 518 B

The structure of the E 518 B cladding due to the high carbon content consists of ledeburite and regarding the high content of chromium primary and secondary carbides are found in the structure morphologically segregated as both the massive and dispersion, Fig. 7. Hardness of the matrix and carbides is high, which is reflected in low values of weight loss at impact angle 90°. Although the material is high-strength (hard), but its supply of plastic deformation is small, that is brittle. In addition to these features material shows low strength of the grain boundaries. It can be said that the cohesion strength of boundaries and sub-boundaries is significantly lower than the strength of the matrix. Separation of material at abrasives impact angles 45° and 75° is realized by decohesion of particles and separation by fissile mechanism [5,8,11]. The result is high levels of wear at tested impact angles of particles. Mentioned interpretation is necessary to verify by research of mechanism of claddings wear in specific conditions.

Since it is an intensive erosive wear with high kinetic energy of impinging particles there was also evaluated their influence on surface hardening intensity after 500 cycles. Results of microhardness measurement are showed in Fig. 8, 9 and 10. Maximal surface hardening of evaluated materials was achieved at impact angle 90°, because at this angle the highest forging effect of impinging particles occur. In the direction from surface to core material microhardness values decrease. Maximal surface hardening appeared up to depth of 0.25 mm below the surface of the material.

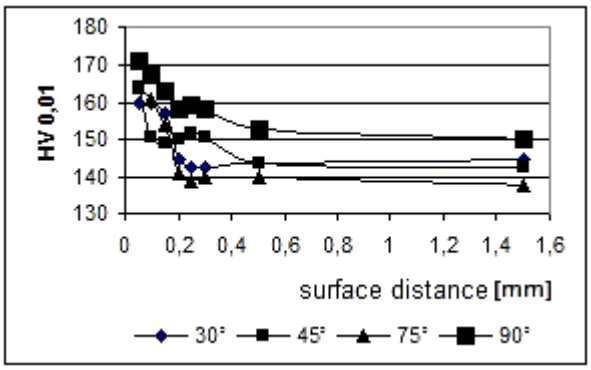

Fig. 8. Microhardness of reference material

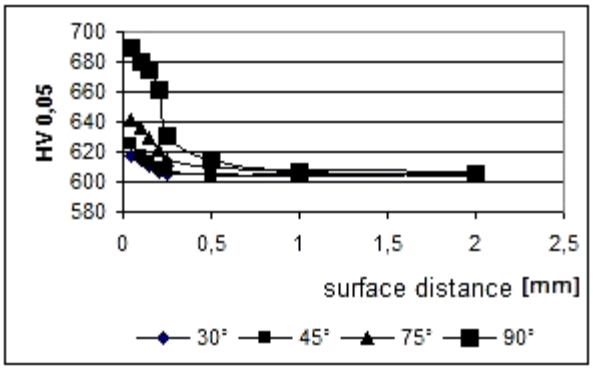

Fig. 9. Microhardness of E 508 B cladding

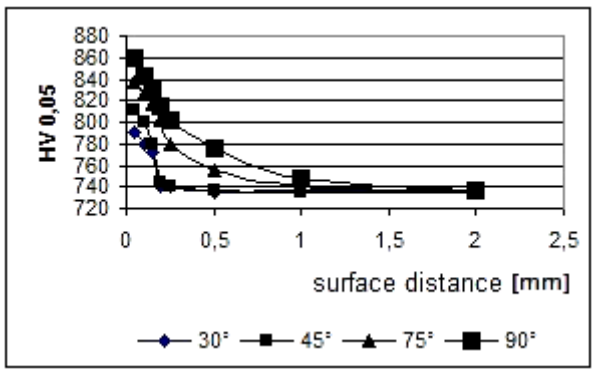

Fig. 10. Microhardness of E 518 B cladding

Obtained results basically confirm the assumption that hardness is one of the main factors influencing the wear resistance of the material. Wear of reference material is high order than in claddings. Effect of particles impact angle on wear intensity of materials of lower hardness (S235JRG2) is consistent with literature findings. [5] Maximal wear intensity was achieved at lower impact angles, at higher impact angles prevails forging effect of abrasive.

CONCLUSIONS

In terms of chemical composition and the possibility of their realization without special heat treatment claims welding wire E 508 B presents economic type of claddings. The achieved hardness values indicate that the optimum properties of claddings appear only in the third layer. For all tested materials and the impact angles of particles a substantial surface hardening of the material up to a depth of approximately 0.25 mm was achieved. The highest surface hardening values were achieved at an angle of 90°. Examined claddings showed a significant dependence on the impact angle of the abrasive particles in given erosive wear conditions. Intensity of wear of E 508 B claddings and the reference material, depending on the particle impact angle is consistent with the literary knowledge. In E 518 B cladding reached results of wear at high impact angles are in contrast with literature data. Different wear values of claddings that don't significantly differ in hardness relate to their different structural building. Comparison of evaluated claddings showed significantly higher wear values of E 508 B cladding than in E 518 B cladding with the exception of the angle of 45°. Hardness of the material is crucial factors in wear resistance, which resulted in different wear values for reference material and claddings. There was confirmed the significant influence of the impact angle on abrasive wear.

Resistance to erosion wear in addition to the hardness significantly depends on the type, distribution and mutual linking of structural components. The structure of materials is another factor that significantly affects their tribological properties [12].

REFERENCES

1. Czichos M.: *Tribology*. Elsevier Sr. Publ. komp. Oxford, New York, 1978.
2. Blaškovitš P., Balla J., Dzimko M.: *Tribológia*. Alfa, Bratislava 1990.
3. Vocel M.: *Tření a opotřebení strojních součástí*. Praha,SNTL,1976
4. Blaškovitš P., Čomaj M.: *Renovácia naváraním a žiarovým striekaním*. Alfa, Bratislava, 1991.
5. Brezinová J.: *Štúdium zákonitostí procesu tryskania z aspektu degradačných javov*. Doktorandská dizertačná práca, SjF TU Košice, 2002.
6. Jankura D., Brezinová J.: *Vplyv uhlu dopadu abrazívnych častíc na tribologické vlastnosti tvrdonávarov*. In: Acta Mechanica Slovaca. roč. 6, č. 2, 2002, s. 217-221. ISSN 1335 - 2393.
7. Bhusnan B., Gupta B.K.: *Handbook of tribology*. McGraw-Hill, Inc., New York, 1991.
8. Adamka J., Petríková G.: *Vplyv štruktúry návarov na odolnosť proti abrazívnemu opotrebeniu*. In.: Intertribo 93, Bratislava, 1993, s. 70.
9. Hammer P.: *Some metallurgical aspects of wear*. In.: Eurotrib 89, I, Warszawa, 1989, s.197.
10. Kovaříková rod. Sukubová, I., Szewczyková B., Blaškovitš P., Hodúlová E., Lechovič E.: *Study and characteristic of abrasive wear mechanisms*. In: Materials Science and Technology [online]. - ISSN 1335-9053. - Roč. 9, č. 1, 2009.

11. Knoško P., Kovaříková rod. Sukubová I., Hodúlová E.: *Metodika návrhu modelu predikcie opotrebenia trecích vrstiev*. In: Vedecké práce MtF STU v Bratislave so sídlom v Trnave. - ISSN 1336-1589. - č. 25, s. 83-88, 2008.
12. Mohyla P., Koukal J.: *Vliv mikrostruktury na mechanické vlastnosti svarových spojů oceli T24*. In: Sborník Nové materiály, technologie a zařízení pro svařování, *19-21.9.2005,* Ostravice - Ostrava, Český svářečský ústav s.r.o., s. 175-180. ISBN 80-248-0898-6, 2005.
13. Blaškovitš P. et al.: *Návarové materiály pre abrazívne a erozívne opotrebenie*. Zváranie, č.11-12, ISSN 0044-5525, 2001.

Contribution was processed within the frame of Grant Scientific Project VEGA No. 1/0510/2010.

Ján VIŇÁŠ
Ľuboš KAŠČÁK
Milan ÁBEL
Dagmar DRAGANOVSKÁ

Technical University of Košice, Slovakia

THE QUALITY ANALYZE OF MIG SOLDERING ZINC-COATED STEEL SHEETS BY DESTRUCTIVE TESTING

In the paper results of metallographic analyses of joints made by MIG brazing on high strength galvanized steel sheets of H 340LAD + Z EN 10292 are presented. The quality of brazed joints made by SG CuAl8 braze with fluctuating welding rectifier CLOOS 303 MC4 was evaluated. Argon 4,80 was used as gaseous shield. Soldering joints quality was evaluated by destructive testing. The bearing capacity joints were evaluated by STN EN ISO 895 and STN EN 1321. Macrostructure and microstructure analyze of joints were realized too.

INTRODUCTION

Automotive manufacture is the most dynamic developing branch of engineering industry. In world markets only those concerns can achieve successes which are able to flexibly react to the needs of customers, dynamically innovate manufacturing, and implement productive technologies into manufacturing. Demands on product quality are more and more strict. The need of process optimization of welding, soldering and adhesive bonding arises from the reason of application various qualities of iron and non-iron materials, their combinations for the purpose of weight reduction of automobile body parts. Along with conventional methods of welding which are resistance point welding and shielded arc welding, in manufacture also unconventional methods find their application which are laser welding, brazing in shielding gas [1, 2, 3].

Surface-modified steel sheets are used in car body production. Surface modification is made by hot-dip zinc galvanizing. Both types of Zn coating cause problems mainly in fusing methods of welding when by the influence of high temperatures comes to the failure of coating continuity in the joint place that decrease the corrosion resistance in joint place [4, 6, 9].

The paper deals with analyzing of the joint quality made by method GMAB – (Gas Metal Arc Brazing) method.

MATERIAL AND TREATMENT

Micro alloyed sheets H 340LAD + Z EN 10292 were used for the experiments. It is high-strength micro alloyed deep-drawing steel with ferrite-pearlite structure. The sheet surface modification is realised by hot-dip zinc coating. The thickness of Zn coating is 12 µm. Chemical composition of tested sheet is shown in Table 1.

Table 1. Chemical composition in % wt. and mechanical properties of steel H 340LAD + Z EN 10292

Material EN 10292	C	Mn	Si	Ti	Al	Nb	P	S	R_m	$R_{p0,2}$	A_{80}
	[%]	[%]	[%]	[%]	[%]	[%]	[%]	[%]	[MPa]	[MPa]	[%]
H 340LAD+Z	0,1	0,8	0,4	0,08	0,011	0,06	≤ 0,0025	≤ 0,0025	410 - 510	340 - 420	≥21

Chemical consistence of used soldering metal types and their strength characteristics are in Table 2. Soldering metals of A 384 from UTP productions were used.

Table 2. Chemical composition and mechanical properties of solders [5]

Material DIN 1733	Cu	Mn	Al	R_m	$R_{p0,2}$	A_5	KU	Melting temperature
	[%]	[%]	[%]	[MPa]	[MPa]	[%]	[J]	[ºC]
SG CuAl8	92,0	0,2	7,8	380	180	40	70	950 - 1080

The methodology of joint quality valuation

The samples with parameters 1000 mm x 200 mm were cut with table shears from the sheets of 1 mm thickness with dimensions of 1000 mm x 2000 mm.

Before brazing, joint places of the sheets were degreased with concentrated CH_3COCH_3 from the reason of prevention of negative influence of the emulsions on the process and the quality of brazing joints. The steel sheet brazing was realised in the laboratory of welding and defectoscopy at the Department of Technology and Materials on programmable fluctuating welder machine CLOOS 303 MC4 equipped with four-trolley regulating mechanism in Ar 4.80 shielding gas. The parameters of brazing are in Table 3.

Table 3. Used brazing parameter

Thickness of Brazing Sheets	Type of Braze	Wire Diameter of Braze	Impulse	Brazing Current [A]	Voltage [V]	Inert Gas
1,0 + 1,0	CuAl8	1,0 mm	Yes	80	16 - 18	Argon 4,80

During brazing the slope of lap sheet constitution was used from the reason of better gas venting and Zn vapours from the place of arch burning on the basis of recommened literature, Fig. 1 [4, 9, 10].

Fig. 1. Used grade angle of brazed sheets

The process of brazing was realized from left to right in the position PB according to STN EN ISO 6947. The lenght of brazing arch is 1.5x braze diameter. The wire braze unloading from burner was 10 mm. The flow of gaseous shield was 14 $l.min^{-1}$.

Carrying capacity of braze joint was evaluated by static tensile test according to STN EN 895. This experiment is used for determination of maximal carrying capacity of brazied joints in tensile stress. The experiment was made on experimental machine for determination of metal strength TIRA test 2300 of producer VEB TIW Rauenstein with measuring scope from 0.08 kN to 100 kN. The speed of loading was 10 m/s. Experimental samples were of 100x20 mm dimensions. Thirty samples were used for the experiment.

Macro and microstructural analysis of the braze joint quality was evaluated according to STN EN 1321 standard on metallographical scratch patterns with using optical lighting microscope Olympus CX-31. For visualization of microstructures of basic material the corrosive NITAL (HNO_3) in concentration 3% and for visualization of microstructure of braze $CuAl_8$ the solution peroxysulphate ammonium (10 g peroxy-sulphate ammonium + 100 cm^3 destilated water) was used.

The analysis of achieved results

The average values of carrying capacities of braze joints observed with static tensile test are presented in Table 4. The samples after destruction are documented in Fig. 2. The sample held in the jaws of experimental machine TiraTest 2300 is presented on the Fig. 3.

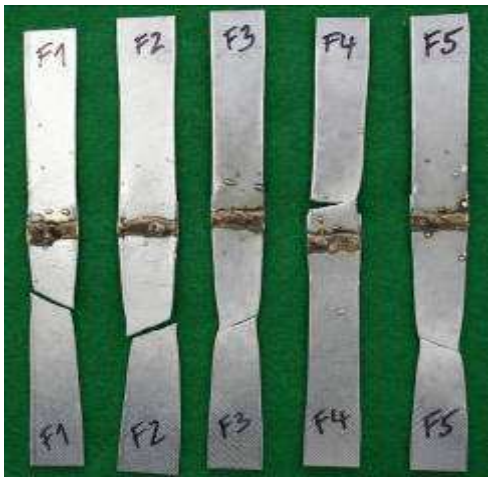

Fig. 2. The samples with mark F after destruction

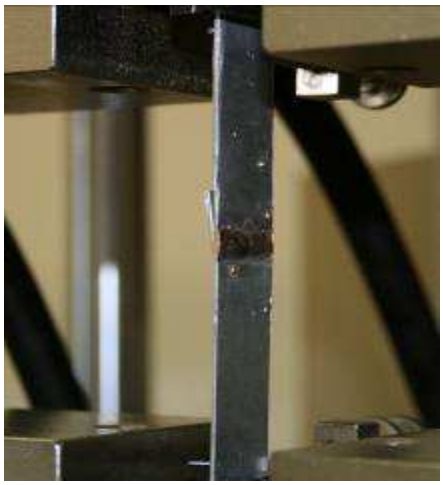

Fig. 3. The sample F2 during the experiment

Table 4. The average values of carrying capacities of the braze joint

Series of samples	Max. force F_m [N]	Max. strenght Rm [MPa]
A	5808	7394,86
B	5877	7483,10
C	5631	7171,83
D	5442	6929,99
E	5762	7336,50
F	5371	6838,13
Total average value of carrying capacity	5648,5 N	7192,4 MPa

Destruction out of the braze joint in all experimental samples was observed, i.e. in the base material that presents great carrying capacity of the joint or braze adhesion to basic material.

The results of macroscopic and microscopic analysis

Great wettability and diffluence on metallographical scratch patterns were observed, that is also documented in Figure 4 and 5. Both connected sheet were covered by braze in the joint place without cavities, respectively cracks. On evaluated cuts no existence of pores or cavities in the metal CuAl8 was recorded when observing macro and microstructures with help of lighting macroscopic what is in line with statement [2, 10] that this braze type has lower tendency for the creation of pores in a braze when comparing to the braze type CuSi3.

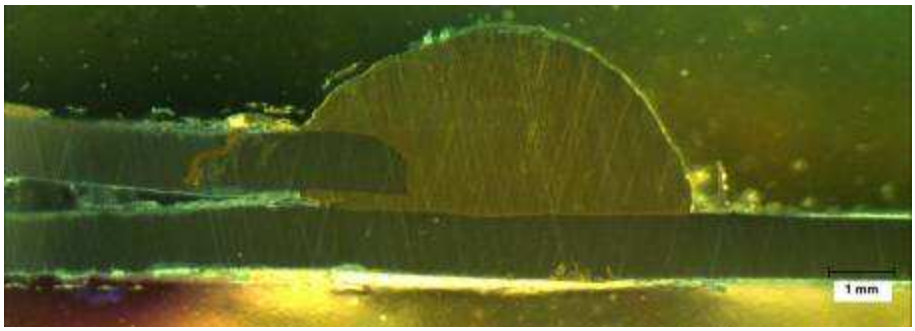

Fig. 4. Macrostructure of brazed joint of the sample B6

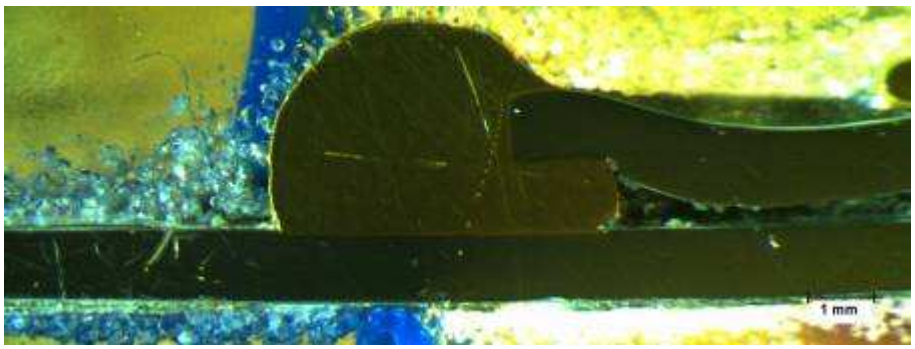

Fig. 5. Macrostructure of brazed joint of the sample F6

The width of braze joint and also the incline degree of braze pass response to the used parameters of braze stream and braze diameter. The braze speed influences the pass height in a marked way. The robot workplaces for connecting of car body parts are used for GMAB. Evaluated samples were brazed by the hand conduct of burner in laboratory conditions.

Microstructure analysis (Figs. 6, 7) confirmed the great quality of joints. In the joint places, the existence of any pores or cavities was recorded which would have a negative effect on the joint quality.

The microstructure of heat non-influenced basic material H 340LAD + Z is presented in Fig. 8. It is fine-grained feritic-pearlitic structure. Steel is regulated Al and Ti.

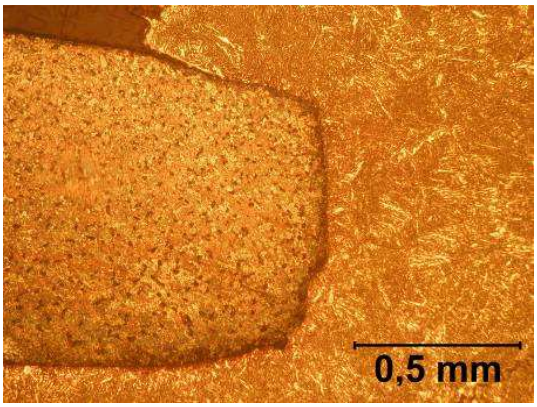

Fig. 6. Microstructure of joint of sample C6

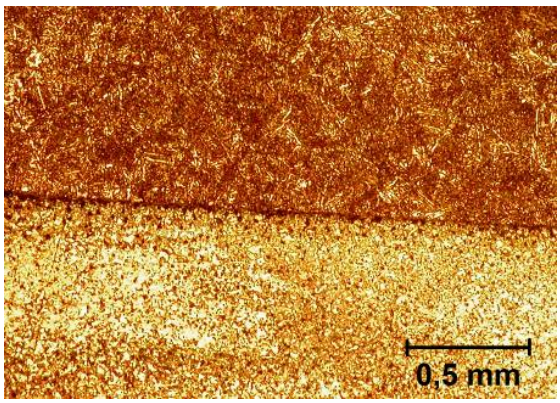

Fig. 7. Transition from base material to braze of sample A6

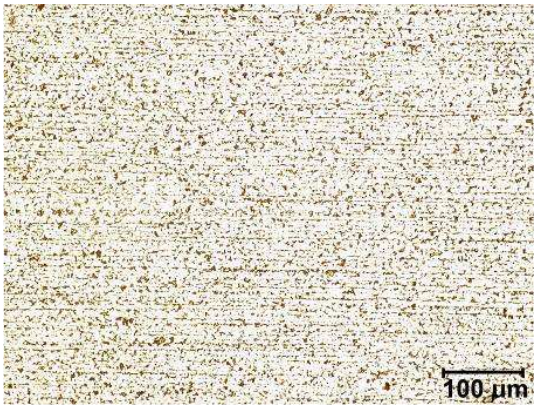

Fig. 8. Microstructure of base material

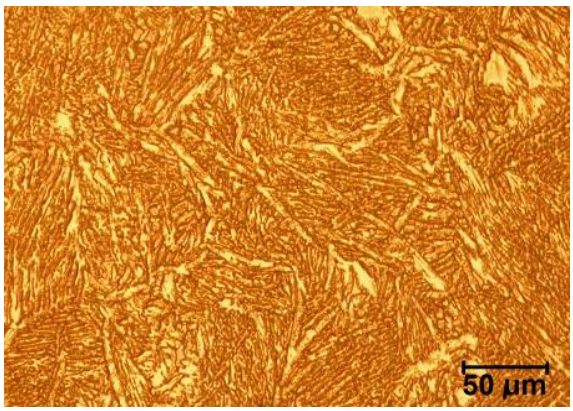

Fig. 9. Microstructure of braze CuAl8

In Fig. 9 is the microstructure of CuAl8 braze. The structure of alloy is dendrite and it is possible to observe Al in form of lighting acicular forms.

CONCLUSION

The braze joints quality of zinc-coated sheets H 340LAD + Z joined with MIG braze with CuAl8 braze in shielding gas Ar 4.80 was evaluated with the destructive tests. The braze current of 80A was used for evaluation of sheet thickness. On the base of the analyses it is possible to state that used parameters of braze are suitable for brazing and guarantee the great joint quality. The average carrying capacity F_m = 5648,5N of the joint was measured with tensile test. Destruction in the base material was observed in all tested materials. Macroscopical and microscopical analysis also confirmed suitable joint quality. No cavities, pores or cracks occurred in joints.

The CuAl8 braze has two times higher electric conductivity and higher strength in comparison to CuSi3 braze. It is suitable mainly for brazing of zinc-coated dual-phase steels [8, 11, 12].

The influence of used shielded gas for MIG brazing must be considered in optimization of pulse brazing parameters. On the base of studied literature and the results of experiments it is possible to state that mixed gases are suitable for MIG brazing. Pure Ar gas during experiments caused the pollution of adjacent areas of

braze by combustion product. By the reason of arch burning stabilization it is suitable to use blending gas Ar + O_2 or Ar + CO_2. By the stabilization of arch, the pollution of the joint place by the influence of the braze will be decreased, burning performance will be increased, the braze fluidity will be increased what will improve the wettability and diffluence [7, 8, 9].

Contribution was elaborated within the solving the grant project VEGA №. 1/0206/08.

REFERENCES

1. Sejč P.: *Optimalizácia vybraných parametrov oblúkového MIG/MAG spájkovania pozinkovaných plechov*. Zváranie- Svařování 53, 2004, č.3, str. 57-62.
2. Sejč P.: *Špecifikácia oblúkového zvárania a spájkovania pozinkovaných plechov*. Bratislava, 2005.
3. Hodúlová E. Et al.: *Štúdium rozhrania bezolovnatých spájkovaných spojov*. In: Zváranie 2008. Welding 2008 : Zborník prednášok z XXXVI. medzinárodnej konferencie a diskusného fóra. Tatranská Lomnica, 5.-7. novembra 2008. - Bratislava : Slovenská zváračská spoločnosť, 2008. - ISBN 978-80-89296-05-7. - S. 296-300
4. Roubiček. M.: *Problematika spojování pozinkovaných ocelí*. Seminář nové materiály, technológie a zařízení pro svařování, Ostravice, 2003.
5. *Bohler Thyssen Welding*, UTP Schweiβmaterial FmbH, Bad Krozingen, 2004, 435 s.
6. Hodúlová, E., Kováčik Ľ.: *GMAW brazing of steels*. In: Engineering Sciences 2 / nadát. 4th international conference of PHD. Miskolc, Hungary, 11-17 August 2003. - Miskolc : University of Miskolc, 2003. - ISBN 963 661 585 3 ö. - ISBN 963 661 591 8. - S. 103-108.
7. Kersche A., Trube S.: *Schutzgase zum MSG-Loten*. Linde Technische Gase GmbH, Hollriegelskreuth, 1998.
8. Hodúlová E., Maňka Ľ., Turňa M.: *Metalografické hodnotenie spájkovaných spojov vyhotovených bezolovnatými spájkami*. Metallographic analysis of Pb-free slodered joints. In: Přínos metalografie pro řešení výrobních problémů : Sborník přednášek / nadát. Konference. 10. Lázně Libverda, 14.-17.6.2005. - Praha : České vysoké učení technické v Praze, 2005. - ISBN 80-01-03251-5. - s. 342-345.
9. Roubiček M.: *Příspěvek do problematiky spojování pozinkovaných plechu*. Air Liquide CZ, s.r.o 2003.
10. Palcut M. Et al.: *Thermal analysis of selected tin-based lead-free solder alloys*. In: TOFA 2008 : Discussion Meeting on Thermodynamics of alloys. Krakow, Poland, June 22th-27th, 2008. - Krakow : Katedra informatiky FPV UCM Trnava, 2008. - s. 89.
11. Hodúlová E., Gatial M.: *Alternative lead-free materials and alloys for the soldering*. In: ELITECH 2002: The Fifth Scientific Conference on Electrical Engineering & Information Technology for Ph.D. Students. - Bratislava: STU v Bratislave, 2002. - ISBN 80-227-1760-8. - S. 33-35.
12. Hodúlová E.: *Bezolovnaté spájky v mikroelektronike*. Lead-free solders in microelectronics. In: Zvárač. - ISSN 1336-5045. - Roč. 4, č. 3 (2007), s. 21-25.

ZESZYTY NAUKOWE POLITECHNIKI RZESZOWSKIEJ NR 274
Mechanika z. 81 2010

Franciszek WOLAŃCZYK

Rzeszów University of Technology, Poland

THE INVESTIGATION OF THERMAL CONDUCTIVITY OF LOW-ALLOYED HIGH SPEED STEELS

In the presented work the effective thermal conductivity of three alloyed high speed steels: SW3S2, SW7M and SW2M5 were compared. The thermal conductivity was received from the simple experiment in which the change of phase metrology-matter was applied. As the metrology-matter gallium was used. The value of the thermal conductivity for high speed steels was compared with date of science literature.

INTRODUCTION

Cutting tools made of high-speed steels still make up about 50 % of the general number of tools [1]. High speed steels which have been used for about a hundred years, are less frequently used in manufacturing cutting tools (particularly for a high cutting speed) whereas their use in manufacturing structural elements, forming tools, and for plastic product forms has increased.

The chip formation process in machining is accompanied by heat generation, which influences the mechanical and physical properties of both the workpiece and the cutting tool. The cutting energy is dissipated as heat in the cutting zone. The temperature distribution during the process is able to stand decisive effect on waste of tool. The temperature field measured into cutting tool also as well as knowledge of the thermal conductivity of tools material permit to define heat flux . This heat flux permits on optimization of tool quality and of all technological process too. The difficult of regard of effect of the alloy addition also technology of production of steel cause, that literature given of the thermal conductivity of steel have approximate character. Begun into the work [4], and [6] thermal measurements were used of qualification the thermal conductivity for the three low-alloy high-speed steels: SW7M, SW3S2 and SW2M5 and presented. At present paper the results of the effective thermal conductivity of three alloyed high speed steels: SW3S2, SW7M and SW2M5 were compared with given of literature the thermal conductivity of three alloyed high speed steels: P12, P18 and 3X2B8Φ about the close chemical composition.

Chemical constitution of low-alloy high speed steels

Three the thermal conductivity samples for steel SW2M5, SW3S2 and SW7M, which chemical composition shown (Tab.1) and of diameter is equal to 6 mm, were

selected as being very typical material used in the production of cutting tools. The measurement of thermal conductivity in materials with very high conductivity, such as metals and their alloys, requires special measuring technics. The measurement thermal conductivity are used the quasi-stationary method in are shown [5]. Measurement of thermal conductivity quasi-stationary method is practised for the Department of Thermodynamics at Technical University of Rzeszów. This method has application in measurement of thermal conductivity of good conductors.

Table 1. Chemical composition of low-alloy high speed steels

Steel grade	Chemical constitution in %							Ref.
	C	W	Mo	Cr	V	Si	ΣW%+Mo%	
SW2M5 (Poland)	0,9-1,0	1,5-2,0	4,5	5,5	-	-	9,5	[2]
SW3S2 (Poland)	1,1-1,2	3,1-3,4	1,1-1,2	4,3-4,7	1,6-1,8	1,3-2,3	5,2	[2]
SW7M (Poland)	0,8-0,88	5,5-6,5	5,0-5,5	3,8-4,4	1,7-2,1		13	[2]
P12 (Russia)	0,8-0,9	12,0-13,0	≥1,0	3,1-3,6	1,5-1,9		14	[3]
P18 (Russia)	0,7-0,8	17-18	≤1,0	3,8-4,4	1,0-1,4		19	[3]
3X2B8Ф (Russia)	0,3-0,4	7,5-8,5		2,20-2,70	0,2-0,50	0,15-0,4		[3]

EXPERIMENTAL DETAILS

The thermal conductivity was received from the simple experiment in which the change of phase metrology-matter was applied [5]. As the metrology-matter gallium and tin were used. The change of phase process plays role of the heat source. During the change of phase period the temperature is constant a quasi-stationary temperature fields which allows to use the stationary model of heat transfer calculations. The model is a cylindrical spine of finite length and losing heat out one face to melting-substance and by radiation from surface, respectively. All process measurement was carried out in vacuum.

The mean thermal conductivity λ was calculated from the equation:

$$\frac{T_w - T_o}{T_l - T_o} = ch(m \cdot L) - \left[\frac{\dot{Q}_l}{(T_w - T_o) \cdot A \cdot \lambda \cdot m \cdot ch(m \cdot L)} + tgh(m \cdot L) \right] sh(m \cdot L) \qquad (1)$$

where: *w* subscript stands for temperature of the hot end of the sample, *l*- for temperature of the cool end of the sample *o* - for temperature of sides of vessel vacuum, *L* is length of sample, $\dot{Q}_l$ is the heat power of the cooler as the sum of heat power of fusion of melting-substance and heat power lost from the surface of the

cooler by radiation, the A is metrology cross section of the sample, O is a circuit of sample, λ is the mean thermal conductivity of the sample,

$$m = \sqrt{\frac{\alpha_r \cdot O}{\lambda \cdot A}} \tag{2}$$

and the mean heat transfer coefficient by radiation

$$\alpha_r = \frac{C_o}{(T_{sr} - T_o)\left(\frac{1}{\varepsilon_1} + \frac{d}{D}\left(\frac{1}{\varepsilon_2} - 1\right)\right)}\left[\left(\frac{T_{sr}}{100}\right)^4 - \left(\frac{T_o}{100}\right)^4\right] \tag{4}$$

where d, D are diameter of sample and vessels vacuum respectively, ε_1, ε_2 are the effective emissivity of the sample and of the vacuum vessels respectively, the mean temperature of the sample is

$$T_{sr} = \frac{T_w + T_k}{2} \tag{5}$$

The temperature T_w and T_k of the sample, during measurement of the thermal conductivity, defined from three points measuring, appointed from T_1 to T_3, (see Fig. 1), by use of thermocouples chromel-alumel and graphically extrapolate.

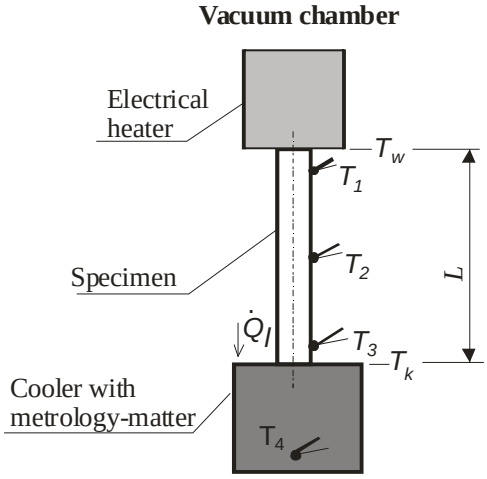

Fig. 1. Schematic cross-section of the experimental setup for thermal conductivity measurements by the quasi-stationary method

RESULTS AND DISCUSSION

Results of calculations of the thermal conductivity from (1) and measurements of λ are estimated with function linear: λ = 16,66+0,0158$T_{śr}$,- for steel SW2M5, λ = 18,67-0,01303$T_{śr}$-for steel SW3S2 and λ = 13,32+0,00798$T_{śr}$-for steel SW7M for temperatures changing from 50°C to 450°C. Results of calculations of the thermal conductivity from function linear are given in Table 2 and show in Fig. 3.

Table 2. Thermal conductivity of low-alloy high speed steels

Steel grade	λ, [W/(m·K)]						
	27 ^{O}C	127 ^{O}C	227 ^{O}C	327 ^{O}C	427 ^{O}C	527 ^{O}C	
SW2M5		18,7	20,3	21,8	23,4		
SW3S2		17,0	15,7	14,4	13,1		
SW7M		14,3	15,1	15,9	16,7		
P12	15,5	16,6	19,1	22	25,6		[3]
P18	21,5	25,6	26,2	26,2	25,9	25,8	[3]
3X2B8Ф					28,5	25,7	[3]

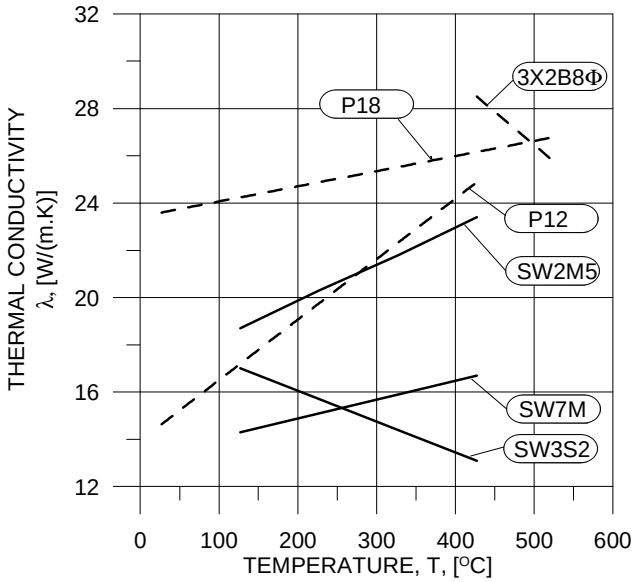

Fig. 2. Thermal conductivity of low-alloy high speed steels

Counted the thermal conductivity for steel SW3S2 in measured range of temperatures is decreasing the same us for the steel 3X2B8Φ. Both the steel SW3S2 and steel 3X2B8Φ contain a silicon (see Tab.1), which may be the cause of the decrease in their thermal conductivity.

REFERENCES

1. Sinopalnikov V.A.: *Some Problems of Increasing in Durability of Tools Made of High-speed Steel*. High-productivity Designs of Cutting Tools. — Moscow: 1976. MDNTN.
2. Jaworski J.: *The study of thermal processes as a basis for quality production of tools of low-alloy high-speed steels*. Int. J. of Applied Mechanics and Engineering, vol. 9, No.3, pp.493-503.
3. Охотин А. С.: *Теплопроводность тверых тел*. Справочник. Москва Энергоатомиздат 1984.
4. Wolańczyk F.: *Preliminary results of the measurements of thermal property of low-alloy high-speed steel SW7M i SW3S2*. Proceedings of the International Scientific Conference, Vol. II, Rzeszów 1998, pp.453-459.
5 Wolańczyk F.: *Pomiar przewodności cieplnej metali i ich stopów*. XI Zjazd Termodynamików, Materiały Zjazdowe Cz.II, Szczecin-Świnoujście, 1981 pp.551-554.
6 Wolańczyk F.: *The thermal diffusivity of low-alloy high-speed steels*. Acta Metallurgia Slovaca, Vol. 3, Košice 1999, pp. 247-250.

ZESZYTY NAUKOWE POLITECHNIKI RZESZOWSKIEJ NR 274
Mechanika z. 81 2010

Grzegorz ZAJĄC
Paweł KRZACZEK

Uniwersytet Przyrodniczy w Lublinie

COMPARISON OF RAPESEED ETHYL AND METHYL ESTERS UTILIZATION INFLUENCE ON ENGINE ENERGETIC PARAMETERS

Use of plant oil methyl esters as a fuel for diesel engines is popular practice however it is also possible to utilize ethyl esters. In this paper, results of research concerning utilization of methyl esters (FAME) and ethyl esters (FAEE) of rape oil for powering diesel engine were presented. Results enabled comparative analysis of effects of powering diesel engines with these fuels. Research was based on taking, for each of the investigated fuels, measurements which enabled elaboration of data necessary for drawing external characteristics, on basis of which effect of esters utilization on energetic parameters was evaluated. Research was carried out on, installed on dynamometric stand, 2CA90 engine. Results of the research did not prove determining influence of utilized ester type on engine energetic parameters.

INTRODUCTION

Produced in process of transesterification, higher fatty esters of plant oils are commonly used for powering diesel engines. They can be used as a separate type of fuel parallel to diesel fuel (DF) or as a mixture of esters and mineral diesel fuel containing specified amount of esters [2, 6, 12].

Most commonly used, in process of transesterification, is methyl alcohol. It has numerous advantages among which its low price, resulting mainly from cost of its production, is most often noticed one. Ethyl alcohol can be considered an alternative for methyl alcohol. Its production is based on process of fermentation and, in contrary to methanol, which is currently obtained through synthesis, it can be considered renewable material. However, its utilisation is limited. It results from price of ethanol, and, required in process of transesterification, necessity of its deep dehydration.

Having similar qualities, methyl (FAME) and ethyl (FAEE) esters, both have properties predisposing them to being utilized as fuel for diesel engines.

Moreover, ethyl esters have slightly higher, than methyl esters, caloric value for they contain one more carbon atom in their particle. Products of incomplete combustion of ethyl esters do not contain formaldehydes, which are formed during combustion of methyl esters. Additionally, ethyl esters characterize with lower than methyl esters solidification point, what influences low temperature properties of fuel [5, 12]. Absence of this fuel on EU list of biocomponents and lack of formal-legal regulations inhibits development of investment.

Goal of presented research is comparison of effects of, used as fuel for powering diesel engines, methyl and ethyl esters of higher fatty acids on work parameters of 2CA90 diesel engine.

MATERIAL AND TREATMENT

Object of this experimental research were rapeseed methyl (FAME) and ethyl (FAEE) fatty acids esters and, for comparison purposes, conventional diesel fuel. Rapeseed oil fatty acids methyl ester was obtained from factory installation. Rapeseed oil fatty acids ethyl ester was obtained from experimental installation.

Requirements and results of diesel fuel and esters samples analyses were presented in Table 1.

Table 1. Properties of diesel fuel, methyl and ethyl esters and their reference to PN EN 590:2006 norm

Property	Unit	Requirements by norm PN-EN 590:2006	Marked value to DF	Marked value to FAEE	Marked value to FAME
Cetane number	–	min. 51,0	53,1	-	51
Cetane index	–	min. 46,0	54,0	n.d.	n.d.
Density at 15°C	$kg \cdot m^{-3}$	820-845	835	873	881
Viscosity at 40 °C	$mm^2 \cdot s^{-1}$	2,0-4,5	2,8	4,16	4,42
Distillation recovered at 250 °C Distillation recovered at 350 °C 95%(V/V) recovered at	% obj. % obj. °C	max 65 min. 85 max 360	33 95 350	n.d.	n.d.
Flash point	°C	min. 55	61	60	130
Sulphur content	$mg \cdot kg^{-1}$	max 50	9,6	n.d.	1,9
Polycyclic aromatic hydrocarbons	% m/m	max 11	2,1	n.d.	n.d.
Lubricity, corrected wear scar diameter (wsd 1,4) at 60 °C	μm	max 460	351	n.d.	n.d
Oxidation Stability	$g \cdot m^{-3}$	max 25	6,0	n.d.	n.d.
Ash content	% m/m	max 0,01	0,001	-	-
Copper strip corrosion (3 hours at 50°C)	rating	Class 1	1	-	1
Carbon residue (on 10% distillaiton residue)	% m/m	max 0,30	0,01	n.d.	0,04
Water content	$mg \cdot kg^{-1}$	max 200	65	80	148
Total contamination	$mg \cdot kg^{-1}$	max 24	11	8	16

The marking of energetic parameters was performed in the test bench of the research laboratory in the Department of Power Engineering and Vehicles of the Agricultural University of Lublin. The test bench included following apparatuses:

- diesel engine 2CA90;
- electro whirl brake AMX 210;
- control and measurement system AMX 201, AMX 211;
- fuel consumption measurement system;
- surroundings measurement system: surroundings temperature tot, atmospheric pressure and air humidity φ.

Fig. 1. presents a diagram of the test bench containing the particular apparatuses.

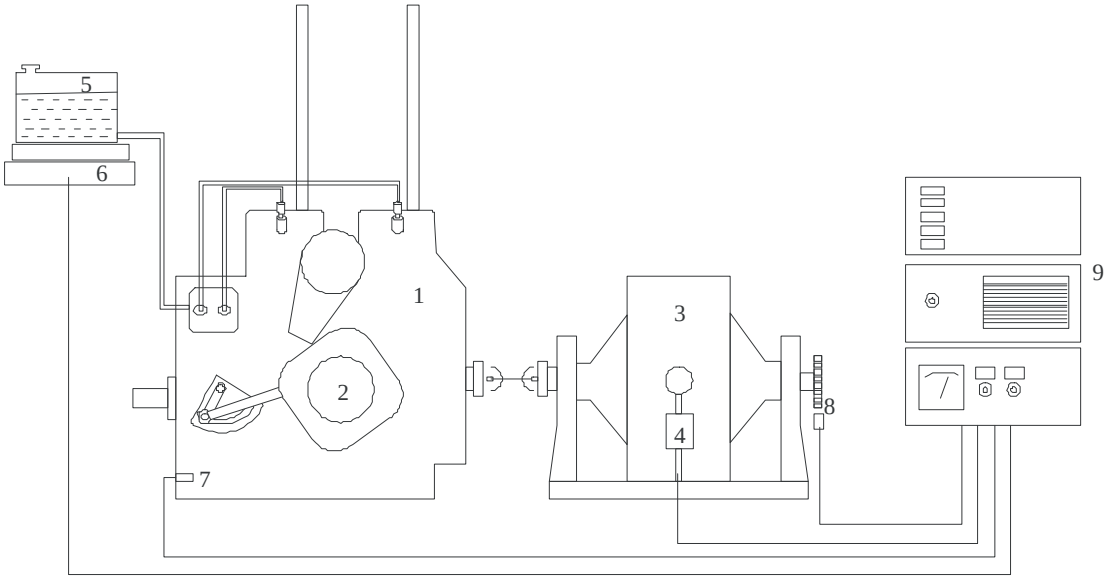

Fig. 1. Test bench diagram: 1 – 2CA90 engine, 2 – engine control, 3 – AMX 210 electro whirl brake, 4 – tensometer, 5 – fuel tank, 6 – scales for measuring fuel consumption, 7 – oil temperature sensor, 8 – engine speed sensor, 9 – control measurement panel

Investigation of energetic parameters was based on set of measurements conducted for each of investigated fuels with regard to PN norm, which enabled elaboration of data essential for determining external characteristics with engine's rotation speed ranging from minimal to nominal. In this research following kinematic and dynamic parameters of engine: torque – Mo, rotation speed –n, time in which set amount of fuel was used – τ. Amount of fuel used in determination of this parameter was 50 g. Methodology of measurements and methods of torque and power reductions were conformed to following norms: PN-78/S-02005, PN-88/S-02005, BN-79/1374-03 and BN-74/1340-12.

Statistical analysis of research results embraced assessment of variation of energetic parameters, significance analysis of differences between value of these parameters and determination, based on curvilinear regression method, of function dependencies. Analysis of biocomponent addition influence on energetic parameters was conducted by means of univariate variance analysis (ANOVA), and estimation of differences significance between investigated fuels and diesel fuel by means of Tukey's least significant difference (LSD) with significance level $\alpha = 0.05$.

RESEARCH RESULTS AND THEIR ANALYSIS

Influence of fuel type on energetic parameters was evaluated relying on external characteristics prepared during powering engine with prepared prior to investigation fuels. Changes were compared to characteristics prepared for diesel fuel powered engine. Results of FAME and FAEE influence on engine energetic parameters were presented in Figure 2.

Analysis of, presented in Fig. 2, torque curves proves that utilization of esters as fuel, when compared to diesel fuel, causes change of engine energetic parameters. Reduction of torque value, decrease of power and increase of specific and hourly fuel consumption are noticeable. Also, character of curves course is slightly different than characteristics elaborated for diesel fuel.

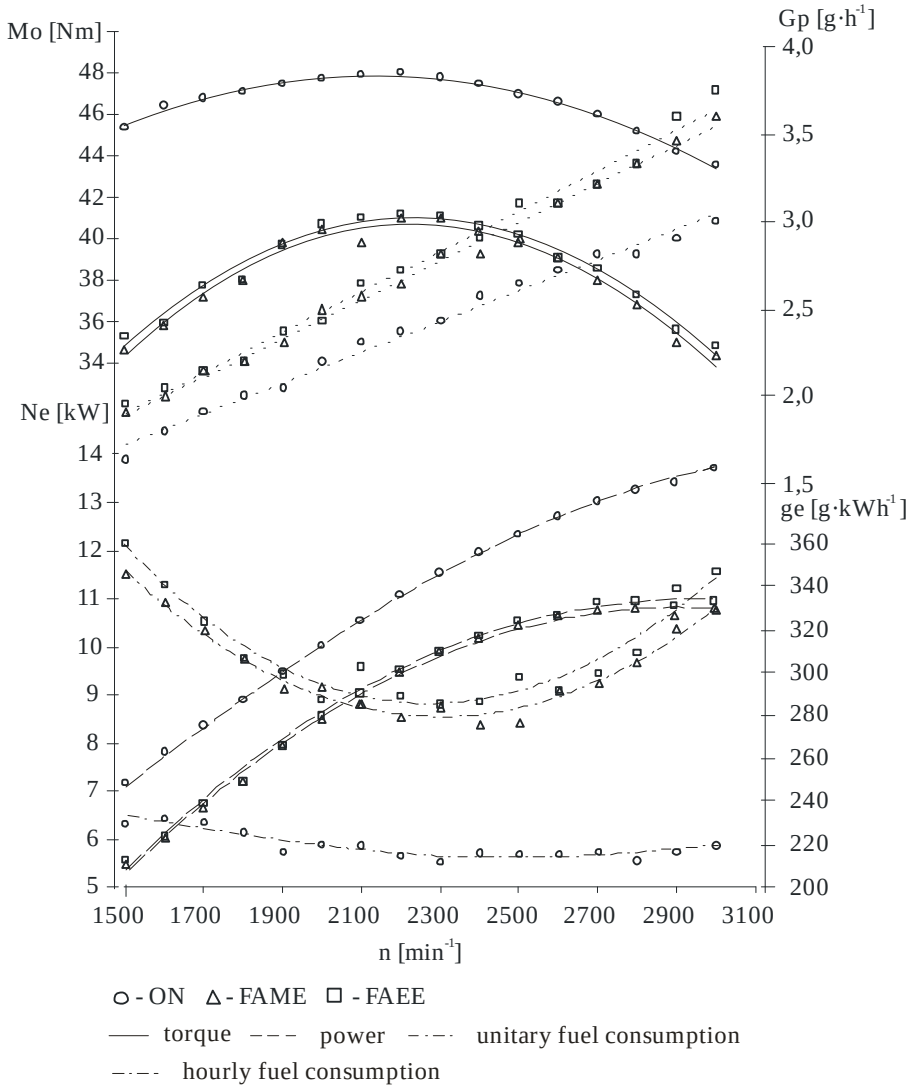

Fig. 2. Comparison characteristic of 2CA90 engine powered with diesel fuel and rapeseed oil methyl and ethyl esters

Analysing relative changes of energetic parameters of engine powered with ester fuel to engine powered with DF (Fig. 3) it can be stated that change was not big and remained within range presented by other authors [3, 4, 9-11] Change of maximal torque was about 5%, maximal power about 7%, specific fuel consumption about 16% and hourly fuel consumption about 10%.

Statistical analysis of obtained results, concerning influence of ester addition on engine energetic parameters, showed that changes of power, specific and hourly fuel consumption for fuel mixtures containing ester addition significantly differ from ones observed for DF (significance level 0,05).

Regression models for torque, power, specific and hourly fuel consumption for particular fuels, were described with equations presented in Table 2. In this table, coefficients of determination R2 were also presented.

Analysing diagrams presented in Figure 3, it can be stated that type of ester used in mixture does not have significant effect on obtained energetic parameters of the engine. Maximal torque recorded for FAME was 0,5 Nm higher. Type of ester used in mixture does not have significant effect on obtained maximal power, what was presented in Fig. 3b. Higher values of torque were observed for FAME based mixtures, with the highest observed difference of 0,4 kW. Analysis of mean hourly fuel consumption, Fig. 4c, shows that the highest consumption was noted for ethyl esters - with difference up to 0,1 kg • h^{-1}. Similarly, higher specific fuel consumption was observed for mixtures based on ethyl esters with difference reaching 5 g • $(kWh)^{-1}$.

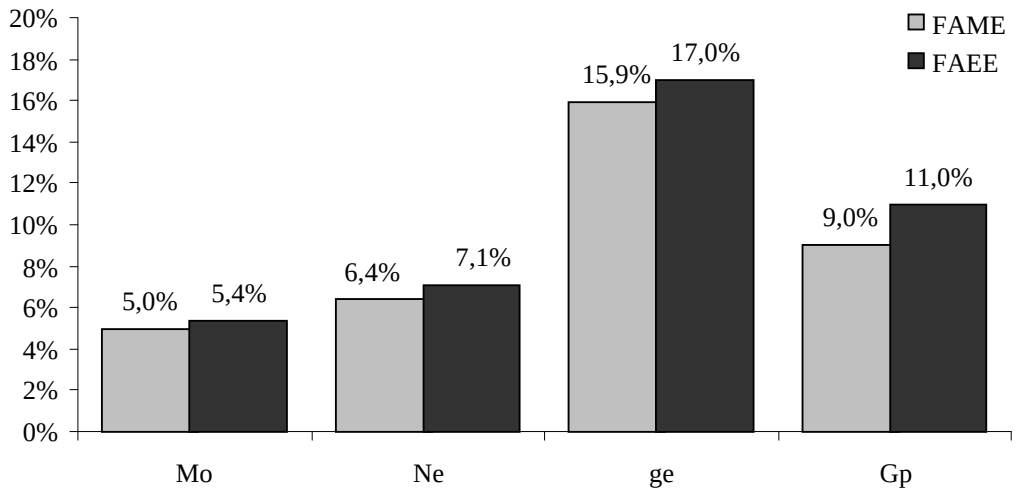

Fig. 3. Relative changes of engine maximal torque, maximal power, minimal fuel consumption, mean hourly fuel consumption of 2CA90 engine powered with methyl and ethyl ester.

Table 2. Regression equations for variables calculated relying on research results

Dependent variable y	Fuel	Regression equations	Coefficient of determination R^2
Mo [Nm]	ON	$y = -0{,}000006 \cdot n^2 + 0{,}0253 \cdot n + 20{,}848$	0,9931
	FAME	$y = -0{,}000001 \cdot n^2 + 0{,}0508 \cdot n - 15{,}862$	0,9752
	FAEE	$y = -0{,}000001 \cdot n^2 + 0{,}0523 \cdot n - 17{,}763$	0,9474
Ne [kW]	ON	$y = 5 \cdot 10^{-10} \cdot n^3 + 2 \cdot 10^{-6} \cdot n^2 + 0{,}003638 \cdot n - 1{,}036471$	0,9643
	FAME	$y = -1 \cdot 10^{-9} \cdot n^3 + 4 \cdot 10^{-6} \cdot n^2 + 0{,}0006 \cdot n - 1{,}036471$	0,9983
	FAEE	$y = 1 \cdot 10^{-9} \cdot n^3 + 4 \cdot 10^{-6} \cdot n^2 + 0{,}0016 \cdot n - 2{,}4606$	0,9977
ge [g · (kWh)$^{-1}$]	ON	$y = 7 \cdot 10^{-9} \cdot n^3 + 8{,}1 \cdot 10^{-5} \cdot n^2 - 0{,}257178 \cdot n + 465{,}911$	0,7282
	FAME	$y = 0{,}0001 \cdot n^2 - 0{,}4893 \cdot n + 842{,}7$	0,9755
	FAEE	$y = 0{,}0001 \cdot n^2 - 0{,}5429 \cdot n + 903{,}88$	0,9361
Gp [kg · h^{-1}]	ON	$y = 0{,}0009 \cdot n + 0{,}360898$	0,9675
	FAME	$y = 0{,}0011 \cdot n + 0{,}2377$	0,9939
	FAEE	$y = 0{,}0012 \cdot n + 0{,}1658$	0,9892

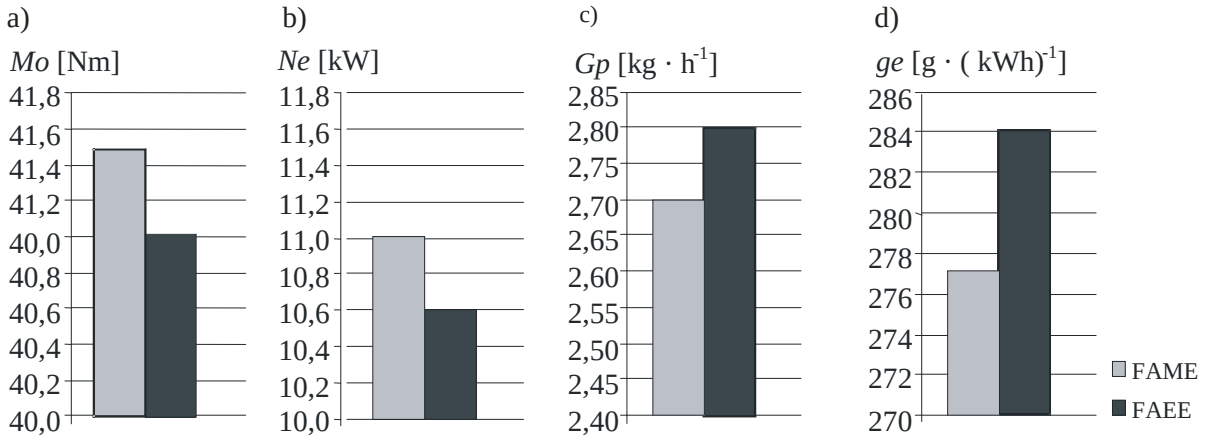

Fig. 4. Comparison analysis of FAME and FAEE influence on: a) maximal torque, b) maximal power, c)mean hourly fuel consumption, d) minimal specific fuel consumption of 2CA90 engine

CONCLUSIONS

1. Esters of higher fatty acids of plant oils characterise with different physico-chemical properties than conventional diesel fuel. It has an effect on process of supplying and injection of fuel, and therefore, its combustion [1], and directly results in changes of energetic effects of engine powered with such fuels.

2. Utilization of methyl and ethyl esters of rapeseed oil fatty acids, for powering diesel engines, causes change, when compared to powering with diesel fuel, of engine work energetic parameters Analysis of results of research conducted on 2CA90 engine justifies statement that: addition of FAME and FAEE into DF significantly affected change of the engine effective power, maximal torque and led to increase of hourly and unitary fuel consumption.

3. Research did not prove determining effect of ester type used in mixture with DF on engine energetic parameters.

4. Lack of legal regulations concerning quality of ethyl esters may cause problems related to possibility of wider scale introduction of this fuel.

REFERENCES

1. Ambrozik A., Kruczyński S., Orliński S.*: Influence of diesel engine fuelling with selected hydrocarbon and vegetable fuels on injection and self ignition angle delay*. P05-C024, PTNSS-Kongres, Międzynarodowy Kongres Silników Spalinowych, Bielsko-Biała –Szczyrk, 2005.
2. Baczewski K., Kałdoński T.: *Paliwa do silników o zapłonie samoczynnym*. WKŁ, Warszawa, 2004.
3. Graboski M. S., McCormick R. L.: *Combustion of fat and vegetable oil derived fuels in diesel engines*. Prog. Energy Combust. Sci. Vol. 24, 1998, pp. 125-164.
4. Lotko W.: *Zasilanie silników wysokoprężnych paliwami węglowodorowymi i roślinnymi*. Wyd. WNT, Warszawa, 1997.
5. Ma F., Hanna M. A.: *Biodiesel production: a review*. Bioresource Technology 70, 1999, pp. 1-15.
6. Merkisz J., Kozak M.: *Przegląd techniczno-eksploatacyjnych korzyści i zagrożeń związanych ze stosowaniem biopaliw w silnikach spalinowych*. II Międzynarodowa konferencja Naukowo-Techniczna „Biopaliwa 2003", SGGW Warszawa.
7. PN-EN 14214:2004 *Paliwa do pojazdów samochodowych.* Estry metylowe kwasów tłuszczowych (FAME) do silników o zapłonie samoczynnym (Diesla). Wymagania i metody badań.
8. PN-EN 590:2009 *Paliwa do pojazdów samochodowych*. Oleje napędowe. Wymagania i metody badań.
9. Srivastava A., Prasad R.: *Triglycerides-based diesel fuels*. Renewable and Sustainable Energy Reviews 4, 2000, pp. 111-133.
10. Szlachta Z.: *Zasilanie silników wysokoprężnych paliwami rzepakowymi*. WKŁ, Warszawa, 2002.
11. Williamson A-M., Badr O.: Assessing the Viability of using Rape Methyl Ester (RME) as an Alternative to Mineral Diesel Fuel for Powering Road Vehicles in the UK Applied Energy, Vol. 59, No. 2±3, 1998, pp. 187-214.
12. Zając G. Węgrzyn A.: *Analysis of Work Parameters Changes of Diesel Engine Powered With Diesel Fuel and FAEE Blends*. Maintenance and Reliability 2 (38), 2008, Lublin.

ZESZYTY NAUKOWE POLITECHNIKI RZESZOWSKIEJ NR 274
Mechanika z. 81 2010

Eva ZDRAVECKÁ
Lukáš FRANTA*
Miroslav ONDÁČ

TU of Košice, Slovak Republic; *FME CTU in Prague, Czech Republic

THE CARBON LAYERS FOR BIO-TRIBOLOGICAL APLICATIONS

One of alternatives for improving the wear resistance and corrosion of biomaterials is the application of protective coatings. DLC coatings are one of the most attractive proposal of the last years for biomedical applications. The aim of this contribution is to compare the mechanical properties for CoCr materials surfaces deposited with DLC coatings under different deposition parameters. DLC coatings were deposited by PVD method (physical vapor deposition) on CrCo alloy-substrate used for bioimplants.

INTRODUCTION

Mechanical load which presents in orthopedic implants can affect drastically the properties of implants materials. Damage of these materials usually occurs due to contact and is connected with abrasion, adhesion, fretting, delamination, pitting and fatigue. Damage depends on friction, lubrication, contact area, surface finish and level of loads (stresses). For these materials are important mainly the physical properties: yield strength, toughness and contact fatigue. Fatigue wear occurs when the fatigue limit of a material is exceeded or when subsurface shear stresses and contact stresses lead to subsurface crack growth. This leads to delamination and pitting (larger debris than generated through adhesive/abrasive mechanisms). The most of materials applied in medicine are composed of basic material (substrate) and coating. Diamond-like carbon (DLC) coatings cover a wide range of different types of carbon-based coatings, which generally have properties such as low friction and high wear resistance [1]. Also many applications of a-C films are permanent actual for bio-tribological applications.

In order to use DLC coatings reliably in different applications, it is important to understand the mechanical and tribological behaviour of the coatings in different operating conditions. This has been studied intensively by many scientists during the last few years. The friction and wear performance of amorphous carbon (a-C) coatings greatly depends on the deposition method and the deposition parameters used as well as the test environment [2, 3]. As a general trend, a-C:H films can provide low friction performance in sliding conditions [4–6].

The aim of this work is to study mechanical properties of a-DLC coatings deposited by PVD cathodic arc method on CoCr substrate used on artificial joints and to compare the mechanical properties under different depositions parameters.

DEPOSITION PROCESS

The DLCs were deposited by low arc discharge vacuum equipment in a UVNIPA-1-001 vacuum system with three sources (gas ion source for cleaning, electric arc source for non-magnetic metal sputtering and pulse arc carbon source). Samples entering were sputtered in one vacuum cycle. All of substrates were cleaned for 10 min with Ar ions. DLC layer was deposited at down to 150°C temperature. Nitrogen and Ar gasses were added during the DLC deposition into a working chamber [7, 9]. The coatings were produced on a highly polished flat CoCr materials substrate R_a = 0.05 µm. One fine polished face of every CoCr substrates was coated by a-C film. The hardness were determined from dept sensing indentations (DSI) of curves measured Nano TEST NT600. Type LabRam Scanning electron microscope (SEM) LEO 1550 was used to study the microtopography of DLC layers.

EVALUATION OF NANOINDENTATION

The hardness H, elastic modulus E_{eff} and mechanical characteristics were determined from depth sensing indentations (DSI) curves measured by the NanoTest NT600 apparatus (Fig. 1) at different maximal loads from 5 to 100 mN with diamond Berkovich tip [8]. The indentation cycle was repeated five times in slightly different places for each maxima load. The samples were indented at the different maximal load 5, 10, 20, 50 and 100 mN [10]. Records DSI curves served to determination of maximal penetration depth h_{max}, at maximal loading force F_{max}. Values of H_{IT}^3/E_{eff}^2 for type of films marked U II and U III are almost similar. The lowest value H_{IT}^3/E_{eff}^2 was observed for coating marked U IV what can be connected with lower content of N [7, 9] - (Fig. 2, 3).

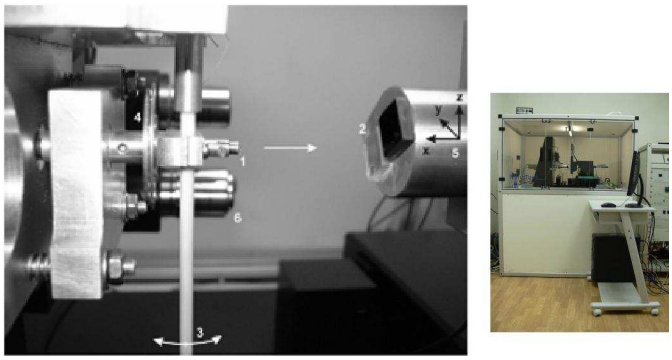

Fig. 1. View and measuring node of apparatus**,** 1-indenter, 2-samples, 3-pendulum, 4-capacitor plates, 5-sample holder (x-y-z directions of moving), 6-microscope

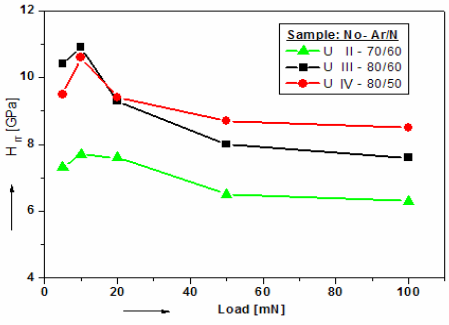

Fig. 2. Dependence H_{IT} on different load

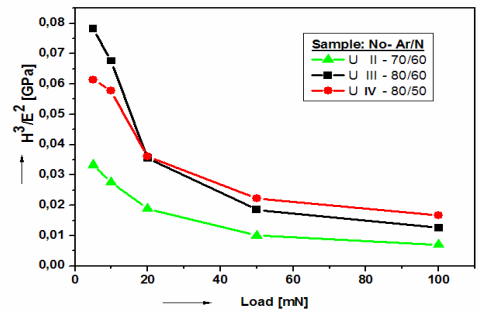

Fig. 3. Dependence of H_{IT}^3/E_{eff}^2 on different load

TRIBOLOGICAL TESTS ON LARGE 3D SUBSTRATES

Due to specific shape of knee joint the standard wear methods (pin-on-disk, ring-on-disk, and etc.) are not suitable, because it is not the stylization of functional geometry. Methodics of non-standard test is selected for prevailing conditions of wear process and respects the functional geometry of knee joint, conditions of non-standard test equal the condition of so-called „locked knee“[11]. This non-standard method represents the test method with contact area line-on-plate. Test conditions are characterized by linear distribution of load. Geometry of 3D shaped sample is similar to geometry of total knee implant. From the view is under full load on the contact line 30-40 mm the min. load 750 N is acting (1 BW-Body Weight) but also 2000 N (2,5 BW). Load is in the range from minimum 20 N/mm to maximum 65 N/mm. Shaped samples were with width 15 mm and loaded under normal force 340 N. (load is equal 22,6 N/mm). All experiments were carried out on minimum limit of realistic loading. Parameters of the test are shown in Tab. 1.

Tab. 1. Parameters of non-standard test

Path	18	Mm
Frequence of movement	1,43	Hz
Lubricant	H_2O+0,9 g/l NaCl	
Normal loading force	343	N
Time of 1 cycle	0,70	s
Middle-sized speed	51,6	mm/s
Temperature	25	°C

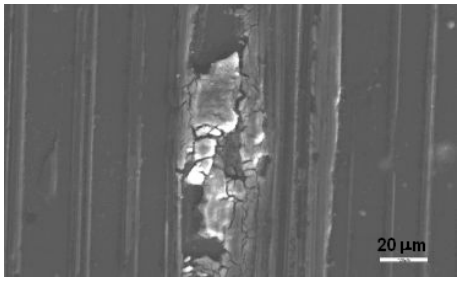

Fig. 4. Initiation of mircracking

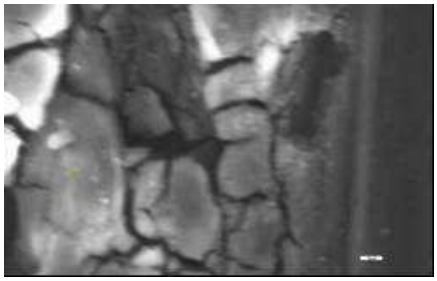

Fig. 5. The generation microcracking

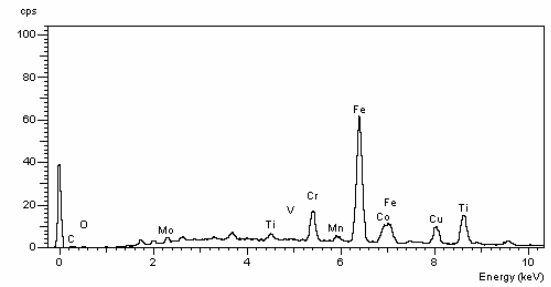

Fig. 6. EDX analysis of DLC coating from microcraking

DISCUSSION

From mechanical and tribological properties obtained from standard test the following conclusions can be made:

- The lowest value H_{IT}^3/E_{eff}^2 was observed for coating marked IV what can be connected with lower content of N,
- The highest value H_{IT}^3/E_{eff}^2 was obtained for coating U III [with Ar 80 sccm and N 60 sccm].

Tribological properties obtained from non-standard test the following conclusions can be made:

- Morphology of DLC surface contains microcrack (Figs. 4, 5) what can be connected with high internal stress, EDX analysis is in Fig. 6,
- These microparticles from microcrack were transferred on UHMWPE and created contact stresses whereby the crack spreads farther,
- Design of tested samples affects stress states and failure for coating. High hardness, in turn, causes high internal stress. These stresses can contribute to microcrack of coating and creation debris than generated through adhesive/abrasive mechanisms. Together with transfer of debris from coating on UHMWPE is produced a damage score.

CONCLUSION

Characteristics like hardness H, elastic modulus were obtained from indentation loop and were investigated in range of film deposited by low arc discharge vacuum equipment UVNIPA-1-001.

The presented work shows that conditions for wear and debris formation are connected with conditions of deposition parameters. More investigations are needed for obtaining excellent behaviour of DLC coating during depositions on 3D shaped surfaces.

REFERENCES

1. Dion I, Baquey C, Monties JR.: *Diamond: the biomaterial of the 21st century?* Int J Artif Organs. 1993 Sep.16(9); 623-7.s.
2. Grill A.:, Wear 168, 1993; 143.
3. Grill A.:, Surf. Coatings Technol. 94/95, 1997; p. 507–513.
4. Erdemir A., Switala M., Wie R., Wilbur P.: Surf. Coatings Technol. 50, 1991; p. 17.
5. Marchon B., et al.: IEEE Trans. Magnet. 26 (5), 1990; 2670.
6. Kim D.S. et al.: Surf. Coatings Technol. 49, 1991; p. 537.
7. Vojs M., et al.: *Properties of amorphous carbon layers for bio-tribological aplications*. Microelectronics Journal (in press)
8. OliverW.C., Pharr G.M.: Journal of Materials Research, Vol. 7. 1992; p. 1564-1583.
9. Zdravecká E., et al., Study of DLC coatings on micro and macro level. Eurocorr 2007, Freiburg; p.1-9
10. Boháč P., et al.: Beijing. 2007. Elsevier UK. 2007; P 2.37
11. Pražák J., et al.: *Možnosti umělé lubrikace umělých kloubů*. Ustav termomechaniky AV ČR. 2002.

This work has been supported by grants VEGA 1/0390/08 and COST 533 from of the Ministry of Education of the Slovak Republic.